TITLE PAGE

Report Title: Solid State Energy Conversion Alliance Delphi SOFC

Type of Report: Topical

Reporting Period Start Date: 01/01/02

Reporting Period End Date: 06/30/02

Principal Author(s):   Steven Shaffer
           Sean Kelly
           Dr. Larry Chick
           Dr. Subhasish Mukerjee
           David Schumann

Date Revised Report Issued: May 20, 2003

DOE Award Number: DE-FC26-02NT41246

Submitted By: Delphi Automotive Systems
           5725 Delphi Drive
           Troy, Michigan 48098

In Collaboration with: Battelle/PNNL
           Electricore, Inc.

DISCLAIMER

TABLE OF CONTENTS

List of Figures – Topical Report

List of Tables – Topical Report

1.0   ABSTRACT

The objective of Phase I under this project is to develop a 5 kW SOFC power system for a range of fuels and applications. During Phase I, the following will be accomplished:

1. Develop and demonstrate technology transfer efforts on a 5 kW stationary distributed power generation system that incorporates steam reforming of natural gas with piped-in water (Demonstration System A).

2. Initiate development of a 5 kW system for later mass-market automotive auxiliary power unit application, which will incorporate catalytic partial oxidation (CPO) reforming of gasoline, with anode exhaust gas injected into an ultra-lean burn internal combustion engine.

This topical report covers work performed by Delphi Automotive Systems from January through June 2002 under DOE Cooperative Agreement DE-FC-02NT41246 for the 5 kW mass-market automotive (gasoline) auxiliary power unit. This report highlights technical results of the work performed under the following tasks for the automotive 5 kW system:

1. System Design and Integration
2. SOFC Stack Development
3. Reformer Development

The next anticipated Technical Progress Report will be submitted January 30, 2003 and will include tasks contained within the cooperative agreement including development work on the Demonstration System A, if available.

2.0   EXECUTIVE SUMMARY

The subject effort includes development of the SOFC stack and reformers. Also included are system design and integration, fabrication of demonstration systems, testing of demonstration systems, and reporting of results. Development of other balance-of-plant components (e.g., the air delivery system, fuel delivery system, sensors and controls, control algorithms and software, safety systems, insulation, enclosure and packaging, exhaust system, electrical signal and power conditioning) will be privately funded by Delphi, and is considered outside the scope of this program. However, Delphi will report on the general status of the privately funded effort when significant milestones are achieved.

The following accomplishments were achieved under the following tasks for this reporting period.

2.1 System Design and Integration

The requirements for the 5 kW Auxiliary Power Unit (APU) have been generated with the automotive (mobile) application as the focus. Progress towards the automotive requirements will satisfy many of the stationary power plant requirements. The general requirements of the power plant include the overall target volumetric and gravimetric power densities, overall conversion efficiency as well as the typical service life and duty requirements. Additionally, the start-up time, or latency has been specified. The requirements are shown for prototype design levels (1-5 years) as well as target commercial levels (5-10 years). (Refer to Section 4.1.1.1 General Requirements.)

One of the most highly influential requirements in the pursuit of an automotive APU conceptual system design is the volumetric power density. 10 liters/kW was the target used for initial system work. For the conceptual system design, a fixed package envelope was adopted as a starting point. This fixed package envelope necessitated some initial concept system integration and the definition of additional conceptual design requirements. Of these, the most important requirement pertains to the definition of a high temperature module (Hot-Zone-Module, HZM) and low temperature module (Plant-Support-Module, PSM) organization in the APU.

To support the conceptual design activity and meet the system requirements, an APU system mechanization has been created. This mechanization features several innovations that improve potential system performance and system packaging.

Two initial concepts were generated given the system requirements, conceptual design requirements and system mechanization. The concepts investigated were classified as the "T" and the "Square" based upon the general shape of the Hot-Zone-Module within the enclosure boundaries.

Within the prevailing design concept, two main concepts for modular APU insulation have been investigated. Each has apparent advantages and disadvantages. Additionally, the requirement for insulation performance has been determined in consideration of design constraints.

Process air blower requirements have been generated for the 5 kW APU. While the requirements of the blower are atypical, and commercial choices are limited, two technologies that offer promise for the automotive APU have been identified and characterized.

For the SOFC APU, much effort has been focused on the integration of system models and controls. Towards this end, a plant model with integrated controls has been developed to jointly support system analysis and concurrent control strategy development. The system model has been used to run many simulations of the 5 kW APU featuring both straight POx reformer operation and anode tail gas recycling. The plant model has allowed for the verification of fundamental assumptions about the response and control of the SOFC APU.

Working within the fixed package size has been an extremely challenging engineering task; however, one that has produced many innovations in both system mechanization and design concept. The integration of the subsystems into the APU product was undertaken in an engineering evaluation mock-up. While executed mainly as a packaging verification exercise, many functional parts were used. The subsystems, now in various stages of development, have been guided by the integrated product requirements. The emphasis on the end-product form factor has produced a workable concept with realizable performance in a much smaller size than would normally have been attempted.

2.2   SOFC Stack Development

Huge progress has been made between January and June 2002 in stack development. The key achievements are:

- Generation 2 stack design with metal cassettes as the repeating unit has been developed.
- Steady state modeling of this design has been carried out to understand flow, thermal and electrochemical behavior.
- Transient modeling has been carried out to understand the stresses for fast start-up in these designs.
- Cathode development has progressed with 7x7 cm cell stacks demonstrating high power densities. Further work is ongoing to understand the processes that contribute to stable high power density performance of the cell.
- Fabrication of large cells of 12cm x 12cm dimensions has been successful for implementing into cassette builds.
- Bonding using the existing glass ceramic seal G18 has been further improved by new coating processes.
- New glass ceramic seals with better thermal expansion coefficient matching has been tested for adhesion. Further development ongoing.
- Alternate seals have been developed like a silver based braze which is being evaluated. Initial results from rupture test is very encouraging
- Multiple 3-cell stacks (7cm x7cm cells) have been successfully fabricated and tested for performance validation.
- 3-cell stack (7cm x 7cm cells) has been tested for 1000 hour of durability.
- Successful fabrication and testing of 1- to 6-cell stacks with full sized (12cm x 12cm) cells.

2.3   Reformer Developments

Reformer

A production minded Reformer system continues to be developed that includes integrated reformer, combustor and reformer air pre-heat function. Testing has been conducted that supports the viability of a homogenous mix combustor to provide clean start up heat to the reactor. Several reactor designs have been built and tested that have pointed out areas of design/process weaknesses in need of further development including:

- Combustor mixing geometry and temperature feedback
- Reactor lead edge temperature control
- Reformer thermal mass reduction / isolation
- Rapid heat up of reformer pre-heat air
- Braze related prototype manufacturing techniques
- Most of these identified weaknesses will be addressed in a new design (H2 reformer) which will undergo evaluation in Q3 and Q4 2002.

Catalyst

Significant improvements to gasoline partial oxidation catalyst formulations resulted in alumina or zirconia based compositions having excellent performance and durability at high operating temperatures for at least fifty hours of testing. Performance and thermodynamic modeling considerations were employed to suggest the best operating regime for gasoline partial oxidation to be between 900 and 950 °C and about 13 to 44 in² of washcoated surface area per g/min of fuel to be processed, for planar reactor configurations

3.0   EXPERIMENTAL APPROACH

The following sections describe, and reference experimental methods, materials, and equipment being used for the research described below.

3.1   System Design and Integration

For the SOFC APU, much effort has been focused on the integration of system models and controls.   Towards this end, a plant model with integrated controls has been developed to jointly support system analysis and concurrent control strategy development.   The system model has been used to run many simulations of the 5 kW APU featuring both straight POx reformer operation and anode tail gas recycling.

3.2   SOFC Stack Development

Typical stack testing is carried out using a test stand that has a hot furnace, electrical load bank, and gas mixing cabinet (Lynntech Inc).   Metallic cassettes for building stacks are fabricated by standard brazing procedures and are creep flattened before use. Cells are fabricated internally or bought from suppliers.   A typical experiment involves measurement of standard polarization curves and power densities at constant voltages for performance evaluation.

The Interconnect Resistance Unit (IRU, Figure 4.2.9-1) is a device that is used to characterize the electronic conductivity of the interconnects at operating temperatures. A current at a density of 0.5 A/cm^2 is run through a double cathode "sandwich" as the specimen is heated at stack operating temperature in air. Various materials combinations and configurations for separator plate, mesh, bonding paste and current collector grid can be conveniently tested in the IRU.   The Area Specific Resistance (ASR, ohm-cm2) is calculated as ½ the measured resistance multiplied by the surface area.

The seal rupture strength test unit (Figure 4.2.10-2) is used for quantitative comparison of seal joint strengths.   A metal washer with the sample is clamped into the fixture and air pressure is increased until the seal breaks and the ceramic bilayer disk pops off.

3.3   Reformer Development

Single Planar / H1 / H2 testing Setup

Reformers were tested in several configurations with respect to feedstream preparation. Early in this time period lab assisted fixtures provided the needed conditioning to feedstreams (i.e. oil heated fixtures to provide vaporization heat and mixing, lab device heated air ducted to either reformer or combustor inlets). As testing and product development progressed, virtually all lab assistance was eliminated by a "product" device or function. For all configurations tested the experimental set up was similar and consisted of the following:

Mass Spectrometer
A gas analysis system was utilized to quantify as many as 9 compounds on a real time basis for both the reformer outlet and combustor outlet streams.

Emissions Bench
An Emissions bench capable of measurement in the typical engine out range was utilized to supplement mass spectrometer data with independent measures of total HCs (propane equivalent), CO, NOx and O^2

Controls and Data Acquisition
Dspace
A flexible I/O component driver and controller (D-Space) was utilized for all reformer testing.
The use of Dspace allows any control algorithm to be shared between the lab environment and vehicle or systems environment so that system control strategies can be exercised in the lab with virtual transparency.

ADAM (Advantech Data Acquisition and Control Module)
All non-system mechanized I/O or devices (those not on the product intent mechanization but present for enhanced lab data or control i.e additional thermocouples) are handled by this controller. This allows the lab environment to have supplemental I/O and devices beyond those on the mechanization. As testing progressed we gradually have begun to rely more on the D-Space I/O and less on those supported by the ADAM controller

Labview
Labview now serves as the "umbrella" controller and provides 2 key functions: 1. Integraton of data acquisition of all other (non product) devices for lab / facility control. 2. Emulation of system components not present in the test via Lab devices (i.e. makes lab environment transparent to Dspace controller)

Lab Fuel / Gas Controls
A gas blending cabinet was frequently used to simulate anode tail gas representative of what might leave the stack at various fuel utilizations. This was particularly important in understanding combustor behavior.
An AVL-735 unit provided accurate fuel measurement and conditioning. This provided a measure of safety given that actual injector hardware was subject to a harsh operating environment and could be subject to flow shifts.

Vaporizer Characterization
In addition to conventional flow visualization, two other Laser based techniques have been employed to help evaluate and improve A/F delivery performance. Mie Scattering techniques provide visual evaluation of the distribution of liquid droplets of an injected spray while Planar Laser Induced Flourescence (PLIF) is used as a subsequent step

and provides a visual evaluation of liquid and vapor distribution. PLIF essentially is an evaluation of fuel mass (in liquid or vapor form) distribution in the flowstream.

Catalyst Testing

Reforming catalysts were prepared using methods and materials currently employed for the commercial manufacturing of automobile exhaust catalysts. Catalysts were tested using a fully instrumented tubular reactor equipped with gas and mass flow controllers and gas chromatography for product analysis. Sufficient process information can be collected for completing of mass balances.

4.0　RESULTS AND DISCUSSION

This section will summarize all relevant data, and interpret how results relate to developing the overall 5 kW SOFC system.

4.1　System Design and Integration (Task 1.0)

This task provides for the overall system design, including product definition, conceptualization, system modeling, preliminary design, and system integration. Task 1 efforts have been coordinated with subsystem development (Tasks 2 and 3) and provide for concept generation support for these tasks. Task 1 efforts are also coordinated with the system fabrication task. Inputs from the privately funded balance-of-plant components and manufacturing efforts will be key elements throughout the project. Progress on the major subtasks under Task 1 include the following:

4.1.1　Define System Requirements

4.1.1.1　General Requirements

The requirements for the 5 kW Auxiliary Power Unit (APU) have been generated with the automotive (mobile) application as the focus. Progress towards the automotive requirements will satisfy many of the stationary power plant requirements along the way. The general requirements of the power plant include the overall target volumetric and gravimetric power densities, overall conversion efficiency as well as the typical service life and duty requirements. Additionally for a fuel cell system, the start-up time, or latency must be specified. The requirements are shown for prototype design levels (1-5 years) as well as target commercial levels (5-10 years). The requirements for the 5 kW automotive APU are summarized in Table 4.1.1.1-1.

APU General Requirements:			
	Prototype	**Commercial**	**Units**
Net Electrical Output (VA)	3	5	kW
Response (10 to 90% load)	5000	500	msec
System Volume	75	44	Liters
	15	10	Liters/kW
System Mass	70	50	kg
Stack Volume	3	2	L/kW
Stack Mass	5	3	kg/kW
Service Duty <10% Power Degradation	>1000	>10000	hours
Service Life w/PM	3	10	years
Cold Start Duration	<20	<10	minutes
Start-Up Energy (at 12 V)	25	25	Ah
Cold Start Cycles <10% Power Degradation	>100	>7000	
Cooldown Thermal Time Constant	4	12	hours
Surface Temperature rise over ambient	40	30	deg C
Fuel Sulphur Content	<50	<50	ppm
Exhaust Emissions			
CO2	6000	600	g/kWh
CO	1	0.1	g/kWh
NOx	0.1	0.01	g/kWh
HC	0.05	0.005	g/kWh
H2	0.5	0.05	g/kWh
PM	0.05	0.005	g/kWh

Table 4.1.1.1-1: APU General Requirements.

These requirements are intended to be a guide for development and are subject to change per application benchmarks. Of particular interest are the service life and service duty requirements. For automotive applications, regular service intervals may be required, as is typical with the powertrain and electrical systems, to achieve the intended service life. This would indicate that serviceability of the critical fuel cell componentry in the APU is required.

Response time requirements are estimated for the APU. Much of this requirement is dictated by the electrical system interfacing with the APU. For instances where the loads are fairly constant and slow changing, or where a storage battery is employed, the response time of the APU may be reasonably slow. Where this is not true, the APU response must necessarily be fast. This presents an engineering challenge to the design of the fuel cell system.

Since the SOFC APU has a relatively high operating temperature, start-up time and cool-down rate are important considerations. Ideally, the start-up time period would be as short as possible and the cool-down rate (shut-down) would be as long as possible. Unfortunately, these requirements are in opposition in that a short start-up time is aided by reducing heat capacity of the hot componentry, while a slow cool down rate is aided by increasing the heat capacity. Treating the system as a lumped thermal mass, the cool-down thermal time constant should be the product of the effective thermal resistance to ambient and the effective thermal capacitance of the hot components. Assuming that neither of these is a strong function of ambient temperature, large thermal resistance and large heat capacity is desirable for temperature maintenance. For start-up performance, thermal capacity must be minimized. Consequently, very high performance thermal insulation will be required to achieve adequate temperature maintenance.

The required time constant referenced in Table 4.1.1.1-1 is targeted for the vehicle application where space for insulation is severely limited. The value of 12 hours for the time constant allows for approximately a 50% system temperature drop in an 8 hour period when no temperature maintenance cycle is employed. Indeed, in all applications, maximizing the thermal time constant is desirable. Insulation may be added where space is available for applications that require longer cool-down times. In stationary applications where start-up latencies are allowed to be longer in duration, both thermal capacity and insulation may be added to improve thermal performance.

4.1.1.2   Electrical Requirements

The electrical requirements are summarized in Table 4.1.1.2-1. Due to the implicit higher-voltage of a fuel cell stack, the requirements are tailored for a 42 V nominal voltage application. The minimum voltage output of 38V and the maximum output voltage of 50 V correspond to the discharge voltage and maximum charge voltage respectively of a 42 V battery system. The minimum input voltage on the 42 V bus correspond to the typical low charge condition. The requirements assume the availability of a 12V bus. This anticipates the application into near-term vehicle applications where many of the balance-of-plant (BOP) components require a 12V circuit; however, where a full 42V vehicle system would be employed this requirement can be eliminated. Note that as is typical in automotive applications, reverse-battery and double-battery conditions on the power bus are anticipated.

Since one of the major advantages of a fuel cell APU is improved economy, the minimum electrical efficiency of the APU is specified as 25%. This is approximately 20-50% better than a typical gasoline powered generator system. While theoretical SOFC Stack efficiencies may be high, resultant system efficiencies are much reduced due to fuel conversion in the reformer, fuel utilization in the stack, parasitic electrical loads and losses, and electrical DC-to-DC or DC-to-AC conversions. The power budgets for both POX reformer systems and anode recycle systems are shown in Table 4.1.1.2-2. For both systems, a 500 W maximum parasitic load is budgeted. Note that in a POX system, to achieve a net 25 % efficiency, very high fuel utilization in the stack is required. This may be an unreasonable expectation at very high power levels. To improve this situation, anode recycle may be employed. This has the potential to increase the reformer efficiency (gasoline to reformate conversion) and allow for much more reasonable fuel utilization. If higher utilization in the stack, or higher reformer efficiencies are allowable, then increases in system efficiency may be realized.

APU Electrical Requirements:

	Minimum	Maximum	Nominal	Units
Net Electrical Output (VA)	0*	5**	3	kW
Electrical Efficiency (Full Power)	25	N/A	N/A	%
Maximum Electrical Parasitic Load	N/A	500	N/A	W
	Non-Isolated **Continuous*			
42 V Output	38	50*	42	V
42 V Input (Operation)	30	50*	42	V
42 V Input (Non-Destructive), 60 sec	-42	84	N/A	V
12 V Input (Operation)	9	16	12	V
12 V Input (Non-Destructive), 60 sec	-14	28	N/A	V
Ripple Voltage	0	2**	0	V
Quiescent current from –10 °C to +40 °C	N/A	0.1	N/A	mA
Electrical isolation @500 V	1	N/A	N/A	Mohm

*Including ripple
** Total amplitude

Table 4.1.1.2-1: APU Electrical Requirements

APU Fuel Conversion Budget:			
		Anode Recycle	
Fuel Conversion:	POX System	System	Units
Reformer Efficiency	76%	100%	
Fuel Utilization	76%	58%	
Stack Efficiency	50%	50%	
Elec Conditioner Efficiency	95%	95%	
Conversion Efficiency	27.5%	27.5%	
Net Elec Power	5	5	kW
Efficiency	25.0%	25.0%	
Fuel Power	20	20	kW
Allowable Electrical Parasitic Load	500	500	W

Table 4.1.1.2-2: APU Power Conversion Budget

4.1.1.3   Environmental Requirements

The climatic requirements are summarized in Table 4.1.1.3-1.

Of particular note is the inlet air temperature requirement. While the ambient surrounding the APU at its installation point may be 80 ºC, the inlet air to the system is limited to 45 ºC, and therefore may need to be ducted from a cool location.

A maximum operating altitude has been specified.   The concern with altitude is similar to any air-breathing power conversion device. At 3600 m (12000 ft), the air density is about 64% of that at sea level and for a constant volumetric flow, like that that would be provided by an air pump or blower at the same speed, the mass flow rate is reduced through the system. Naturally, additional capacity may be specified for the air pumps and blowers, however it is reasonable to expect either a degradation of power rating due to reduced mass flow, or a decrease in efficiency due to increased blower power. Due to space considerations, minimal excess capacity is desirable, so a reduced power rating target is specified. If higher altitude performance is required, additional de-rating of the powerplant would be specified.

The maximum inlet air temperature to the system is specified to be 45^0 C. This air is used for electronics cooling before it is ingested into the blower. The maximum ambient temperature acceptable to the electronics is 105^0 C. The operating temperature of the electronics should be no more than 125^0C.

APU Climatic Requirements:				
	Minimum	Maximum	Nominal	Units
Ambient Temperature	-40	80	25	deg C
Inlet Air	-40	45	25	deg C
Relative Humidity @0-60 C	10	100	50	%
Operation Altitude	Sea Level	3600	Sea Level	m
	Or Below	20% Power Reduction		

Table 4.1.1.3-1: APU Climatic Requirements

4.1.1.4 Acoustic Requirements

The sound emission of the APU is of particular importance in the automotive application. The APU sound should not be notable when inside the vehicle under normal operation, nor outside the vehicle with respect to the background noise of the powertrain. The acceptable acoustic emission is detailed in Figure 4.1.1.4-1.

APU Sound Emission Requirement
(Near Field, Full Power, 2m x 0.5m x 1m Sound Enclosure)
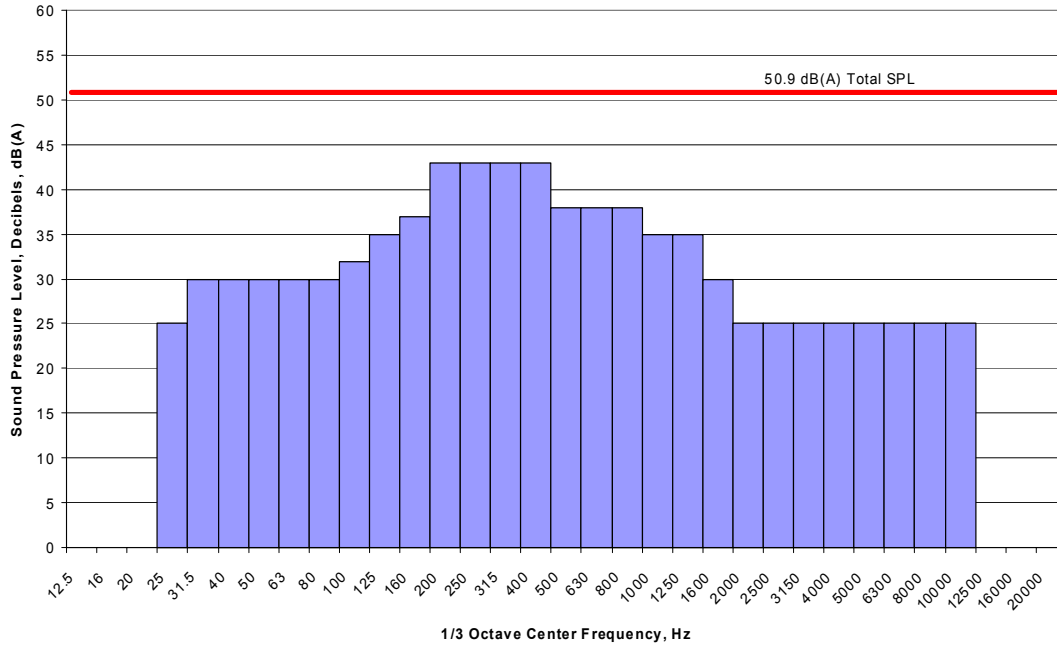
Figure 4.1.1.4 –1: Acoustic Emissions

4.1.1.5 Vibration Requirements

APU Vibration Profile:

(8 Hour Test)

Vertical Axis				Horizontal - Longitudinal Axis				Horizontal - Transverse Axis	
Center Frequency (Hz)	Power Density [(m/s^2)^2/Hz]			Center Frequency (Hz)	Power Density [(m/s^2)^2/Hz]			Center Frequency (Hz)	Power Density [(m/s^2)^2/Hz]
5	0.473			5	0.135			5	0.098
12	4.091			12	1.435			12	1.956
18	4.091			18	1.435			18	1.956
200	0.118			200	0.04			200	0.098

a$_{rms =}$ 12 m/s^2 a$_{rms =}$ 6.8 m/s^2 a$_{rms =}$ 9.0 m/s^2

(1.2 g)   (0.69 g)   (0.92 g)

Table 4.1.1.5-1: APU Vibration Profile

In an automotive environment, the vibration profile is much more severe than what is typical for a stationary application. This presents a special challenge to the stress-

sensitive components like the SOFC stack and an emphasis on overall protection and isolation of the powerplant. The automotive APU is required to survive the vibration profile shown in Table 4.1.1.5-1.

4.1.1.6 Inlet Air Filtration Requirements

The SOFC fuel cell system, like an automotive engine, has requirements on inlet air quality. Since the quality of the ambient air is unknown, the APU requires an air filter. The air filter must demonstrate 99.5% efficiency per SAE J726C variable flow schedule procedure on SAE standard coarse and fine dust. At 14 g/sec, the filter must have a minimum retention of 28 grams of fine dust and 40 grams of coarse dust. At end-of-life, the filter should have no more than a 0.25 kPa pressure drop at 14 g/sec, 25 ºC.

4.1.1.7 Fuel Filtration Requirements

The fuel filtration requirements are per standard automotive application for gasoline.

4.1.1.8 Additional Typical Automotive Requirements

A typical automotive application has additional requirements pertaining to structural integrity and environmental protection. The details of these are highly dependent on application and vehicle installation. Both the structural and environmental protection requirements strongly influence the design of the APU package and enclosure. They may include the following:

Structural:
   Drop test (20 cm) two axis each per 3 specimens
   Crash worthiness (vehicle dependent)

Environmental protection:
   Dust intrusion resistance
    (fine Arizona dust per SAE J 726., DIN 40 050-9 test)
   Hot water jet intrusion test (80 ºC), 1cm/sec
   Water immersion – 0 ºC , 5% salt water
   Salt spray exposure

Electro-magnetic Compatibility (EMC):

The requirements for EMC are typical per automotive standards. For reference, a listing of the typical tests is included in Table 4.1.1.8-1. Level 3 severity is specified for both Radio Interference Suppression and Interference Voltage Peak.

EMC tests according to GS 95002

Measurement required		No.	GS 95002		Type of Measurement
yes	no		Pt.	page	
x		1.	7.1.2	7	Emission of transients on power supply lines
x		2.	7.1.3	8	Immunity to transients on power supply lines
x		3.	7.1.3	8	Immunity to transients on signal, data and control lines
x		4.	7.2.1	9	Measurement of conducted interferences from electromechanical components; Interference suppression level 3; long term interference sources
x		5.	7.2.1	9	Measurement of conducted interferences from electromechanical components; Interference suppression level 1; short term interference sources
x		6.	7.2.2	10	Measurement of conducted interference from electronic components
x		7	7.2.3	11	Measurement of radiated interference using a coupling clamp
x		8.	7.3.1	13	Measurement of radiated interference using a stripline
	x	9.	7.3.2	14	Measurement of conducted emissions using a current probe
x		10	7.3.3	15	Measurement of radiated emissions from carsystems using an anechoic chamber
x		11.	7.4.1	17	Immunity tests using a stripline
	x	12.	7.4.2	19	Immunity tests from components and systems using a Anechoic chamber
	x	13.	7.4.3	20	Immunity tests using the BCI method
x		14.	7.4.4	20	Immunity tests using GSM modulation
x		15.	7.5	21	Component Immunity to electrostatic discharge (ESD)
	x	16.	7.6	21	Attenuation of audio frequencies on supply lines for audio systems
x		17.	7.7	22	Slew rate of voltages and currents on the vehicle electrical system

Table 4.1.1.8-1: Typical Automotive EMC Requirements

4.1.2 Develop Conceptual System Design

One of the most highly influential requirements in the pursuit of an automotive APU conceptual system design is the volumetric power density. For a typical vehicle installation, 10 liters/kW is the target. For the conceptual system design, a fixed package envelope was adopted as a starting point. While inconvenient, this fixed package envelope necessitated some initial concept system integration. In addition to the fixed package envelope, additional requirements were placed on the conceptual system design as enablers for serviceability and product function. These are as follows:

Conceptual design requirements:

1) Top-access of hot zone components.
   To facilitate the build process and easily change out components that have low life in development (reformers, stacks, sensors).

2) Two temperature zone modular construction comprised of low temperature Plant-Support-Module (PSM) and high temperature, insulated Hot-Zone-Module (HZM).

3) Single outer enclosure for environmental protection and containment. Modular high-performance thermal insulation shells to insulate HZM.

4) Integrated gas flow distribution manifold for HZM components (ICM, Integrated-Component-Manifold). Allows for close-coupling of HZM componentry, reduces space requirements, and increases reliability due to reduced plumbing and fittings.

5) Fixed outer dimensional form-factor (550 mm x 400 mm x 200 mm, 44 Liter)

6) Integrated reformer and burner assembly (ReforWER).

7) Two 30-Cell stack assemblies in series electrical and parallel gas stream flow for packaging efficiency and reduced manifold losses. Dual stacks drive high degree of symmetry in manifold design to reduce bias in flow channels and stack flows.

8) Control and power electronics to be contained within the PSM space in the confines of the outer protective enclosure. Thermal management of the electronics must be done internal to the PSM boundaries.

4.1.2.1   Conceptual Design Review

Two initial concepts were generated given the system requirements outlined in Section 4.1.1 and the conceptual design requirements discussed above. The concepts are classified as the "T" and the "Square" based upon the general shape of the Hot-Zone-Module within the enclosure boundaries. These two concepts are detailed in Figure 4.1.2.1-A1 and 4.1.2.1-A2 contained in Appendix A.

4.1.3 Develop System Mechanization (schematic)

To support the conceptual design activity and meet the system requirements, the mechanization shown in Figure 4.1.3-A1 (Appendix A) has been created. This mechanization features several innovations that improve potential system performance and system packaging. The notable mechanization features are as follows:

1) **Integrated air/fuel preparation device, Non-Contact Vaporizer (NCV) and reformer start-up device (start-burner).**
   This integration allows for the elimination of a staged reformer strategy (micro-reformer transition to main reformer) and efficient packaging in the APU.

2) **Electrically heated catalyst (EHC)**
   Located at the APU exhaust, this device provides for low emissions during both cold start-up (electric power mode), and normal service.

3) **ReforWER with integrated air preheat function for NCV**
   A small heat exchanger is integrated into the ReforWER to provide air preheating for enhanced fuel vaporization quality in the NCV.

4) **Catalytic ReforWER combustor plates**
   The catalyst treatment on the combustor acts as a clean-up catalyst for low emissions and complete heat release in the ReforWER.

5) **Inlet air cooling circuit**
   The inlet air of the APU is used to cool the blower motor and motor driver, as well as the control and power electronics.

6) **Anode oxidation protection**
   Flow check valves and oxidation prone materials are used in the anode stream path to isolate and block oxygen from the SOFC anode during periods of APU inactivity.

7) **Elimination of high-temperature control valves.**
   Efforts have been made to eliminate the need for control valves in the HZM. This provides a benefit to control and actuation reliability in the system, as well as a reduction in system complexity.

8) **Anode recycle pump**
   This pump is optional in the mechanization, but it provides for an increase in reformer efficiency and system efficiency. Other benefits include reduced carbon formation in the reformer due to higher O:C ratios.

9) **Exhaust stream stack overwash**
   This improves stack warm-up performance as well as cooling of stacks during operation.

10) **Reformate cooling heat exchanger**
   Hot reformate from the outlet of the reformer exchanges heat with cathode air stream before reaching the stacks. Advantages include preconditioning of reformate to reduce thermal shock to stacks and reduction of preheat

requirement on cathode air. This allows for lower-effectiveness heat exchangers to be used which may have reduced size and pressure drop.

11) Auxiliary burner cooling air circuit.
This feature allows for the modulation of cathode air during warm–up to achieve high preheat temperatures without reducing system fuel flow. This improves heat exchanger function, and heat up performance.

4.1.4 Establish System Thermal Insulation Requirements

Due to the high operating temperature of SOFC, thermal insulation is of special importance. This is even more the case when the space available for insulation is reduced, as in the automotive SOFC APU. Additionally, issues of serviceability, ease of assembly and structural integrity must be considered in this application. Figure 4.1.4-1 shows the two main concepts for APU insulation. Each has apparent advantages and disadvantages as referenced in the figure

The top-loading shell concept is very convenient for development work for its accessibility and flexible geometry. It is the current design path for development APU activity. The package size constraint plays a large role in the choice of insulation technology. There is a large selection of commercial materials with alumina and silica fibers or grains that have the capability to insulate a solid oxide fuel cell system.

Top-Loading Insulation Shell
•Conventional high-performance insulation only
•Very flexible geometry and pass-throughs
•Convenient HZM access and servicability

Front-Loading Insulation Shell
•Conventional or evacuated high-performance insulation (higher performance)
•Less flexible geometry and pass-throughs
•Less convenient HZM access and servicability
•Potential for improved crash containment

Figure 4.1.4-1: Modular Thermal Insulation Concepts

Required Performance for SOFC Insulation
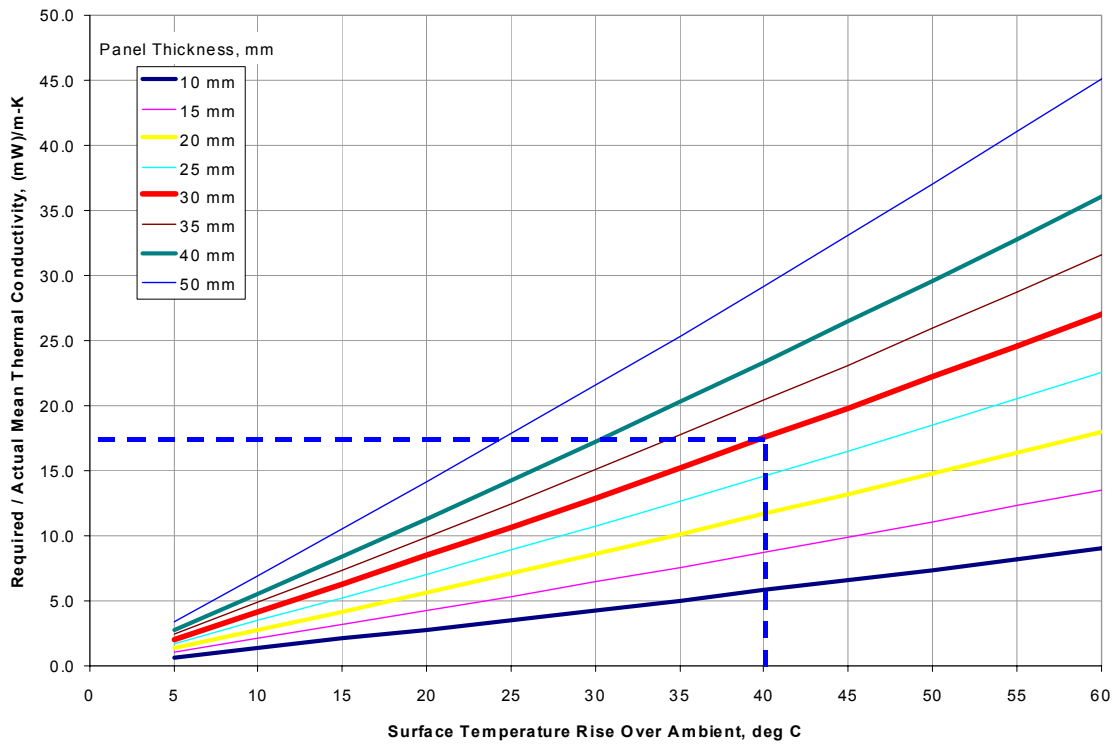
Figure 4.1.4-2: Required Thermal Conductivity of SOFC Insulation

Insulation Material Thermal Conductivity
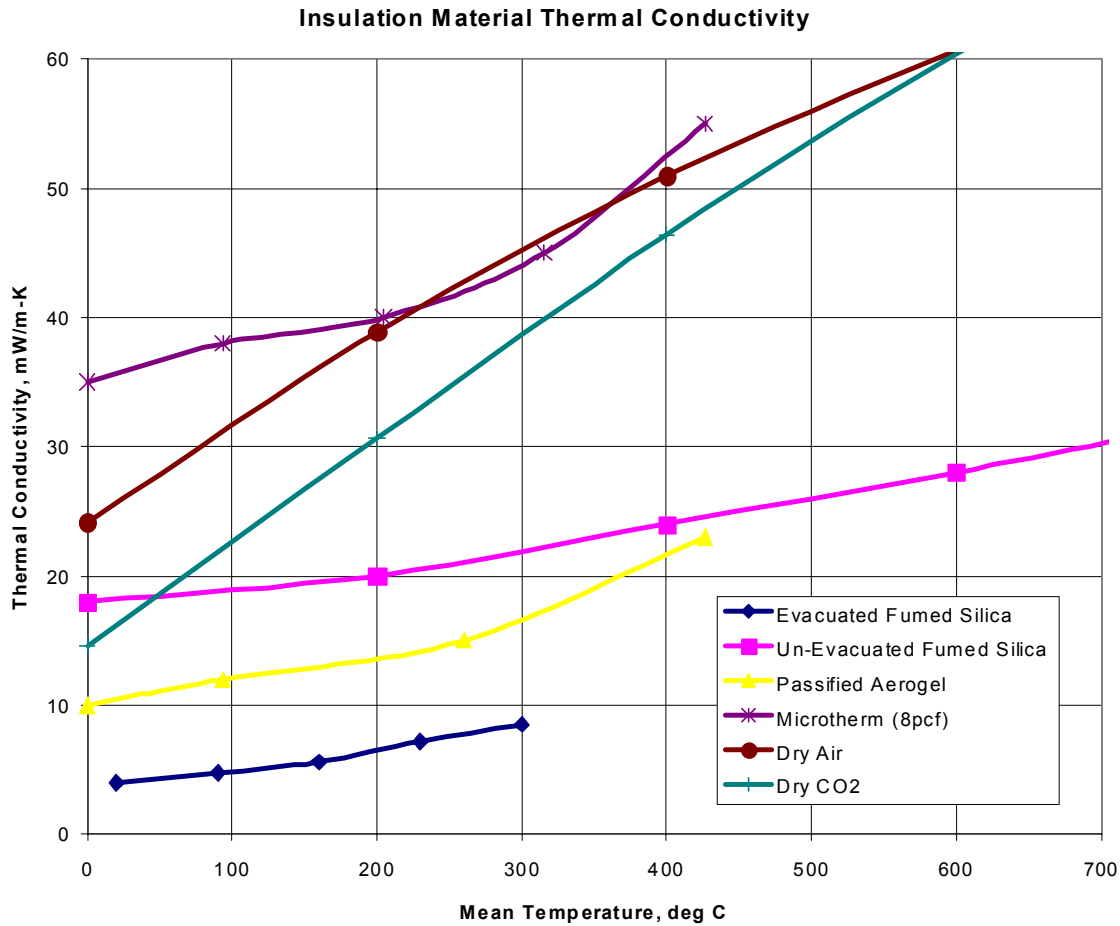
Figure 4.1.4-3: Typical Insulation Thermal Conductivity

Obviously, for the same temperature rating, lower performing insulation may be used if thick thermal barriers can be tolerated in the design. With the automotive APU, and the aggressive target volumetric power density, thick thermal barriers cannot be used, and the choice of thermal insulation is narrowed.

Figure 4.1.4-2 illustrates the required thermal conductivity of insulation material as a function of exterior surface temperature rise and panel thickness. For the near term requirement of no more than a 40 ºC rise over ambient temperature of the insulation surface, and a space budget limitation of 30 mm for insulation thickness, a target mean thermal conductivity is shown in the figure to be 17.5 (mW)/mK. This is the target that applies to a panel with mean temperature of 400 ºC assuming a linear temperature distribution.

Figure 4.1.4-3` indicates typical thermal conductivity values for several tyes of high performance insulation as well as some dry air and CO_2 for reference.

From the figure, it is clear that there are very few choices available for this challenging insulation application. The clear choice for the application is evacuated fumed-silica insulation panels. Unfortunately, these panels require moderate vacuum containment, which is a challenge in high temperature applications, especially with the long service life expectations of the APU. Typically, vacuum insulation is found in cryogenic applications where polymer or thin metal foil bags contain the vacuum adequately for the application. In the SOFC system, these materials will not hold up at temperature and cannot be used. What is required are sheet metal barrier constructions of sufficient thickness, material and design to be robust to the vacuum requirements in service. This places additional constraints on available insulation feature geometry such as pass-throughs and vias, welded joints and high stress concentration areas. For the automotive APU, initial development will allow for the use of non-evacuated insulation and the associated penalty in performance, but provisions are being made to adjust geometry and design to accommodate modular insulation shells that can be evacuated. An example of the performance benefits of vacuum insulation is shown in Figure 4.1.4-4. Note the low surface temperature rise for a panel only 25mm thick. With this performance, for a panel of 30 mm thickness, the predicted temperature rise is only 23 ºC over ambient and the APU should be able to achieve the required 12 hour cool-down thermal time constant assuming other losses to be minimized.

Measured Thermal Performance of Evacuated Fumed Silica Insulation
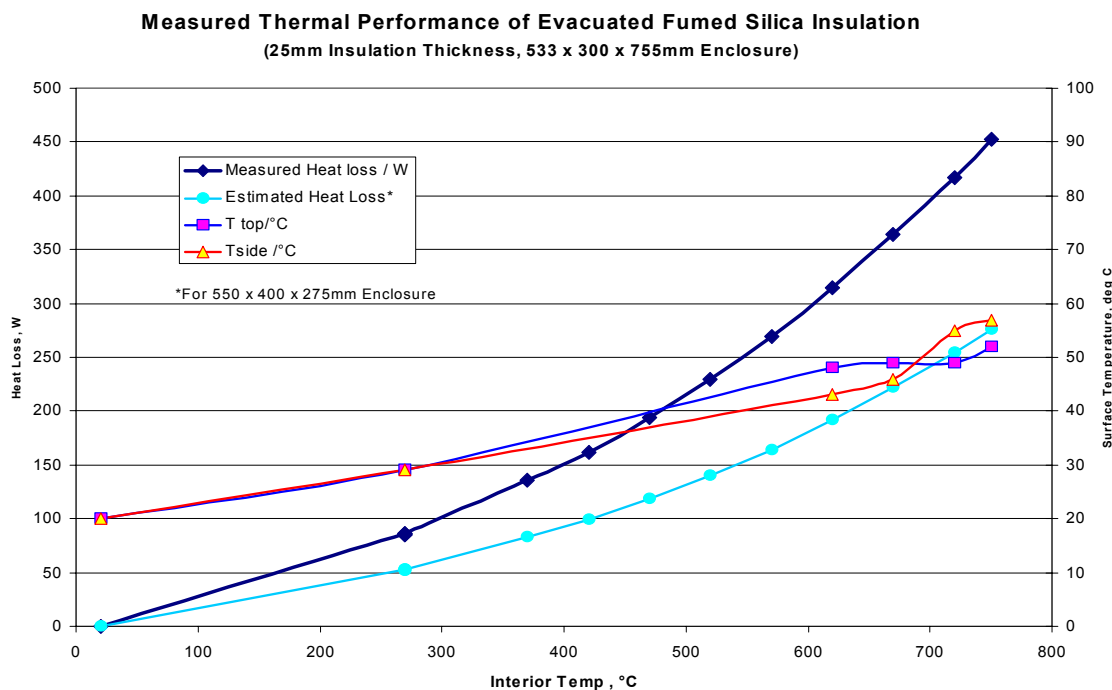**(25mm Insulation Thickness, 533 x 300 x 755mm Enclosure)**

Figure 4.1.4-4: Vacuum Insulation Performance

4.1.5 Provide System Design Support for the Fuel and Air Delivery Systems

The system mechanization detailed in section 1.2 calls for a single process air blower to source air to all of the individual circuit flows. Based upon modeling discussed in

Section 1.7, the blower requirements have been developed. The requirements for the process air blower are summarized in Table 4.1.5-1

Process Air Pump Requirements						
Maximum ambient temperature						
Operation	**85**	C				
Storage	**105**	C				
Elevation	**3600**	m				
Maximum inlet temperature	**45**	C				
Maximum head pressure	**15**	kPa	**148**	mbar	**2.2**	psi
Maximum capacity	**19**	g/sec	**1035**	L/min	**62**	m^3/h
			@45C		**37**	CFM
Noise Level	< **65**	dB(A)				
Mass (pump + motor)	< **5**	kg				
Adiabatic Air Power	**248**	W				
Target Overall Efficiency	> **50%**					
(Pump + Motor)						
Parasitic System Loss	< **496**	W				

Table 4.1.5-1: Process Air Blower Requirements

Typically, the process air blower is the largest power consumer within the powerplant boundaries. In the development of these requirements, particular attention was paid to high efficiency so that system parasitic electrical loads may be minimized and higher net system efficiencies may be obtained. Because of package size restrictions and high operating temperatures (low gas densities), pressure drop in the SOFC APU is a concern. For a 5kW net powerplant, the flow rates drive pressure requirements that exceed typical blower specifications. In the requirements specified in Table 4.1.5-1, the head pressure requirement is 5 to 10 times greater than what is typical for most applications; however, the flow rates are about 5 to 10 times less than typical. The SOFC APU blower requirements fall into an application "hole" where the requirements for pressure are too high for a blower, but not high enough for efficient operation of most compressors, and the flow rates are too high for most compressors while much lower than most blowers produce efficiently. While the application is atypical, and commercial choices are limited, there are two technologies that offer promise for the automotive APU. They are the positive-displacement compressor and the high speed radial blower. Performance curves for the two components currently under evaluation are shown in Figure 4.1.5-1 and Figure 4.1.5-2. Both units meet flow and pressure requirements and target efficiencies are possible with some design optimizations. In the powerplant,

additional considerations and evaluation criteria include reliability, noise output, attenuation potential, and of course, size, mass, and cost.

Performance of 3-Vane Air Compressor
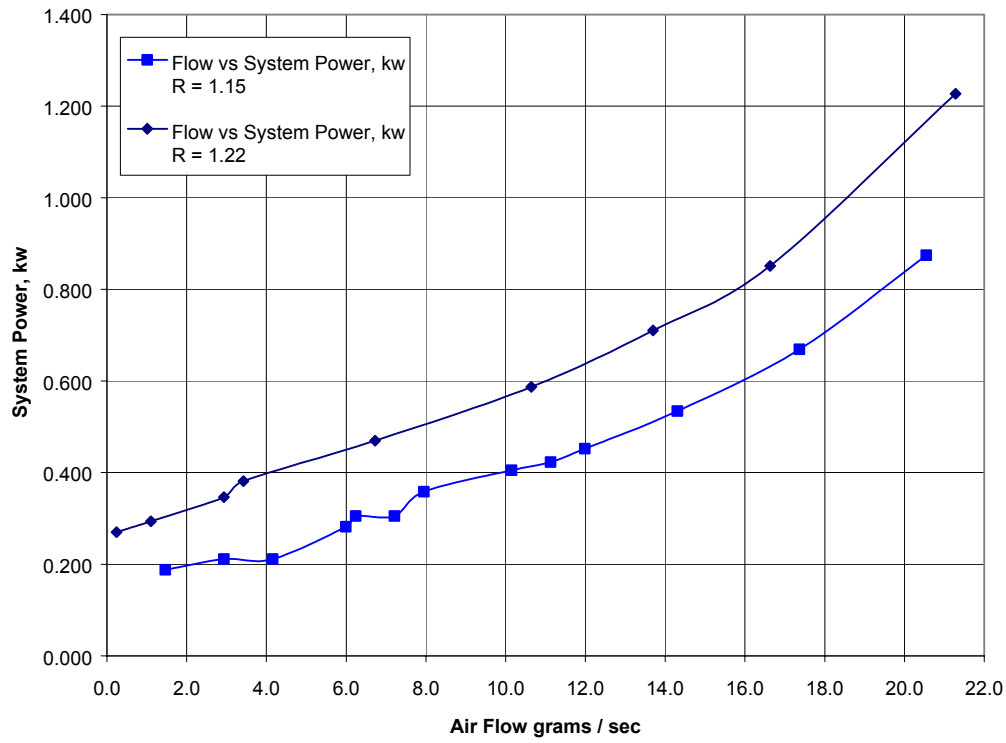
Figure 4.1.5-1: Performance of Positive-Displacement Compressor

Performance Map for High Speed Radial Blower
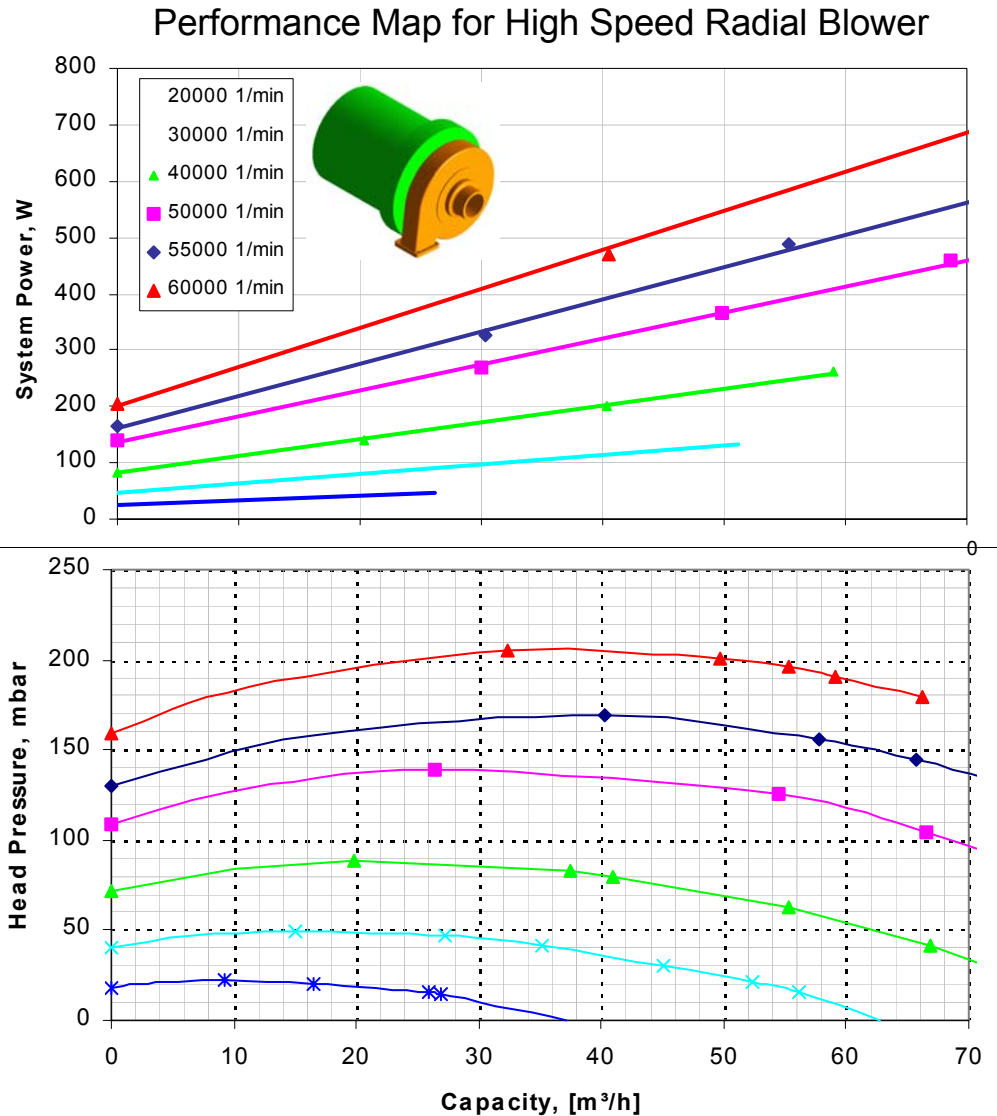
Figure 4.1.5-2: Performance of High Speed Radial Blower

While the blower provides the driving potential for flow through the system, in the system mechanization, it also must provide cooling air to temperature sensitive components in the PSM. Specifically, the inlet air is ducted through a circuit that provides cooling for the blower motor, blower motor electric driver, system controller, and power conditioning module. In addition, it also provides for air exchange in the PSM airspace so that heat loss from the HZM does not create a high temperature condition in the PSM. This circuit is described and illustrated in Figure 4.1.5.4-A1 (Appendix A).

4.1.6 Provide System Design Support for the Systems Control Development

For the SOFC APU much effort has been focused on the integration of system models and controls. Towards this end, a plant model with integrated controls has been developed to jointly support system analysis and concurrent control strategy development. Future phases of the project will feature hardware-in-the-loop controls development as well as plant model-in-the-loop test stand verification and subsystem optimization.

On this project, system plant modeling and controls development has been in the MATLAB/ Simulink^{TM} environment. A system plant model and prototype control strategy has been developed to support the system mechanization discussed in Section 4.1.2. A small section of this model is shown in Figure 4.1.6-1. The figure depicts the cathode air preheat (CHEX) subsystem consisting of controllers, and dynamic heat exchanger and valve models. The model has been used extensively to understand the complex system dynamics of the SOFC APU and develop control strategies. Additionally, model outputs have allowed for better requirements and sizing estimates for Balance Of Plant (BOP) components in the PSM and HZM (heat exchangers, valves and sensors).

The Simulink-based plant model has not been formally validated save agreement with basic hand-calculations and known relations. The Simulink-based plant model was developed as a collection of functional modules that were checked, where possible, against expected results. The Simulink model is a dynamic model that has both plant elements and control elements integrated into a functional simulation. It is inherently limited in that it is all based upon lumped parameter physical elements and estimated properties. The model handles heat and mass balance relationships only. Chemical equilibrium and kinetics are not currently implemented.

Of particular importance with respect to the system requirements is the start-up time of the system. Evaluations have been made using the model to understand control strategy and mechanization enhancements to improve start-up time performance. Some of the findings have proven to be both effective and also counter-intuitive. One example involves cathode air temperature and flow strategies during the warm-up phase. While maximum temperature gradient and maximum mass-flow are an obvious solution, it is not practical when heating a system with real devices and restrictions on capacity. For example, practical heat exchangers in this application are constrained by physical size and pressure drop considerations. Thermal effectiveness may be increased only so far until physical size and pressure drop are out of bounds for the system. For an effective system design, a good compromise, indeed a balance, must be found between competing objectives. With the help of the dynamic system model, an improved control strategy was developed to improve stack warm-up performance. Figure 4.1.6-A1 shows the optimal characteristic of cathode air delivery for maximal heating rate of the stack assembly. (Appendix A)
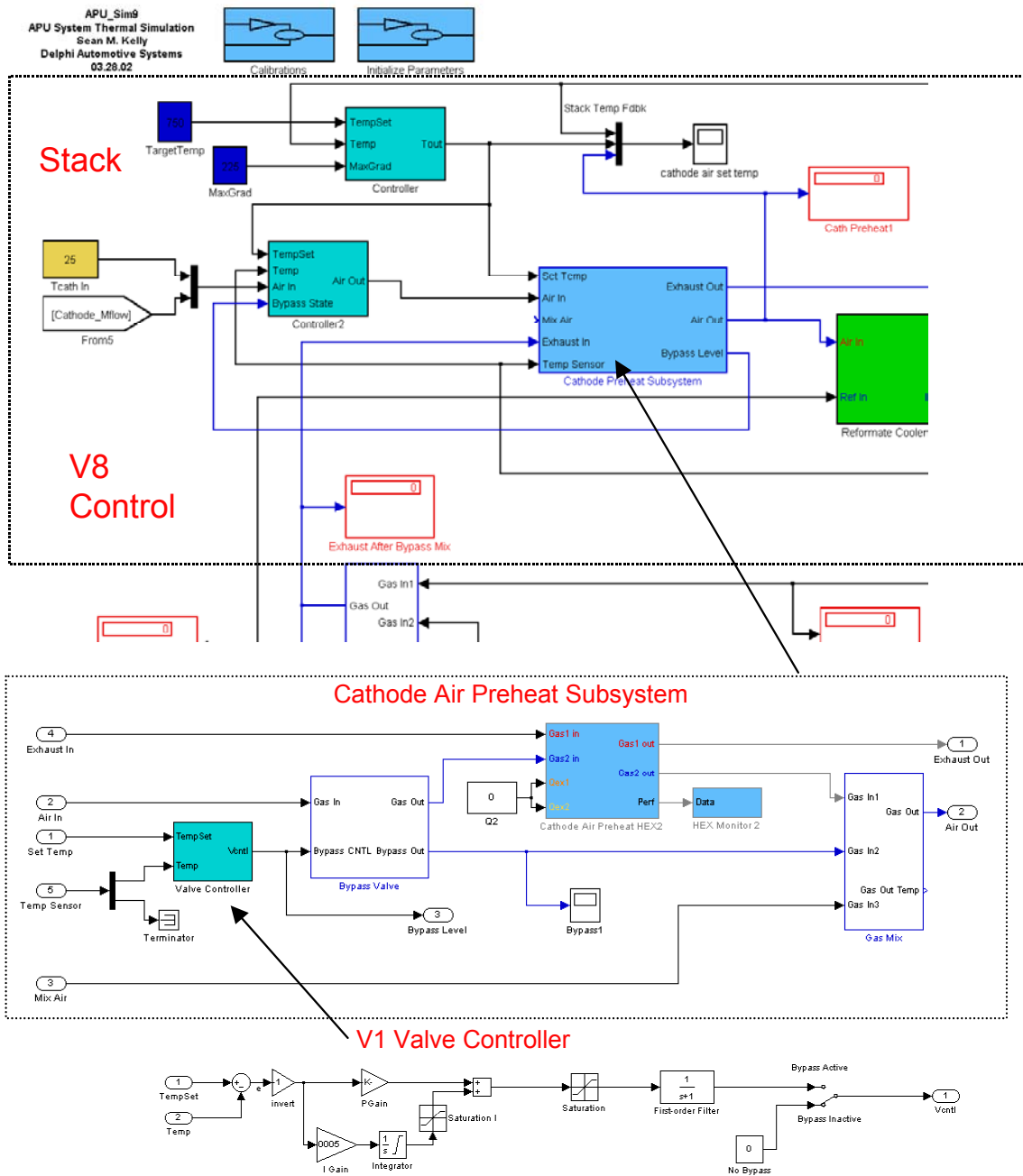
Figure 4.1.6-1: Simulink System/Control Model

4.1.7 Develop and Verify System Models

The system model discussed in section 4.1.6 has been used to run many simulations of the 5 kW APU. An example of the model results are shown in Figures 4.1.7-1 -- 4.1.7-5. The data describes a 5kW net output, gasoline SOFC APU undergoing a cold-start warm-up cycle followed by stepped APU electrical demand loads of 25 to 125 amps. Two cases are investigated. The first case is for straight POx reformer operation, and the second case features anode tail gas recycling.

In Figure 4.1.7-1 the basic warm-up cycle and subsequent stack temperature control may be observed. Note that the control system does a good job regulating the flow and temperature of cathode air to regulate the stack temperature at 750 ºC. Additionally, in this simulation, the operation temperature of 750 ºC was reached in 20 minutes.

In Figure 4.1.7-2, the overall temperature regulation of the burner and ReforWER, as well as the flow circuit mass-flows, may be observed. Of particular note is the fact that in POx mode, the reformer temperatures increase with increased fueling at high load, while with recycle, the challenge is to keep the reformer at the correct operation temperature. This is the expected behavior represented well dynamically in the system plant model. Note that the integrated control algorithms are regulating the plant parameters. This results in the transient response of flows and temperatures during step changes in electrical load.

In Figure 4.1.7-3, the reformer operational characteristics are described for the simulation period. As expected, anode recycle increases reformer O:C ratio and efficiency and consequently results in reduced gasoline fueling for a given electrical load point. This results in an increase in overall system conversion efficiency, as expected.

In Figure 4.1.7-4, the stack characteristics are shown for the simulation. The controls drive the stacks to a predicted 60% fuel utilization operating point. On step load changes, the step fuel flow rate adjustments are easily observed. While the loads and stack behavior are identical between the two cases, in the POx case, system efficiency drops with increasing load due to reductions of stack efficiency. On the other hand, the introduction of anode recycle produces relatively flat and improved system efficiency throughout the load profile.

Lastly, in Figure 4.1.7-5, we may observe the response of the process air blower throughout the simulation. For the simulation, a constant manifold feed pressure has been assumed for simplicity. Clearly, the case with anode recycle has reduced system parasitic load throughout the load profile. This is partially due to the fact that at increased system efficiency, APU exhaust temperatures are reduced and less cathode airflow is needed to cool the stacks since the exhaust gas is allowed to externally cool the stacks. Another factor is that with the anode gas recycle, the reformer outlet temperature is lower which reduces the heat load on the stacks, hence less airflow is

required at higher electrical loads. This effect can be most clearly seen in Figure 4.1.7-1 where the heat transfer of various streams to the stack is displayed.

The plant model has allowed for the verification of fundamental assumptions about the response and control of the SOFC APU.

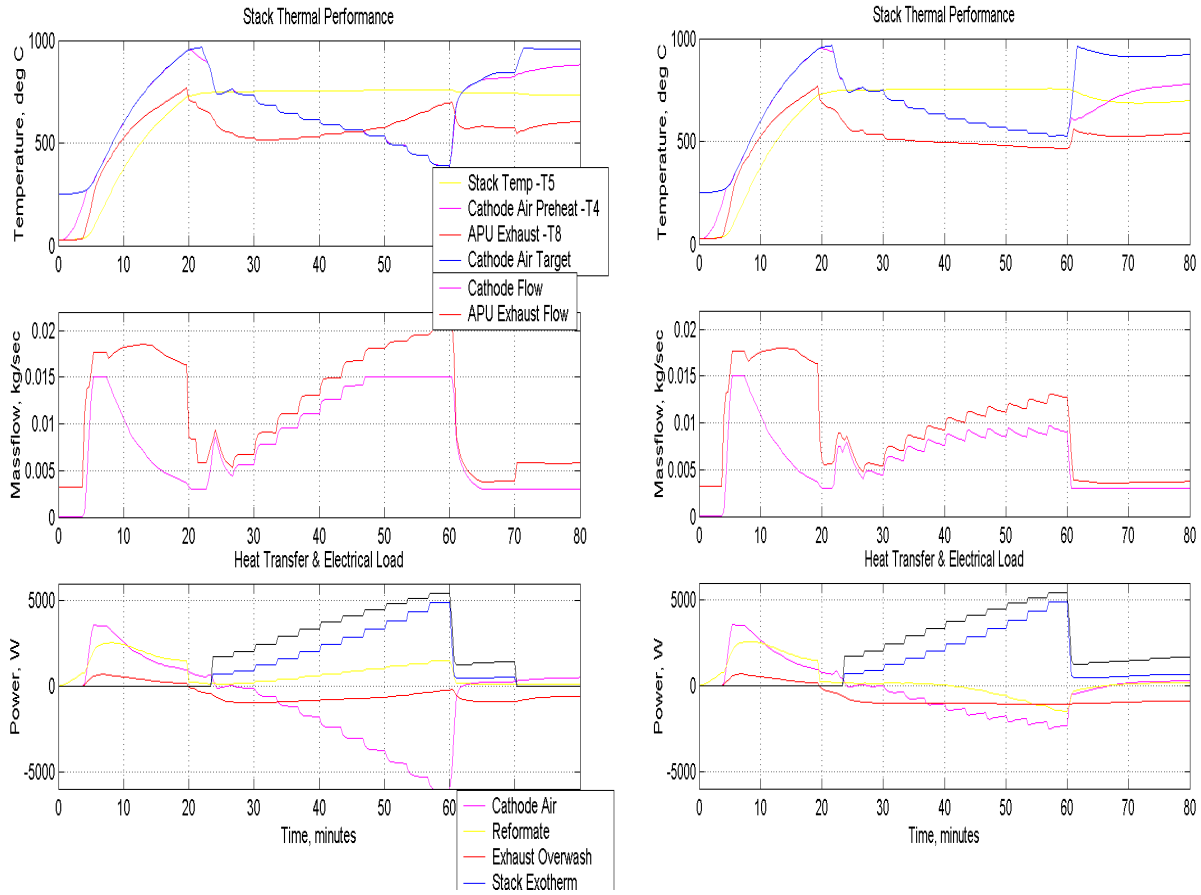

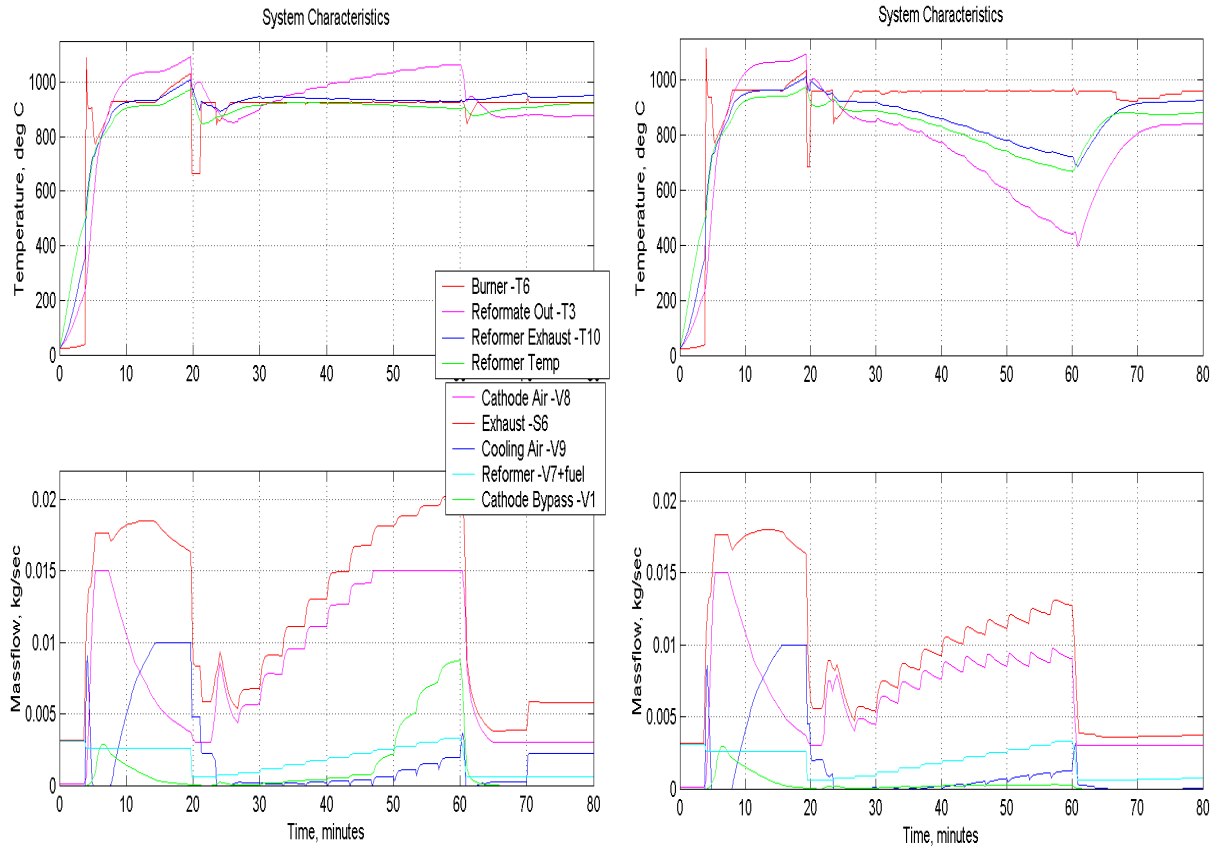**Figure 4.1.7-1: Overall System Performance Dynamic Simulation**
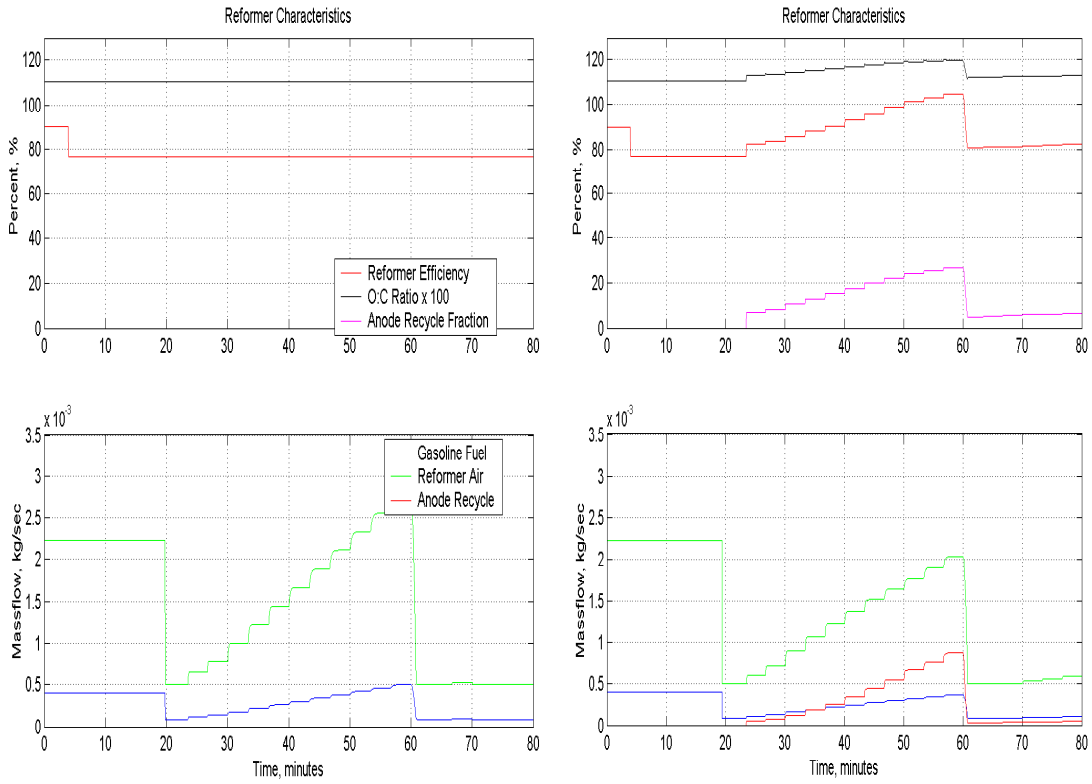
Figure 4.1.7-2: System Characteristics
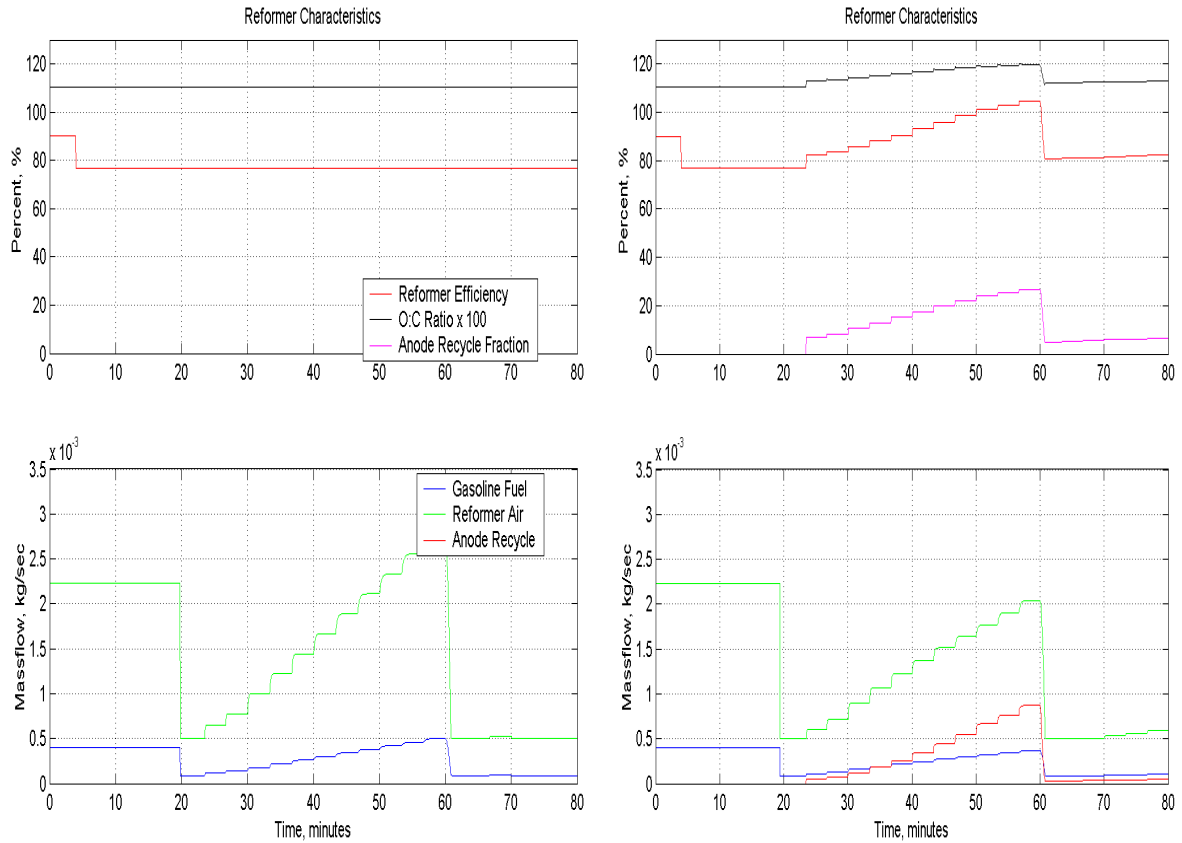
Figure 4.1.7-3: Reformer Characteristics

Figure 4.1.7-4: Stack Characteristics
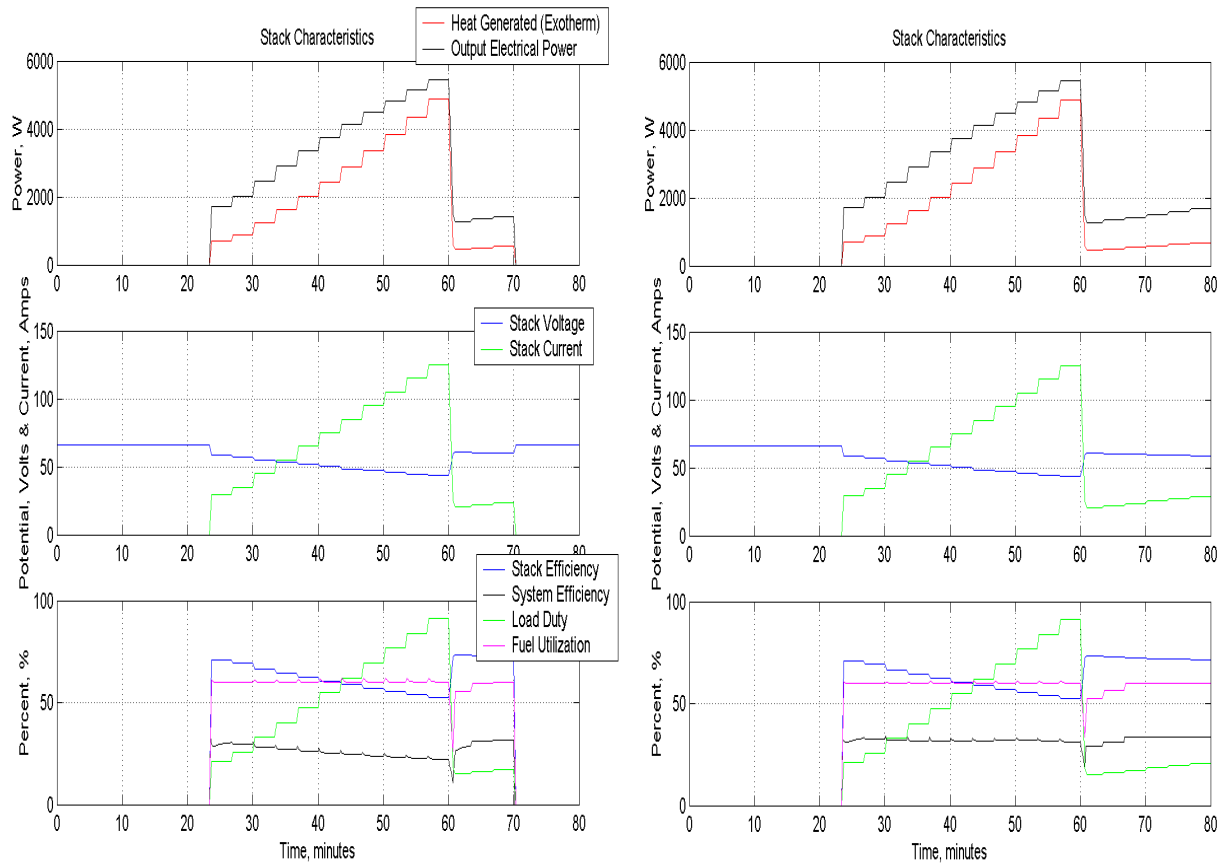
Figure 4.1.7-5: Blower Characteristics

4.1.8 Perform Design Optimization

Section 4.1.8 is addressed above in Sections 4.1.6 & 4.1.7.

4.1.9 Perform System Integration

In the conceptual design phase, one of the requirements was to fix the target volumetric power density of the concept to that appropriate for an automotive SOFC APU. Working within the fixed package size has been an extremely challenging engineering task; however, one that has produced many innovations in both system mechanization and concept. The integration of the subsystems into the APU product was undertaken in a engineering evaluation mock-up. The mock-up is shown in Figure 4.1.9-1. While executed mainly as a packaging verification exercise, many functional parts were used. The subsystems, now in various stages of development, have been guided by the integrated product requirements.
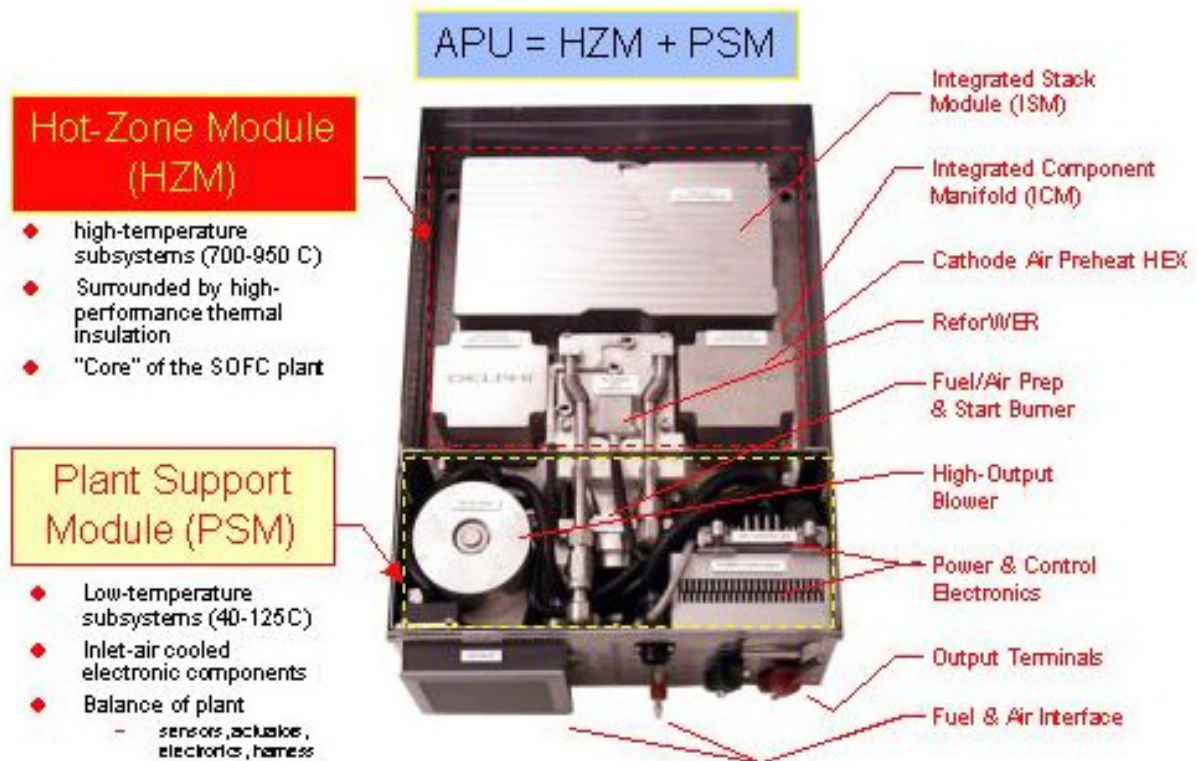
Figure 4.1.9-1: APU System Integration (Engineering Mock-Up)

The emphasis on the end-product form factor has produced a workable concept with realizable performance in a much smaller size than would normally have been attempted. Figure 4.1.9-2 shows an early SOFC APU proof-of-concept, and for comparison, the current design. The current design has a higher power output, more internal content, and a much smaller size and mass than its predecessor.

Figure 4.1.9-2: APU System Integration Progress

4.1.10   Prepare Detailed System Cost Estimate

Progress on the preliminary cost report will be reported on in the next reporting periods.

4.2   SOFC Stack Development (Task 2.0)

This task focuses on the development, fabrication, and demonstration of SOFC stacks. The work scope includes all necessary design and development except for that

pertaining to the electrical connectors used to draw the electrical energy from the stack to the outside load and to the frame and external shell for the stack. These activities are being conducted under Delphi's private funding and will only be reported to the extent to support major task accomplishments. Progress to date under the major subtasks for Task 2 include:

4.2.1 Design Stack

The Delphi-Battelle Generation 2 stack has been designed with anode supported cells, metallic interconnects and optimized manifolding to try to meet the stringent requirements of the transportation industry (Table 4.2.1-1). One of the key features of this design is a robust cassette configuration as the repeating unit of the stack. The cassette involves a cell to cassette (ceramic to metal) bond that is pre-fabricated before the cassettes are assembled into a stack. (See Figure 4.2.1-1).
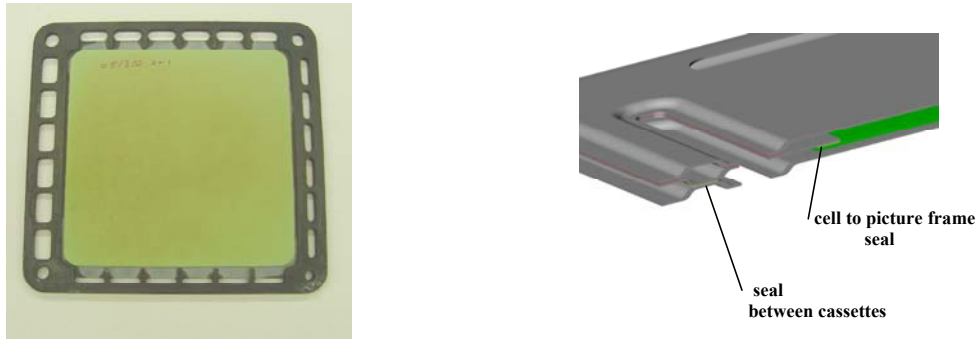

Figure 4.2.1-1: Generation 2 Stack Cassette Configuration

Currently, extensive testing of stack components and assembled stacks is in progress to further optimize the design. Two 30-cell stack modules constitute the stack sub-system in the APU operating at 42V (nominal).

Stack	Targets
Power	6 kW
Fuel	Gasoline based partial oxidation reformate
Durability (continuous)	5000 - 10000 hrs
Durability (thermal cycles)	> 5000
Fuel utilization	> 60%
Start up time	< 20 minutes
Weight	< 4 kg/kW
Volume	1 L/kW

Table 4.2.1-1: Stack Requirements for APU

The stack design has evolved in the last six months (Jan-June, 2002) based on analysis and testing that has provided valuable data for concept evaluation. Multiple concepts have been considered for each individual sub-component of the stack. Some of them are listed below in Table 4.2.1-2.

| SOFC Cells	Seals	Interconnect Metallic	Loading Mechanism	Cell Support	Manifolds air/fuel
Square/ Rectangular	Compressive	Separator plate with Mesh	None (if bonded)	Picture frame	Rectangular chimney
Other shapes	Bonded • Glass • Brazing	Embossed Features	Load frame with compliant member	Edge Cell	Multi holes chimney
		Etched features	Load frame without compliant member		Open Manifolds

Table 4.2.1-2: Design Features Under Consideration for Stack

Based on our assessments and allocated resources, the stack design was chosen to allow for the flexibility to analyze and test the key concepts.

In the following sections we will discuss some of the efforts in the development and testing of the components of the stack as well as the results from testing on stacks.

4.2.2 Model Stack Under Steady-State Conditions

By the beginning of this project, the SECA Core Technology program had developed a Computational Fluid Dynamics (CFD) code that incorporates a stack electrochemistry module. The code is able to predict the temperature distribution within a stack operating under steady-state conditions. These calculations were performed for two stack design configurations, both of which are cross-flow arrangements, in which the flow direction of cathode/cooling air is orthogonal to the flow direction of the anode fuel gas. Figure 4.2.2-1 shows typical steady state electrochemistry results for these designs. Each exhibits a hot spot in the lower right quadrant, which is caused by the presence of fresh, electrochemically active fuel on the anode juxtaposed to air on the cathode side that has already been warmed by flowing over the upper right quadrant. The total temperature difference is near 275 °C for the thin interconnect design, whereas it is about 200 °C for the thicker interconnect design.
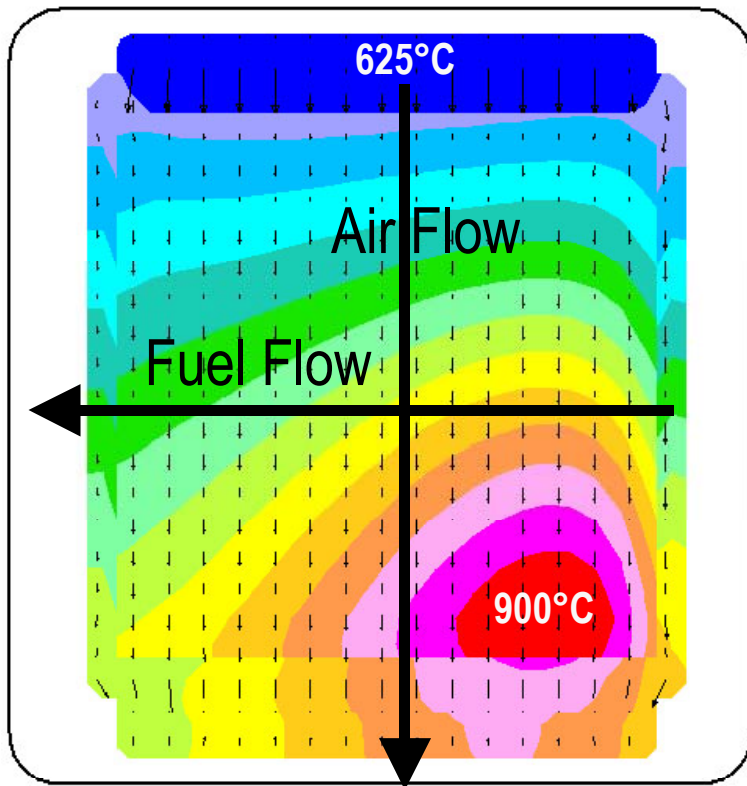
Gen 2 with thin
interconnect
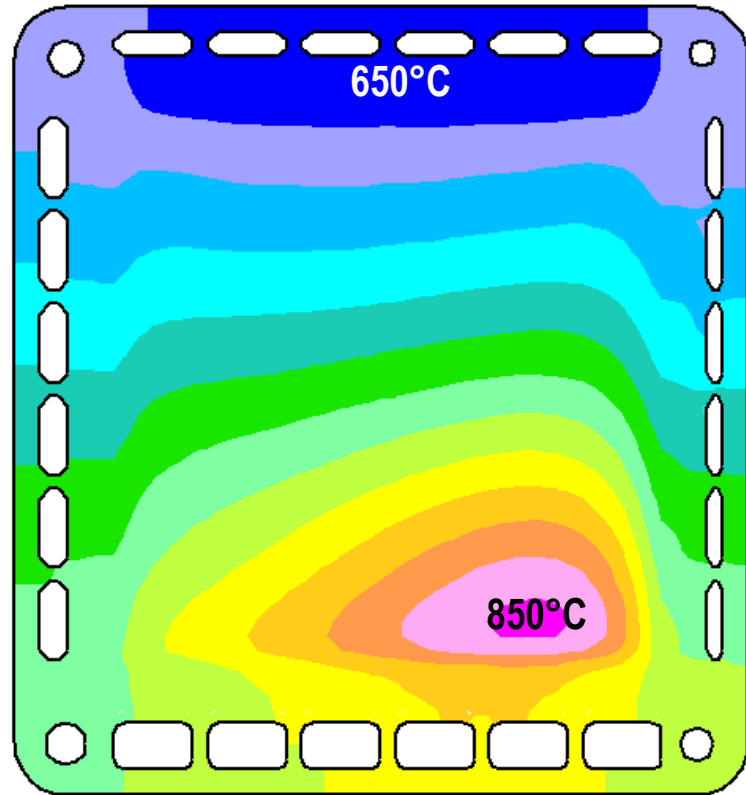
Gen 2 with thick
interconnect

Figure 4.2.2-1: CFD-Electrochemical Model Results Of The Gen 2 Design

4.2.3 Model Stack Under Transient Conditions

Modeling has also been performed to simulate the temperature stress distributions generated during heating of various stack designs. Most of the stack heating is accomplished by blowing hot air through the cathode passages, although hot reformate is also assumed to be circulated through the anode passages. Figure 4.2.3-1 shows transient modeling results for the thin interconnect design. At the left are the CFD model results showing temperature distribution on an anode within the stack at about 23 minutes into the heating cycle, just as the leading edge of the cell has reached 700 °C. The trailing corners are still near 450 °C. This is the moment when maximum stress occurs. As seen in the stress distribution at right, the maximum stress within the anode is 55 MPa.
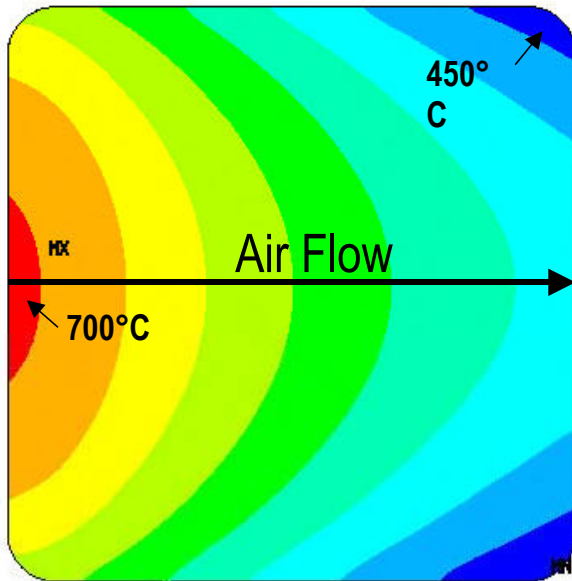
Temperature Distribution
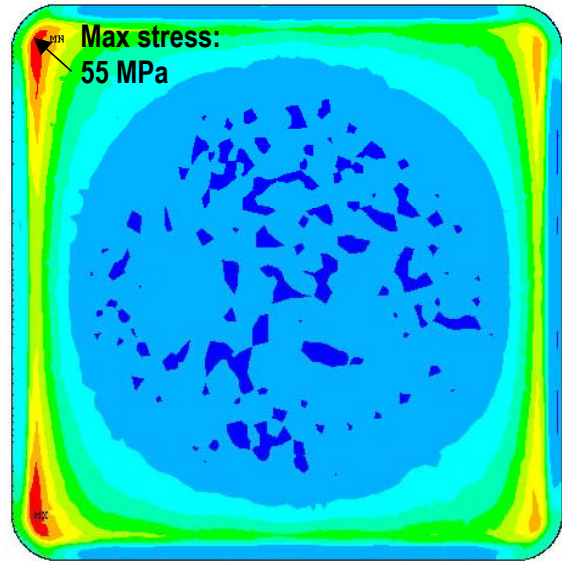
Stress Distribution

Figure 4.2.3-1: CFD Model Results For The Thin Interconnect Design

4.2.4 Develop High-Performance Cathode

A SEM micrograph of a typical cell cross section is shown in Figure 4.2.4-1A in Appendix A. A five micron ceria barrier layer is screen printed and sintered to the electrolyte, followed by screen printing and sintering of the $(LaSr)FeO_3$ (LSF) cathode. At the outset of this project, one inch diameter button cells with LSF based cathodes had exhibited power densities exceeding 0.6 W/cm^2 at 750 ºC, running on 50% hydrogen at 20% fuel utilization. However, these high levels of performance had not yet been attained in larger stack tests. Also, a high degree of variability in cathode performance had been found in nominally identical cells. In addition, cell performance usually increased to a stable level over two to several days of "burn-in". The objectives of this subtask are to:

- Understand the sensitivity of doped lanthanum ferrite to compositional, structural, and micro structural variables to increase reliability of cathode performance.
- Understand the burn-in process affecting cathode performance.
- Develop reliable, high performance cathode powder with a commercial powder vendor.
- Investigate alternate cathode materials to achieve desired power density and lifetime requirements.

Several cathode evaluation tests were performed on the intermediate-scale, single cell test stand. These cells have approximately 30 cm^2 active area. The commercially produced LSF cathode powder from one of the two vendors was found to have acceptable electrochemical activity in intermediate scale cell testing. Reliable commercial supply will require close interaction with the vendor to assure quality.

It was found that there is a trade-off between ceria barrier layer adherence and the subsequent performance of cells. Decreasing the sintering temperature of the ceria layer by 50 °C resulted in about a 40% increase in power density. SEM Micrograph discussion and graphics (4.2.4-A2) are contained in Appendix A.

4.2.5 Develop High-Performance Anode.

Bi-layer Development
In the micrograph shown in Figure 4.2.4-A2 (Appendix A), the three co-sintered layers, including the structural anode, the active anode and the electrolyte can be seen. (The term, "bilayer" refers to the anode/electrolyte composite, considering the anode as one effective layer.) Although the image is truncated, the structural anode is typically 550 microns thick Nickel oxide.

At the outset of this project, both intermediate and full size bi-layers were being produced in limited quantities. However, bi-layers were warped, requiring a separate creep flattening procedure before cathode application. The process time for sintering and creep flattening was 72 hours. Creep flattened bi-layers had residual camber and relatively low strength. The objectives of this subtask are to:
- Decrease residual camber from electrolyte/anode TEC mismatch and increase the strength of the bi-layer.
- Determine the strength-porosity relationship for the current anode formulation.
- Decrease processing cycle times and improve yield.

Characterization was performed, which established the room temperature biaxial flexure strength of baseline anode disks as 240 MPa. This is for the as-sintered

(NiO-containing) anodes. The-reduced (Ni metal containing) anodes had room temperature strength of 147 MPa, 8% std.dev., weibull 15.7.

Further process development during sintering of the bi-layers resulted in eliminating the separate creep flattening process. The resulting moderate camber, shown in Figure 4.2.5.-1, is due to the remaining slight thermal expansion mismatch between the electrolyte and the anode. Efforts were initiated to partially substitute a lower thermal expansion materials for part of the YSZ in the anode.
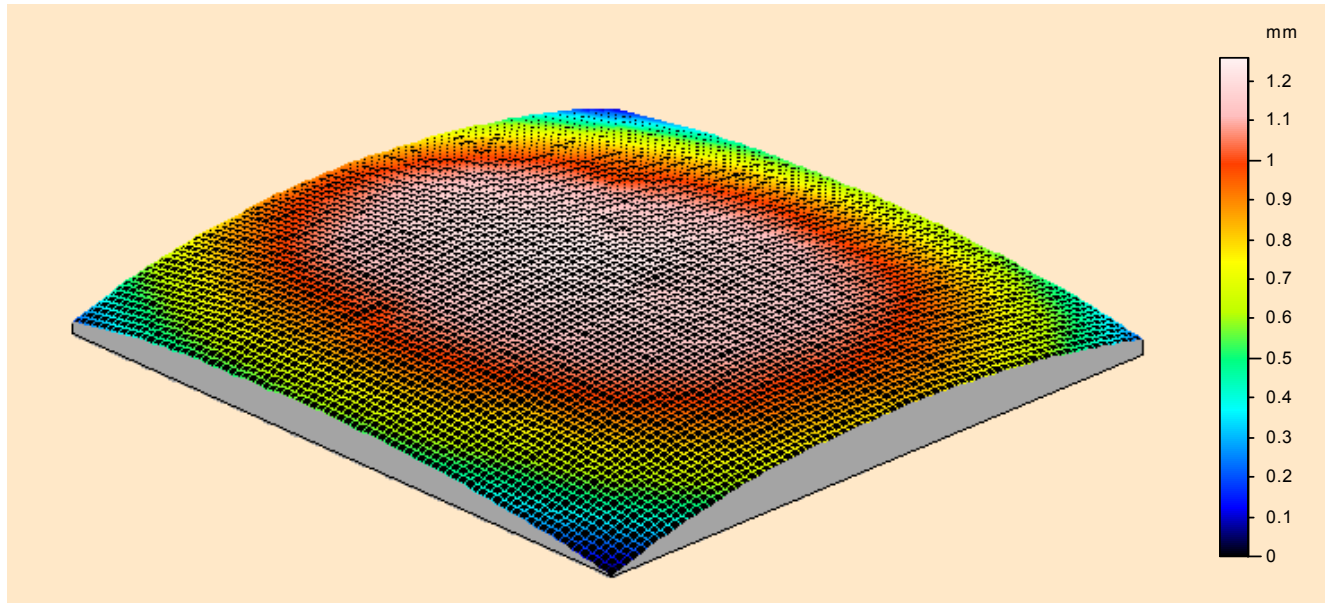

Figure 4.2.5-1: Laser Profilometry Of As-Sintered Bilayer

4.2.6 Develop Cell Fabrication Techniques – Is covered in Section 4.2.5.

4.2.7 Develop Separator and Support Components.

Ferritic steel was chosen as the material of choice for initial separator plate development. It was discovered that glass seal strengths could be greatly improved by altering the sealing surface of the metal. A series of metal coating techniques were developed and tested. The most successful of these involves applying a slurry coating to the metal, followed by firing at near 1000 °C. Metal components often require creep flattening after the coating step. Seal rupture pressure results for metals coated by this technique are included in Figure 4.2.10.3-9. In the case of the glass seal, application of the coating to metal A increases the rupture pressure by a factor of six.

4.2.8 Develop Gas Distribution Meshes

Two key components of the interconnect train are the anode and cathode gas distribution meshes. These structures reside within the gas distribution channels between the separator plate and the requisite electrode. They must allow access of fuel gas or air to the electrodes and, as well, must provide a low resistance pathway for

electrical conduction. In particular, the development of the cathode mesh is challenging because it must survive at operating temperature in an oxidizing atmosphere. Several mesh design concepts are under consideration. Currently, the lead concept for the cathode side is termed the "feather" design. Figure 4.2.8-1 shows pressure drop data for the cathode gas distribution "feather" mesh design. The first plot shows pressure drop as a function of air flow rate for five flow channel heights with mesh "feathers" oriented parallel to the air flow direction. The second plot shows pressure drop as a function of flow channel height for one flow rate, 14 liters per minute, with mesh "feathers" oriented either parallel or perpendicular to the air flow direction.
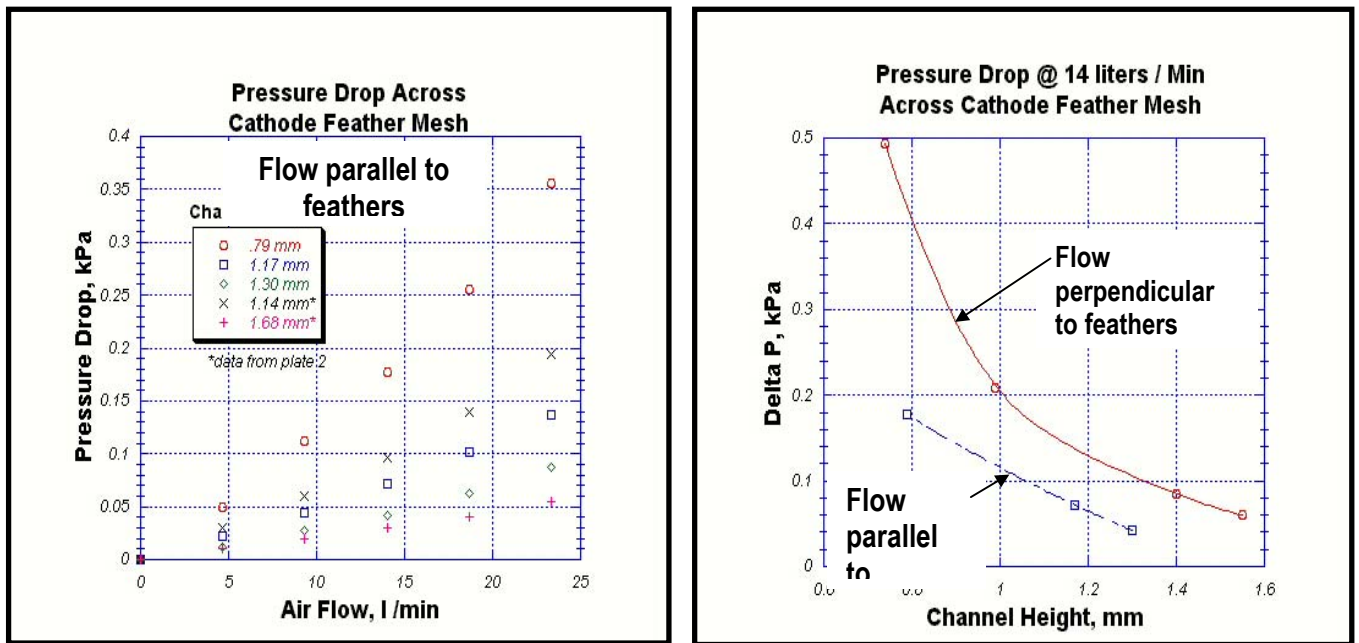

Figure 4.2.8-1: Pressure Drop Data For Cathode "Feather" Mesh Design

4.2.9 Develop Mesh/Electrode Interface Materials

At the beginning of this project, stack testing was being performed exclusively with platinum interconnect components on the cathode side. Platinum mesh was welded to the stainless steel interconnect plate. The Pt mesh contacted the LSF cathode through a Pt bonding paste and a Pt grid, which had been screen printed and then pre-sintered onto the cathode surface. Of course, while this set up provides excellent oxidation resistance, it is prohibitively expensive for commercial applications. The objective of this subtask is to develop a cost-effective interconnect train that provides minimal electrical resistance.

A characterization device was developed, the Interconnect Resistance Unit (IRU), that measures the resistance of the cathode interconnect pathway over time at temperature. A schematic of the IRU is shown in Figure 4.2.9-1. Current at a density of 0.5 A/cm^2 is run through a double cathode "sandwich" as the specimen is heated at stack operating temperature in air. Various material combinations and configurations for separator plate, mesh, bonding paste and current collector grid can be conveniently tested in the IRU. The Area Specific Resistance (ASR, ohm-cm2) is calculated as ½ the measured resistance multiplied by the surface area.
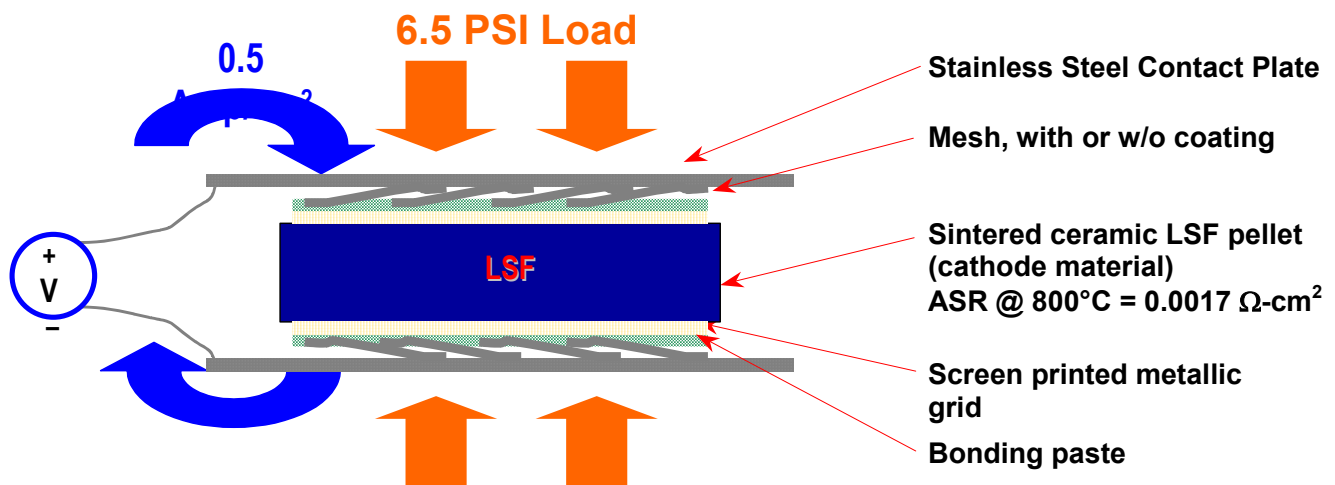

Figure 4.2.9-1: Interconnect Resistance Unit (IRU) Test Set-up

Further IRU discussions are contained in Appendix A including Figure 4.2.9-A1 to 4.2.9-A5.

4.2.10 Develop Glass and Glass-Ceramic Seals

At the beginning of this project, stack sealing was provided by a glass, "G18", which joins ferritic stainless to itself, or in the case of the cell-to-frame seal, to yttria stabilized zirconia. The G18 glass softens near 850 ºC as shown in Figure 4.2.10-1. The G18 glass has a coefficient of thermal expansion (CTE) of 11.7 x 10-6/ºC in the vitreous state. It undergoes de-vitrification with time at temperature, however, and eventually forms low CTE phases that may cause thermal expansion mismatch problems (likely to be apparent during thermal cycling). The G18 glass also reacts with Cr_2O_3 on chromia-forming steels, yielding a barium chromate phase that exhibits a significant CTE mismatch with the underlying substrate and initiates cracking along the metal/glass interface.

One of the objectives of this subtask is to conduct glass composition optimization studies focused on developing a glass ceramic with stable, matching CTE over thousands of hours at 750 °C.

Several candidate glass compositions were investigated. At the time of this reporting, the composition designated La7, had given the best long-term CTE results. The CTE for La7 remains stable over 168 hours at 850 °C.

A rupture strength test was developed to facilitate quantitative comparison of seal joint strengths. Figure 4.2.10-2 shows a photo of the test specimen and a schematic of the pressurizing fixture. The metal washer is clamped into the fixture and air pressure is increased until the seal breaks and the ceramic bi-layer disk pops off. Figure 4.2.10.3-9 shows several rupture strength results. The average rupture pressure for the bare ferritic stainless steel type "A" glass sealed to bi-layer disks was 10 psi. Several factors affect the seal rupture strength. Choice of metal alloy (A, B, C or D) can result in up to a factor of four difference in rupture pressure, for seals to the bare metal surface. Pre-oxidation of metal B resulted in a slight increase in seal strength. Other data in Figure 4.2.10-3 will be discussed in following sections.
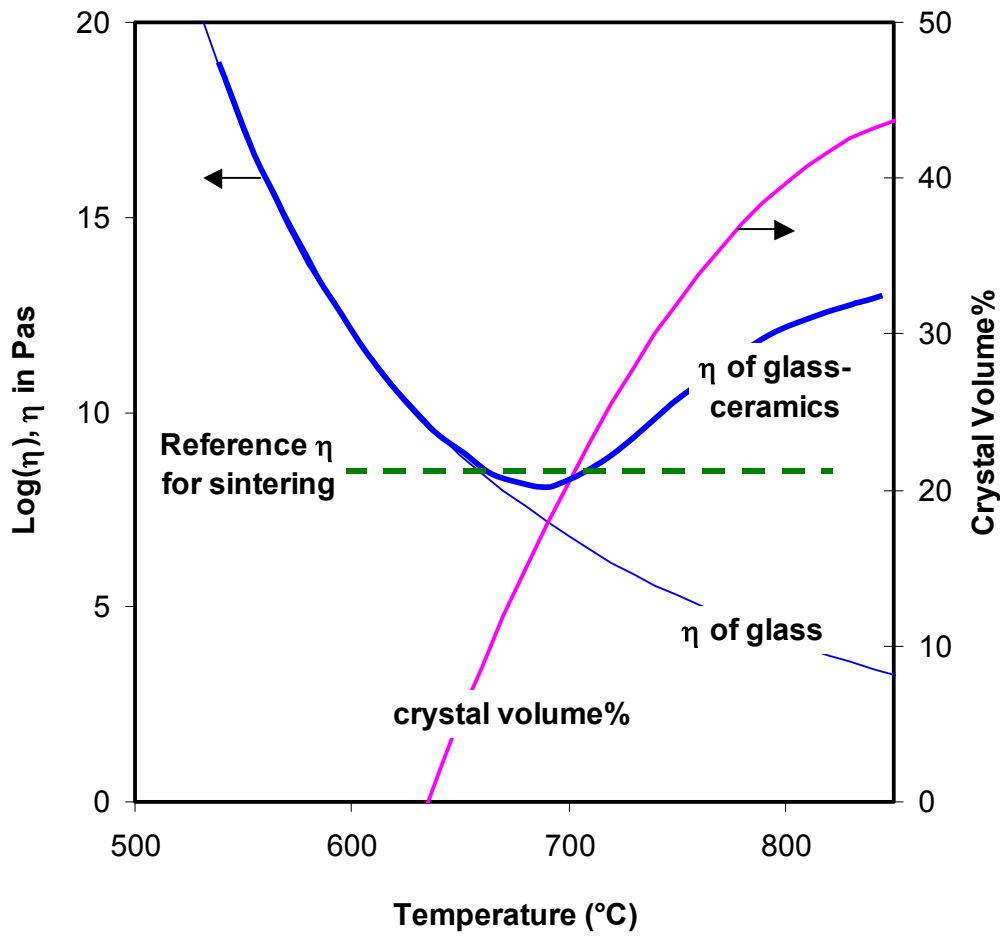
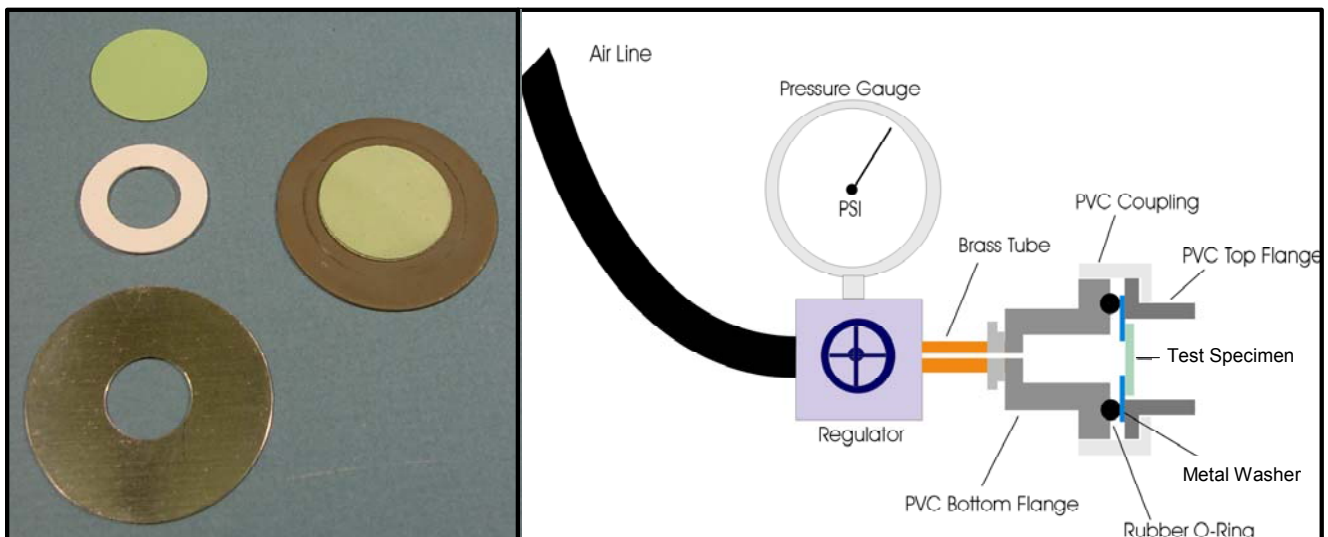**Figure 4.2.10-1: Sealing Glass Viscosity Schematic**

Figure 4.2.10-2: Seal Joint Rupture Strength Fixture and Test Specimen
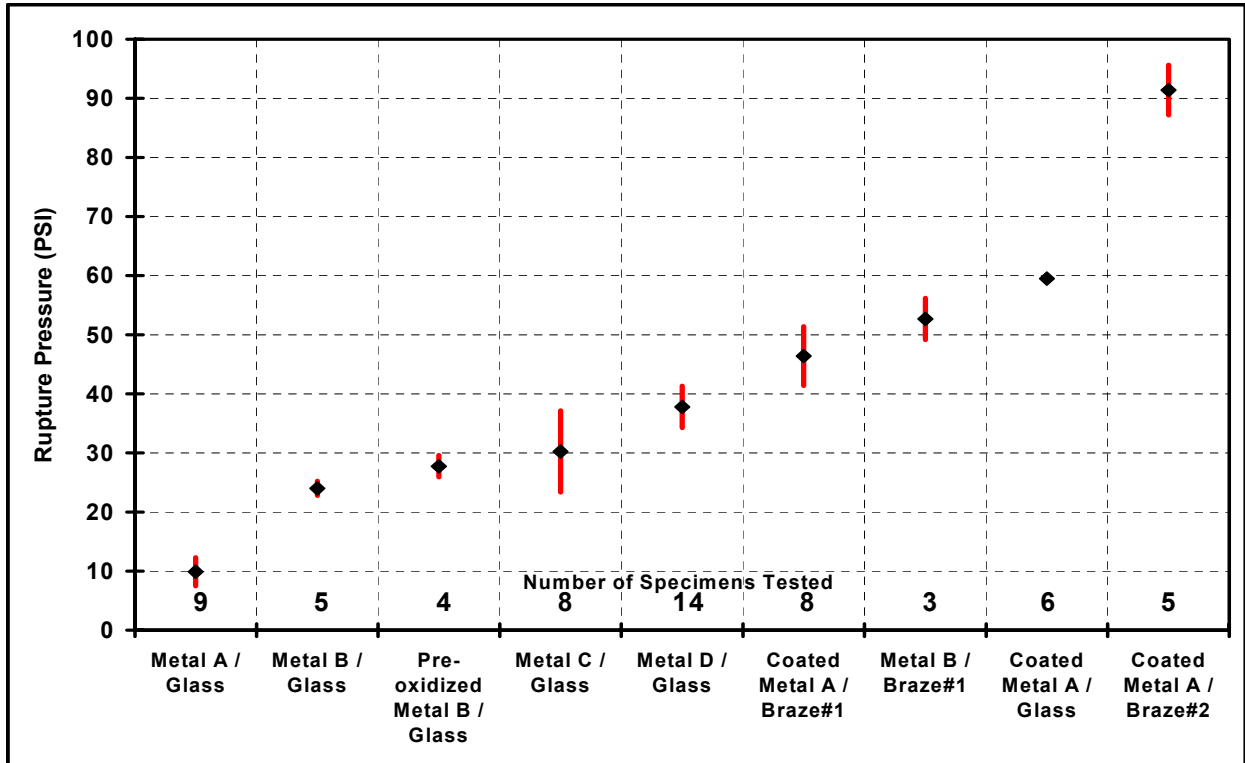
Figure 4.2.10-3: Seal Joint Rupture Strength Test Results

4.2.11   Develop Alternative Seals

A silver-based braze was developed, which appears to be a viable alternative to the glass seal. The braze hermetically sealed a full-scale (~12 cm x 12 cm) bi-layer to a ferritic stainless steel frame. Two braze compositions have been tested using the seal rupture strength method, discussed above. As shown in Figure 4.2.10-3, braze #1 gave average rupture strengths of 46 and 52 psi, on coated metal A and on metal B, respectively. Braze #2 on coated metal A gave an average rupture pressure of 91 psi.

4.2.12   Develop Gas Headers and Manifolds

Different concepts for loading the stack have been developed and are being analyzed and tested. For glass sealed stacks a minimal load is required after the stack is sealed. A metal based "spring" has been designed that can provide this load after the sealing of the stack. This concept is currently under evaluation. Manifolding of the stack has also been designed based on system requirements and ongoing CFD analysis as described earlier.

4.2.13   Fabricate and Test Developmental Stacks

Multiple stacks have been built and tested. The stack tests can be classified into two main categories:

- Stack tests with small active area cells

- Stack tests with full sized cells

Stack test with small active area cells: Multiple stacks have been tested with cells of 4cm X 4cm dimension and cells of 7cm X 7cm dimension. Extensive experience has been gained in the fabrication and testing of these stacks.

Test data from small (4 cm x 4 cm) single cell stack is shown in Figure 4.2.13-1. After stable power was achieved, the stack was maintained at this power for about three days. Some experiments were then undertaken to determine performance versus fuel utilization on concentrated hydrogen. Between 220 and 240 hours, the stack generated 0.4 W/cm^2 at 50% fuel utilization. At the end, the stack generated nearly 0.3 W/cm^2 at 74% utilization of hydrogen for 20 minutes.
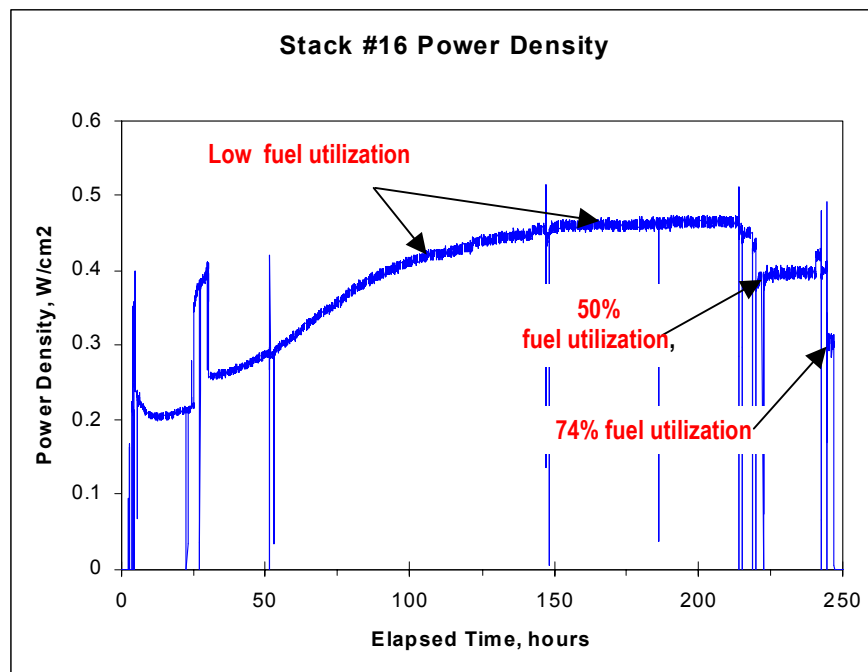
Figure 4.2.13-1: Stack Test (4 cm x 4 cm Cell)

Data from stack testing with 7cmx7cm cells is shown in Figure 4.2.13-2. Extensive testing of these intermediate sized cells have been carried out to understand and improve performance of the stack.
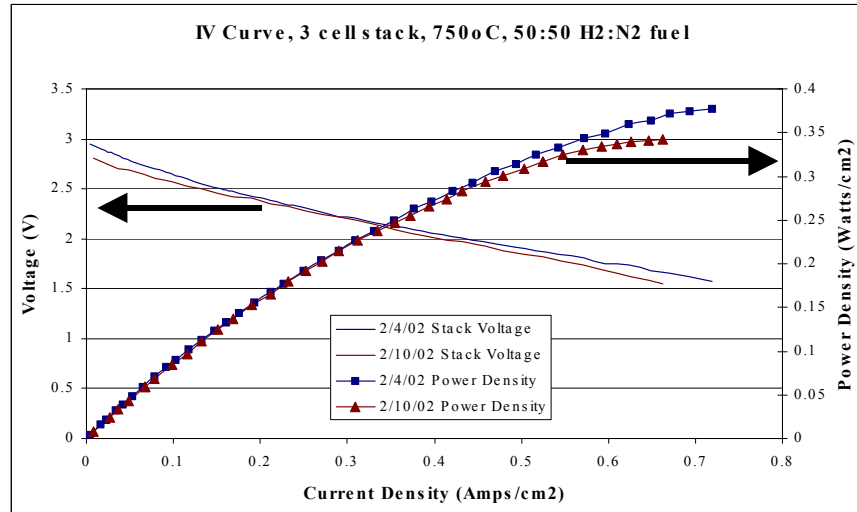
Figure 4.2.13-2: Cell Stack Test (7cm x 7cm Cell)

A 3-cell stack (with 7cm X 7cm cell) was run for 1000 hours on hydrogen at 0.7V/cell to evaluate durability. The degradation was less than 10% of its original electrochemical performance over this period of time. Most of this degradation was observed in the first 200 hours. (Figure 4.2.13-3).
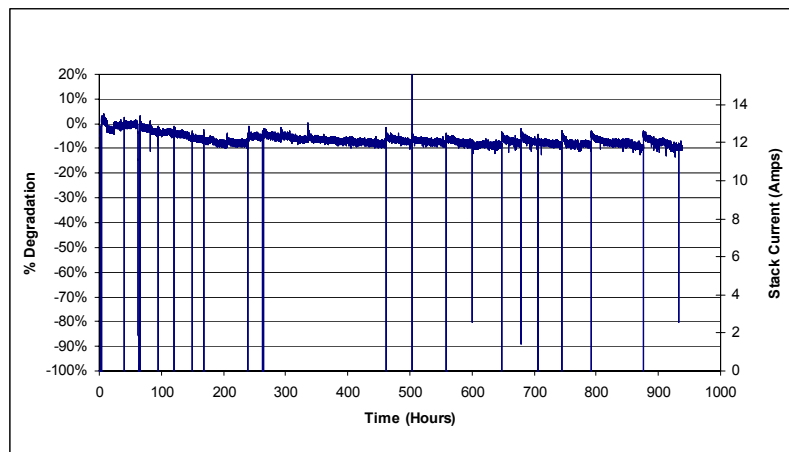
Figure 4.2.13-3: 1000 Hour Durability Test On 3-cell stack (with 7cm x 7 cm Cell)

Stack tests with full sized cells (12cmx12cm): Extensive experience has been gained in building stacks from full size cells. Multiple stacks with number ranging from 1-6 have been built and tested. Testing of full size (~12cm X 12 cm) 1-cell stacks have allowed us to validate and optimize the design. Figure 4.2.13-4 is an example of data obtained from a 1-cell stack test.

Test MG735C72 Polarization Curves
July 19, 2002 - Indec ASC1 Cell at 750C
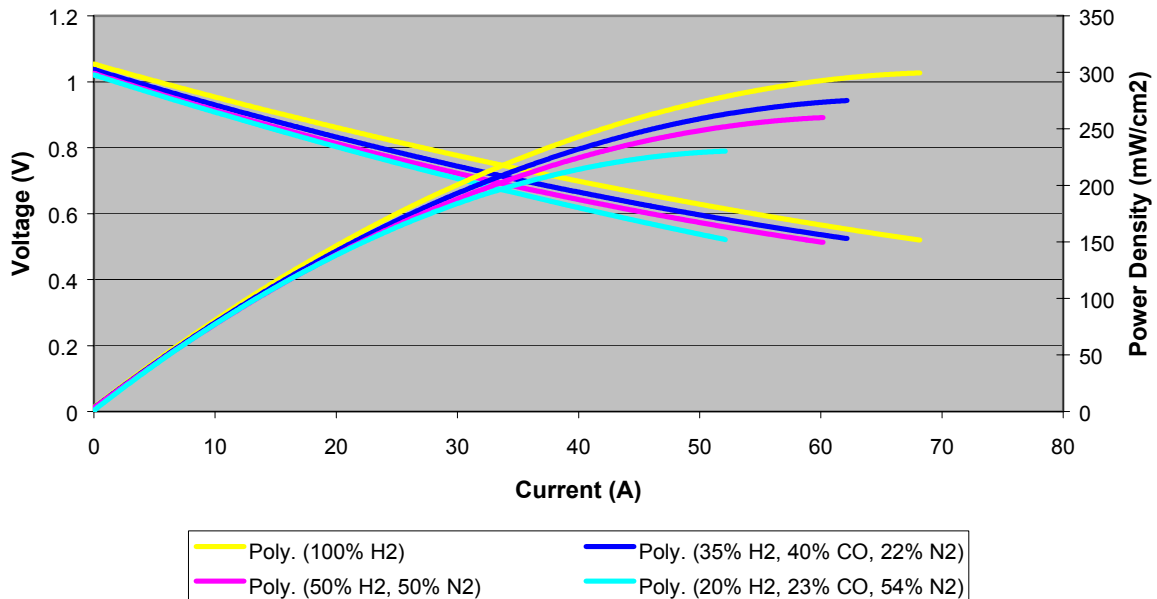
Figure 4.2.13-4: 1-Cell Stack Test (12 cm x 12 cm Cell)

Short stacks have also been built and tested. Data shown in the figure below is from a 6-cell stack using cells from a supplier. The stack was operated at 750 °C and a series of electrochemical tests was carried out to study the stack performance. Figure 4.2.13-5 shows the polarization curves for different compositions of reformate in the stack.

As expected, the 100% H_2 fuel performed the best, closely followed by the simulated reformate composition of 35% H_2, 40% CO, and 22% N_2. Maximum power density of 250 mW/cm^2 was achieved (H_2). The power density is comparable to the power density achieved with single cell stack tests with similar cells.

Test MG735C69 Polarization Curves
6 Cell Stack
June 26, 2002
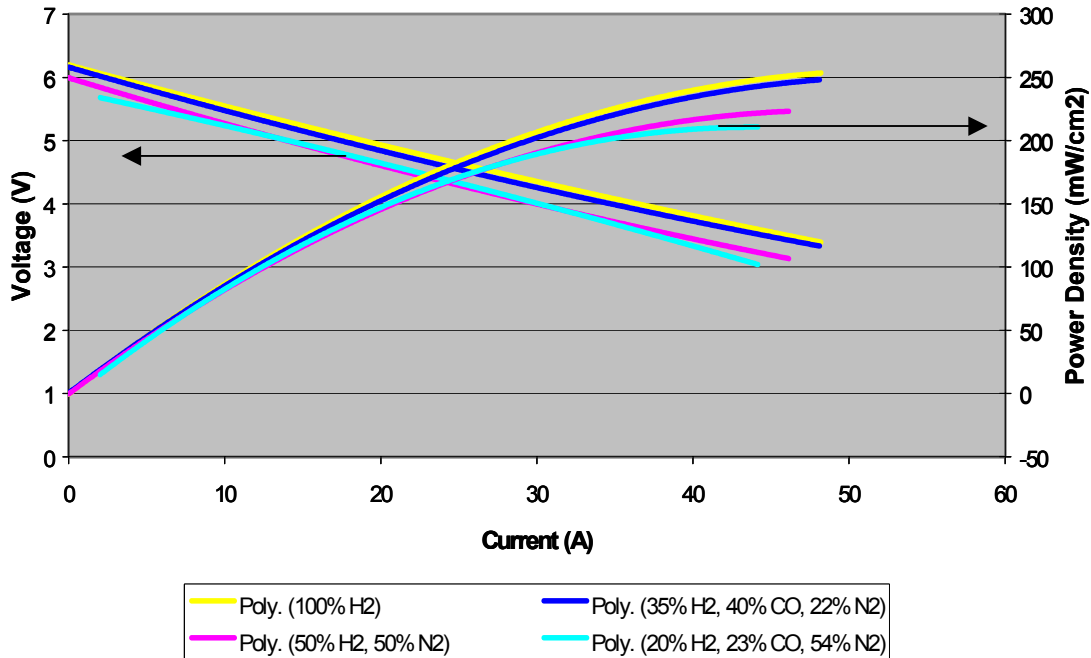
Figure 4.2.13-5:   6-Cell Stack (12 cm x 12cm Cell)

Complete stands to test stacks up to 5kW have been purchased and installed for performance evaluation and durability testing. Figure 4.2.13-6 below shows a picture of a typical Delphi stack test stand.

Figure 4.2.13-6: Test Stand For Electrochemical Stack Testing

4.2.14 Evaluate Stack Performance – Is covered in Section 4.2.13.

4.3 Reformer Development (Task 3.0)

During Phase I, Delphi will focus on two applications: (1) the stationary distributed power generation system fueled by pipeline natural gas, and (2) the gasoline-fueled automoti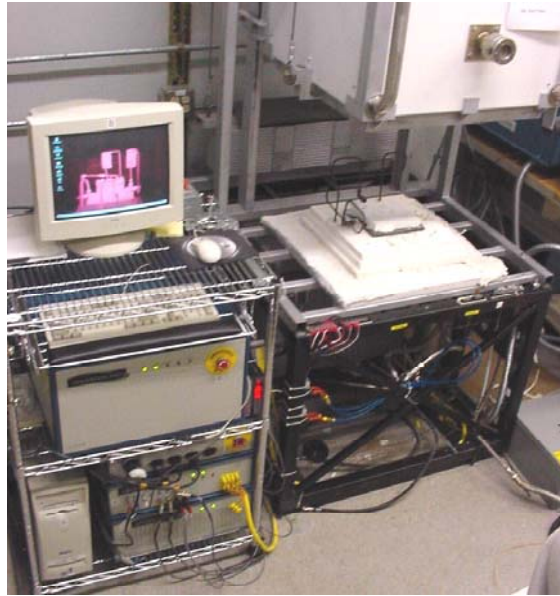ve APU. To date Delphi has focused the entire effort on the gasoline-fueled automotive APU. Major subtasks for the reporting period under Task 3 include the following.

4.3.1 Develop Steam Reformer for Natural Gas

No work complete under this subtask.

4.3.2 Develop CPO Reformer

4.3.2.1 Requirements

All product development conducted on the Reformer subsystem has been either to evaluate the current hardware vs. a stated requirement or to help understand the requirement itself. A general list of reformer requirements is given in Table 4.3.2.1-1 and while it contains some very current revisions, the main areas of concern were present at the close of 2001, the last time the basic reformer system concept was altered.

The significant alteration that occurred at the start of 2002 (and which has remained in effect thru 6/30/02) involved the elimination of "anode tailgas recycle" or simply "recycle" as a feature in the APU system.

Prior to this, Delphi had conducted modeling on several levels and showed the capability experimentally of the single planar reactor, in use at the time, to re-reform both H_20 and CO_2 present in anode tailgas. It is this re-reforming benefit and the 2nd pass thru the stack for increased fuel utilization that improves system efficiency and makes the recycle process so attractive.

However, the complexity and effort required to design a pump to handle the 800 ºC gas was deemed too much for the current project objectives and therefore the reformer system would proceed as a Partial Oxidation (POx) system while the recycle pump was developed in parallel.

The impact of this decision is manifested in the reformer efficiency target being lowered to 70% (from ~110% with recycle) and new attention being focused on carbon formation due to the loss of the beneficial effects of water present in anode tail gas.

The multi-plate planar reformer that was being designed, that included an integrated reformer / tailgas combustor, continued and now had the added burden to show that a combustion process occurring on adjacent plates to the reforming exotherm could provide proper temperature management.

The net result of the systems simplification was to make the reforming task potentially more difficult to make.

	Requirement Name		Units	Targets
				Simplified POx System
				5 kW net
	Fuel			Carb ph 2
	sulfur - ppm		ppm	30
1	Reformate Quality			
	kW - LHV (H2, CO, CH4)		kW	12.8
	Methane allowable - mole %		mole %	1/3 of H2O mole%
	O2 allowable		ppm	1.0E-08
			atm	1.0E-14
	HC (C2s and greater: wrt stack consumption)			C2s < 0.1mole%
	HC (C3H8 equiv) allowable - ppm		ppm	
2	Reformer Efficiency (LHVout/LHVfuel in)			70%
	Recycle Fraction		%	0%
	Fuel In - gps		gps	
3	Tailpipe Emissions (Reformer + WER + EHC)			
	HC ppm		ppm	tbd (~2 est)
	CO ppm		ppm	tbd (~300 est)
	NOx ppm		ppm	tbd (~7 est)
	CO2 @ SS max power (APU)		kg/kWhr	
4	Start-up time: Reformer		min	~3 min
	Start-up time: APU System		min	<20 min
	Reformer Turndown			
5	Carbon Avoidance			
6	Packaging			
	Volume		l	3.5 liters (20 x 12.5 x 14cm)
	Mass		kg	

Table 4.3.2.1-1: Reformer Requirements

4.3.2.2 Reformer System Concepts

While it was accepted that the reformer system reactor would be of a multi-plate planar construction, many of the other aspects of the reformer system were still undetermined relative to start-up devices and emission compliance features. Start time considerations, reformate quality during start-up and tailpipe emissions were considered when deciding which of several system configurations to select.

Delphi had had some success with the cascaded reformer system used in the Proof of Concept unit where an electrically heated micro-reformer fed a main reformer. Because of this experience, this configuration became the baseline for evaluation against our requirements. Due to concerns over the ability of this concept to meet size, start time targets and power consumption limits, it was dismissed in favor of combustion based heating devices. Coincidental with this decision, Delphi was also working on rapid start reformers for SULEV capable / H2 enriched combustion vehicles. This program was having good success in bringing a ceramic foam substrated catalyst to light off in

several minutes and it was felt this could be a viable approach for the SOFC Reformer system as well. Proper integration of a combustion heating process remained to be developed. Four (4) base configurations were considered. Figure 4.3.2.2-1 Reformer Configurations for GPC Location shows a GPC (gas phase combustor) in several locations within the reformer mechanization. After much debate and weighing of trade-offs, configuration 1 was selected primarily on the strength of its simplicity.

It is the only configuration with a single (1) fuel delivery point and therefore only requires a single injector and a single vaporizer (as opposed to 2 for the other 3 configurations). It also has direct heating of the reformer layer for quick heat up with the trade-off of increased risk of fouling the stack with low quality reformate during start-ups.

Each of the configurations analyzed included an electrically heated catalyst (aka EHC or ATC – after treatment catalyst) as a guaranteed "catch all" for emissions. This was viewed as an emissions conservative approach (at the expense of power consumption) and was due to the fact that assessing emissions capability on immature and non-descript concepts would have been highly inaccurate.
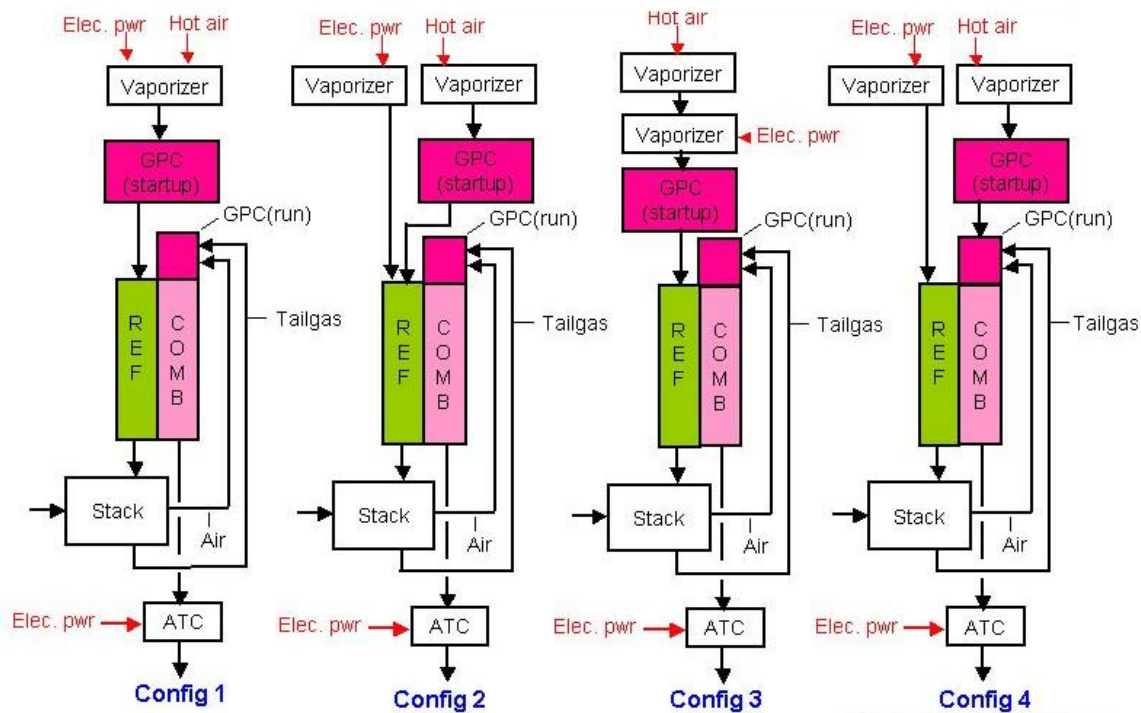

Figure 4.3.2.2-1: Reformer Start Up GPC Location Configurations

4.3.2.3 Non-Contact Vaporizer (NCV) Development

Developments in air assisted vaporization have allowed use of an inline fuel combustion process to provide heat for the start of reforming as well as delivery of the rich Air/Fuel mixture to the reformer during reforming. Figures 4.3.2.3-1 and 4.3.2.3-2 show a Non-contact Vaporizer design and design intent respectively. The approach is referred to as non-contact, in that instead of vaporizing fuel via heat addition due to contact with a heated surface, it is the rapid mixing with heated air that will fully vaporize the atomized injector spray. This approach avoids the fuel cracking deposits that form on heated surface vaporizers. Figure 4.3.2.3-3 shows an example of the fuel and air mass distribution achieved with these devices using Planar Laser Induced Fluorescence (Figure 4.3.2.3-4)
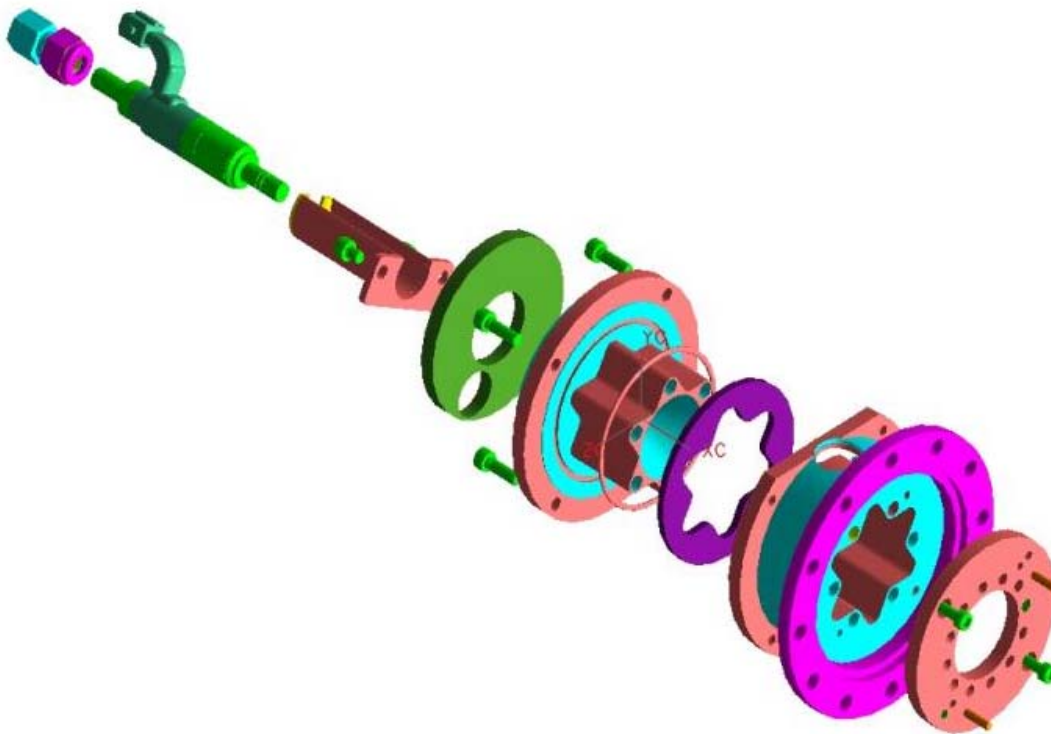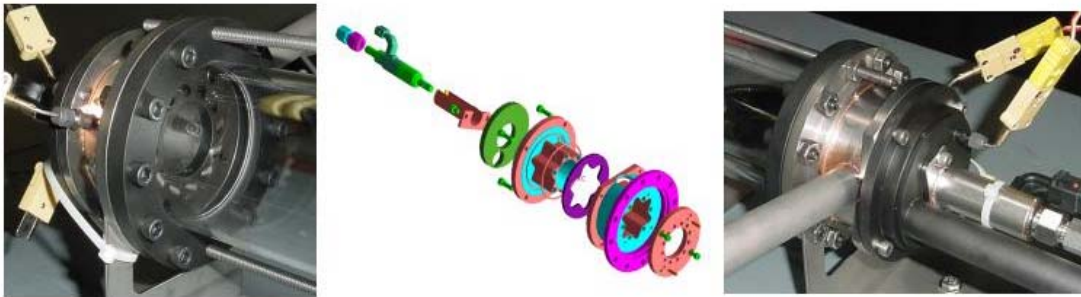

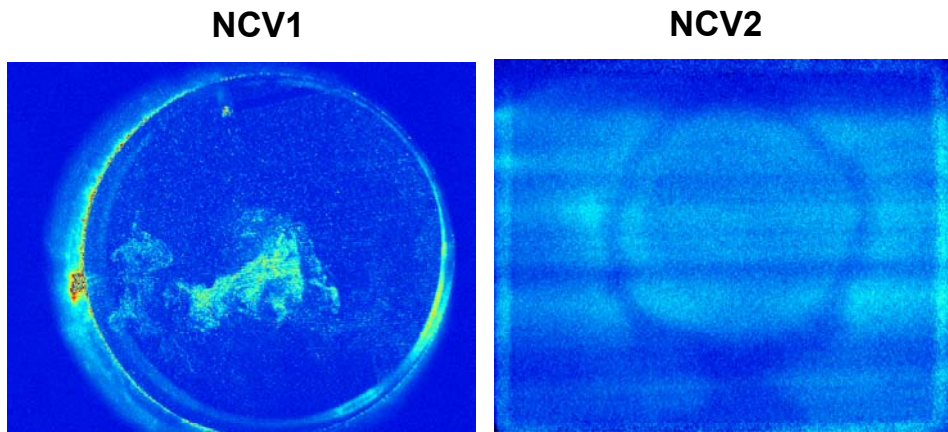**Figure 4.3.2.3-1: Non-Contact Vaporizer**

Vaporizer – Design Intent.

- **Fuel:** Injected via Delphi DI injector (350 kPa to 3 MPa) to control particle size and penetration.
- **Air / Recycle gas:** Introduced via an interchangeable director plate. Plates w/ mutilple exit nozzles for each gas are used to form a controlled mixture: Convergence angle and swirl angle of flow.
- **Goal:** Create gas motion to suspend liquid fuel particles until vaporization is complete (non-contact vaporization) AND mix vapor w/ Air & Recycle to mixture homogenity prior to catalyst introduction.

Experimental Air/Fuel/Recycle Gas
Mixture Fixture: Non Contact Vaporizer
(NCV)

Figure 4.3.2.3-2 Non-Contact Vaporizer – Design Intent

NCV1   **NCV2**

In Figure on left above vapor distribution of an 1st generation non contact vaporizer (NCV1) is shown. The light blue / white colored pixels represent vapor concentrations that flouresce when hit with the sheet laser.

Figure on right shows results from 2nd generation vaporizer (NCV2) Note: NCV2 has a rectangular outlet but the circular pattern due to fuel injection is still evident

Figure 4.3.2.3-3: Vaporizer – Vapor Distribution

NCV Mixture Preparation Evaluation Fixture
Planar Laser Induced Fluorescence (PLIF) and Mie Spray Evaluation

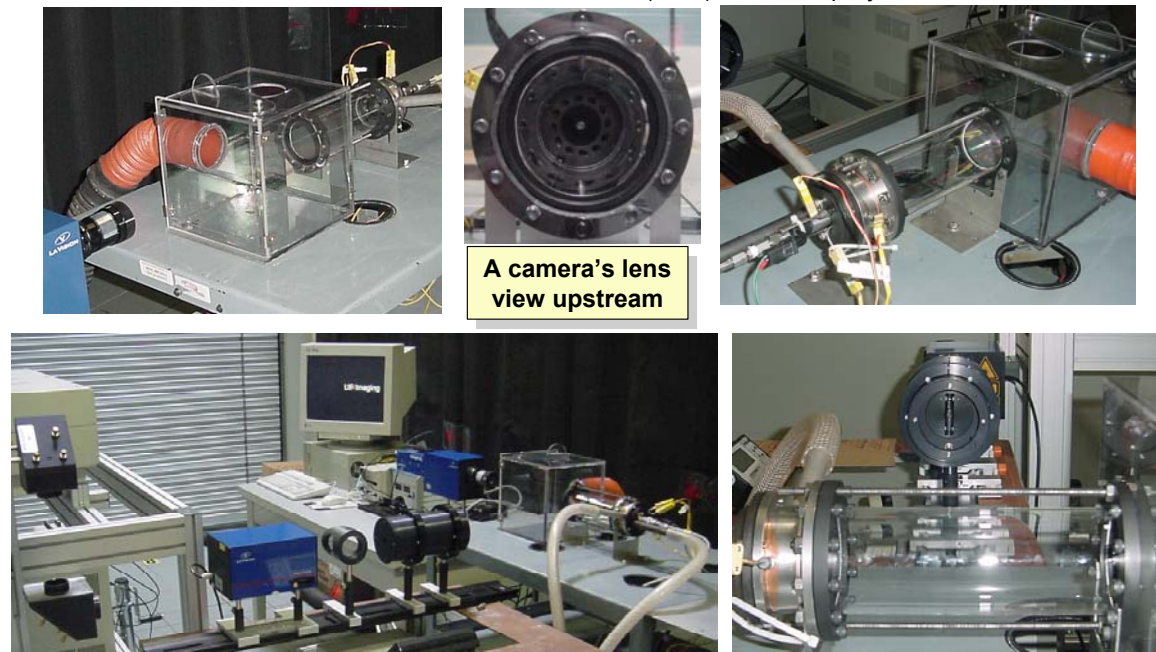
A camera's lens view upstream

Figure: 4.3.2.3-4: NCV Mixture Preparation Evaluation Fixture

4.3.2.4 Homogenous / Heterogeneous Combustor With and Without EHC

In order to better understand the emissions that might occur during start up and to help in the selection of an appropriate GPC approach, a comparison test was conducted.

The start combustor and vaporizer used on Delphi's SULEV / H2 enrichment program was compared with a current production "cabin heater" combustor (aka Webasto) as this was felt to represent a state of the art clean heating device. While the NCV1 (non-contact vaporizer – generation 1) and start combustor represent a homogenous combustion process, the Webasto conversely is a heterogeneous combustion process with a diffusion flame zone and excess air added late in the combustion process. Figure 4.3.2.4-2 show an example of the test setup while Table 4.3.2.4-1 shows both the relative emissions of these 2 configurations, as well as the benefit of using an EHC as the after-treatment strategy.
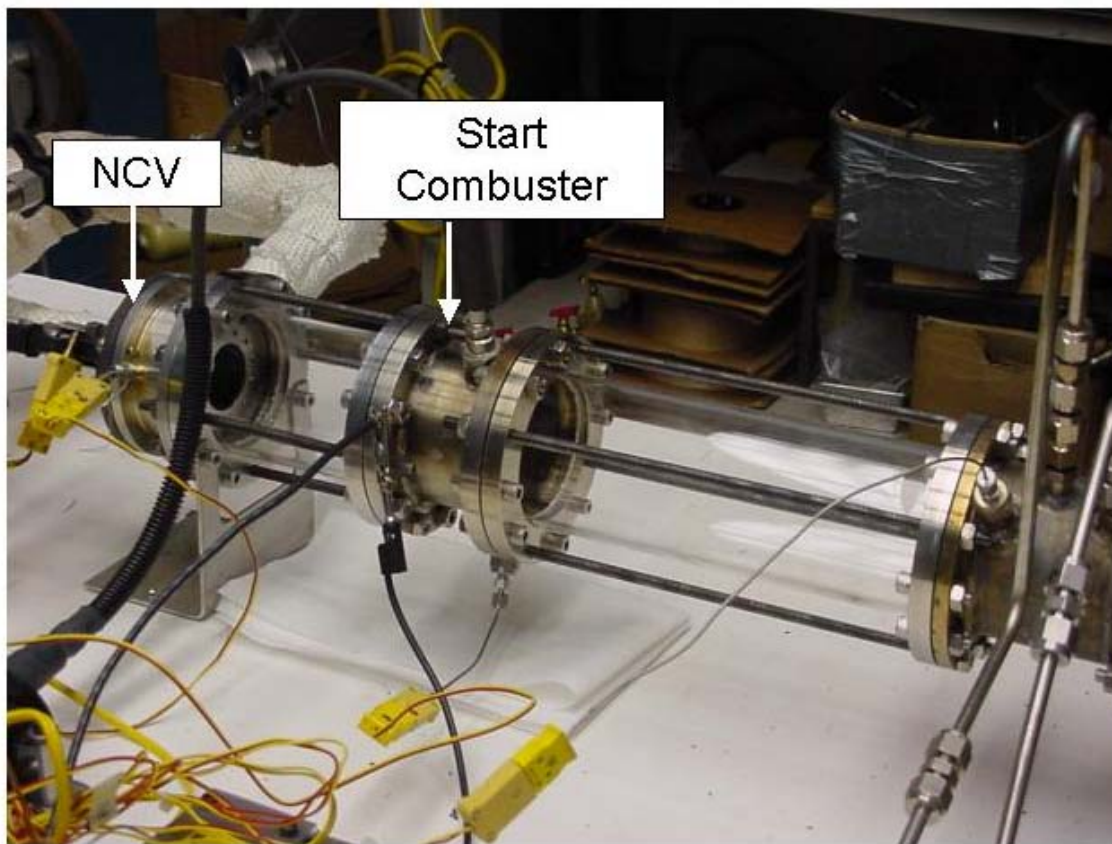

Figure 4.3.2.4-1: NCV1 + Start Combustor

	Peak Values				Steady State Values					
	HC	Nox	CO	CO2	HC	Nox	CO	CO2	ATC Voltage	ATC Current
	ppm	ppm	ppm	mole %	ppm	ppm	ppm	mole %	Volts	amps
European Cabin Heater Emissions Limits (Heaters using liquid fuels)					<= 100	<= 200	1000			
Webasto	14874	51	25251	10	29	38	81	6.6	N/A	N/A
Webasto w' ATC	2628	79	871	8.9	29	28	16	6.2	7	128
Benefit of ATC	*12246*	*-28*	*24380*	*1.1*	*0*	*10*	*65*	*0.4*		*see note*
NCV-1 + SULEV type Start Combustor	7140	47	123	10.9	38	14	25	10	N/A	N/A
NCV-1 + SULEV type Start Combustor w' ATC	2672	23	73	8.8	10	10	22	7.8	12	155
Benefit of ATC	*4468*	*24*	*50*	*2.1*	*28*	*4*	*3*	*2.2*		
				Based on the intended EHC being 0.66 the rated power of the tested EHC… And knowledge of the effect of flow (thermal load) on the EHC the steady state current draw of the intended EHC is estimated at ~100amps with <= 1 g/s flow						

Table 4.3.2.4-1: Start Combustor Emissions

4.3.2.5 NCV1 and Start Combustor Development

Based on the relative success of the start combustor testing, a NCV1 vaporizer and a H1 10 plate planar reformer were assembled together for testing. See Figure 4.3.2.5-1.

The purpose of this test would be to determine general start times (time to light off), emissions during start and run and better develop and optimize the controls strategy.
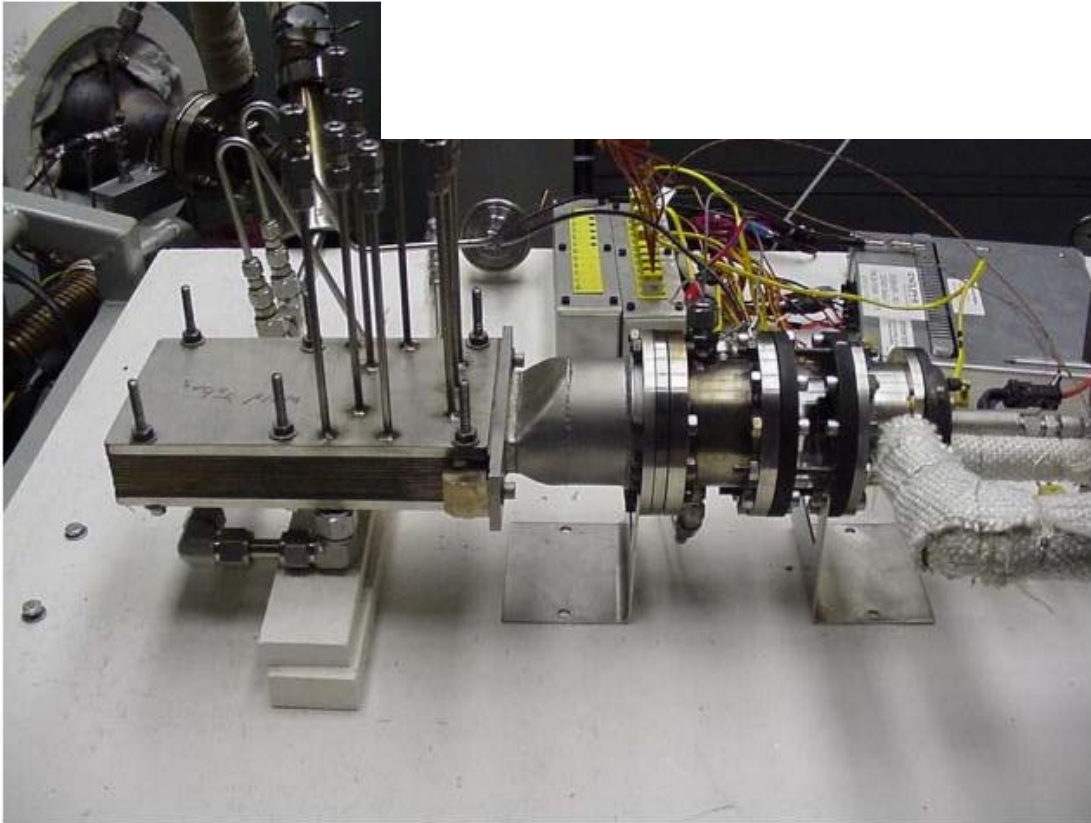
Figure 4.3.2.5-1: NCV1+H1 10 Plate (Partial Fixture)

The basic start sequence is charted in Figure 4.3.2.5-2. While not to scale, it shows how fuel delivery, flame initiation and quench, Reformer LO (Light-off) and GPC (Gas Phase Combustor) are sequenced. FIGURE 4.3.2.5-3 shows the results of initial testing on a minimum function fixture. The significant finding of this testing was that while the lead edge of the reformer can be brought to a LOT (light off temperature – 600 ºC for this discussion), it takes considerably longer, on the order of 20+ minutes before the rear of the reformer is at or near LOT. This testing was only preliminary, as no GPC was used to heat the reformer during most of the ramp to steady state.

Emissions, particularly HCs, were, as expected, quite high during ramp up.

Figure 4.3.2.5-2: ReforWER Modes

Figure 4.3.2.5-3 NCV1 + Start Combustor + H1 SN 2
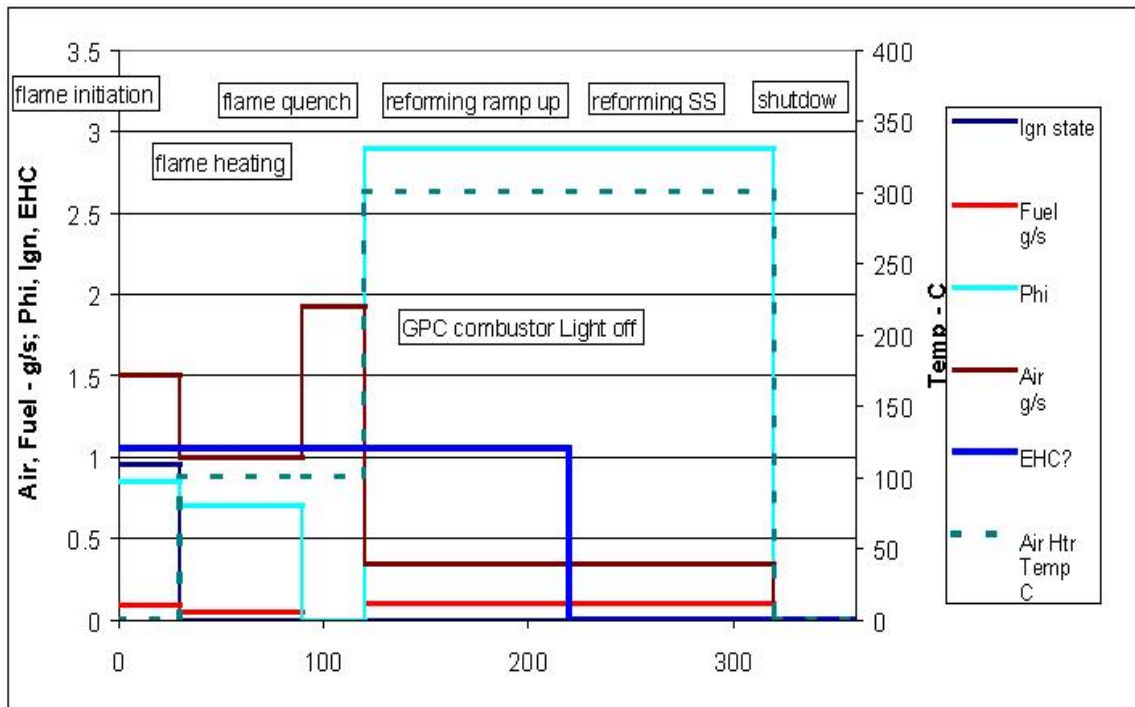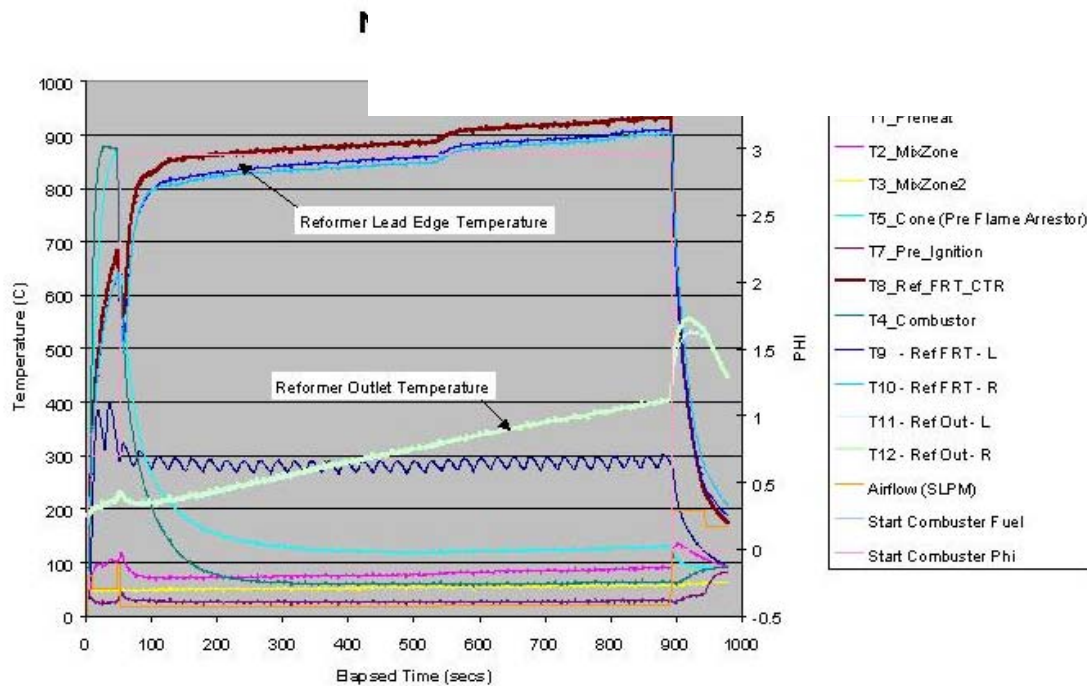
4.3.2.6   NCV1 + H1 on full fixture

Testing of NCV1 and H1 Reformers was continued with a new fully manifolded base fixture that provided a mounting of the GPC igniters. Figure 4.3.2.6-1 shows the test setup used. This setup is assembled onto a test stand inside an insulated zircor box to simulate APU insulation. Figure 4.3.2.6-2 shows temperature and input data for a sample run from this testing. Once again, lead edge temperatures rose quickly, but areas downstream of the reformer inlet take considerable time to reach beneficial reforming temperatures (700 ºC and above). For the rear area of the plate temperature (T3), time to 700 ºC is ~11 minutes, while actual Reformate Out gas temperatures (T5) didn't reach 700 ºC until ~14 minutes. Additionally, the very slow rise of the air pre-heat for vaporization was a concern as it took nearly 45 minutes to reach 150 ºC. A portion of this time can be attributed to the low performance of the lab insulation materials and techniques, as compared to the APU configuration. However a concern remained that the mass of the rear section of the reformer (cathode air pre-heat) presented such a large thermal sink that target air pre-heat temperatures and reformer outlet gas temperatures could not be rapidly achieved. These concerns were directly addressed in the design of the next generation (H2) reactor.

Gas compositions were also recorded during this testing and are found in Figure 4.3.2.6-3.   Reformate quality was found to take some 20 minutes to rise to levels

approaching that required for stack consumption. Note that the latter part of this graph exhibits some variable behavior resulting from changing input conditions.
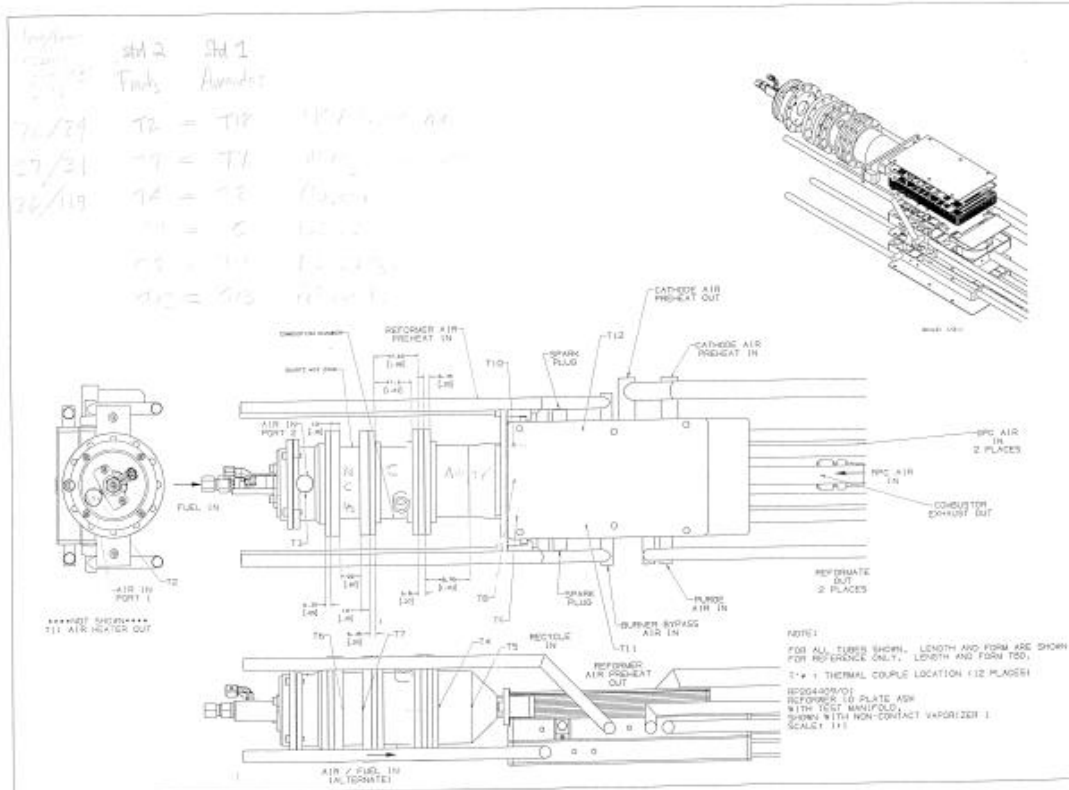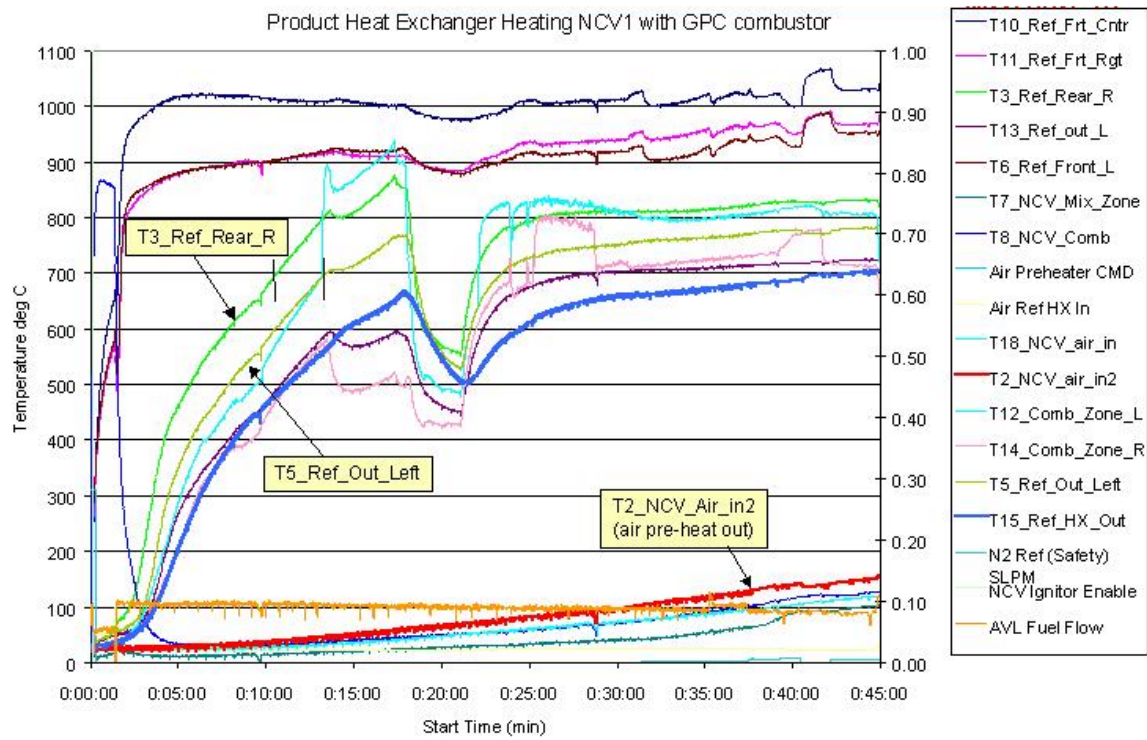

Figure 4.3.2.6-1: NCV1 + H1 10 Plate + Fixture.

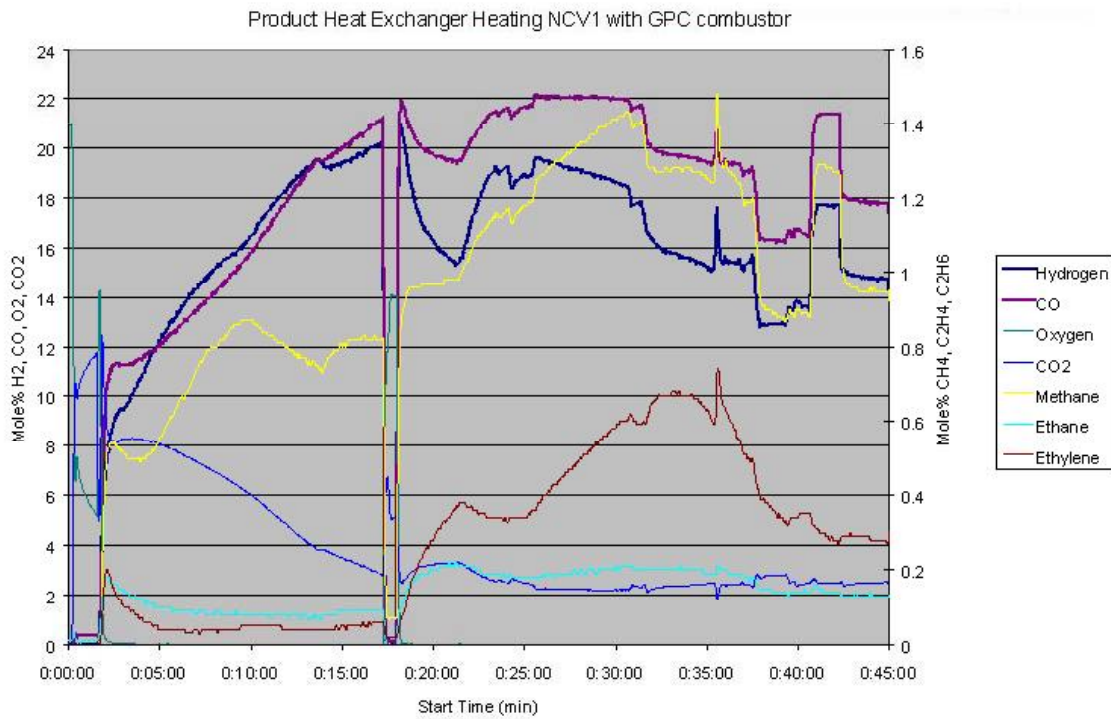**Figure 4.3.2.6-2: Temperatures: NCV1 + GPC**

Figure 4.3.2.6-3: Gas Compositions: NCV1 + GPC

4.3.2.7   Develop Catalytic Partial Oxidation (CPO) Reformer - Reactor

The CPO Reformer Development has been carried out on several reactor platforms covering a range from research level to application specific. Work carried out on each platform will be discussed below.

4.3.2.7.1   1" Nominal OD Tubular Reactor (w/ foam substrate) – See Figure 4.3.2.7.1-1

In general, reaction characterization is carried out on this type of reactor. Use of cylindrical foam substrates makes for ease of wash coating and relatively quick change out. This work continues today and serves as a baseline for reformation performance. This will be discussed in detail in the section on Catalyst Development.
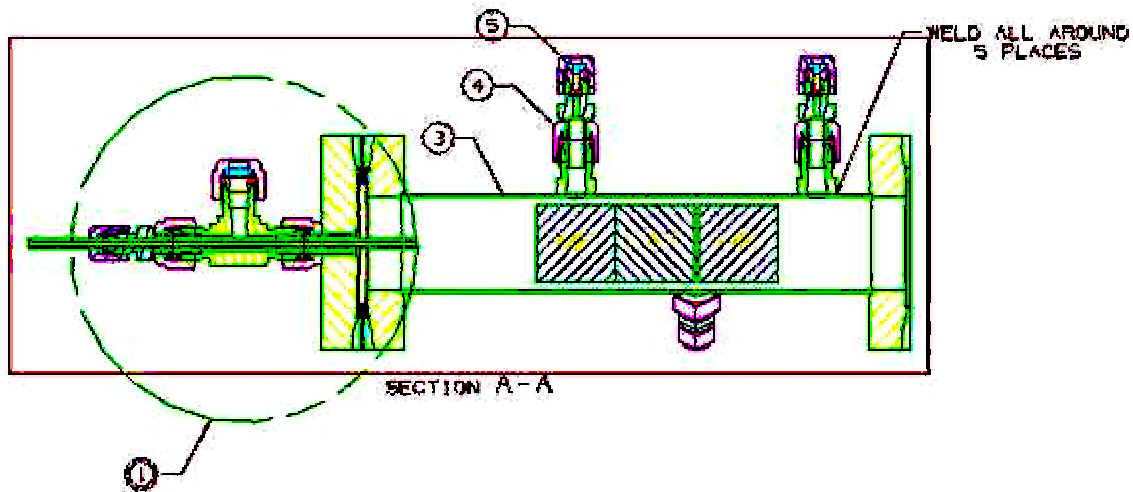
Figure 4.3.2.7.1-1: 1" OD Lab Reactor

4.3.2.7.2   Single Plate Planar Reactor – See Figure 4.3.2.7.2-1

While the use of this reactor pre-dates this report timeframe (Delphi concluded testing on this reactor 12/01 to pursue the H1 design), it is worthy of note as it confirmed key capabilities of a planar reactor. Data was collected that outlined general reformer behavior relative to temperature gradients, species gradients, space velocity capability and the viability of recycle. This information, as it was from a true "channel flow" reactor, was used to design the first generation (H1) reactor.

This reactor also provided our first experience with wash coating of a metal substrate in a reforming application (Delphi has other metal substrate wash coating experience, but for lower temperature exhaust catalysts).

A derivative of this design is in use today as a research reactor in our Delphi Tulsa Catalyst Development facility.
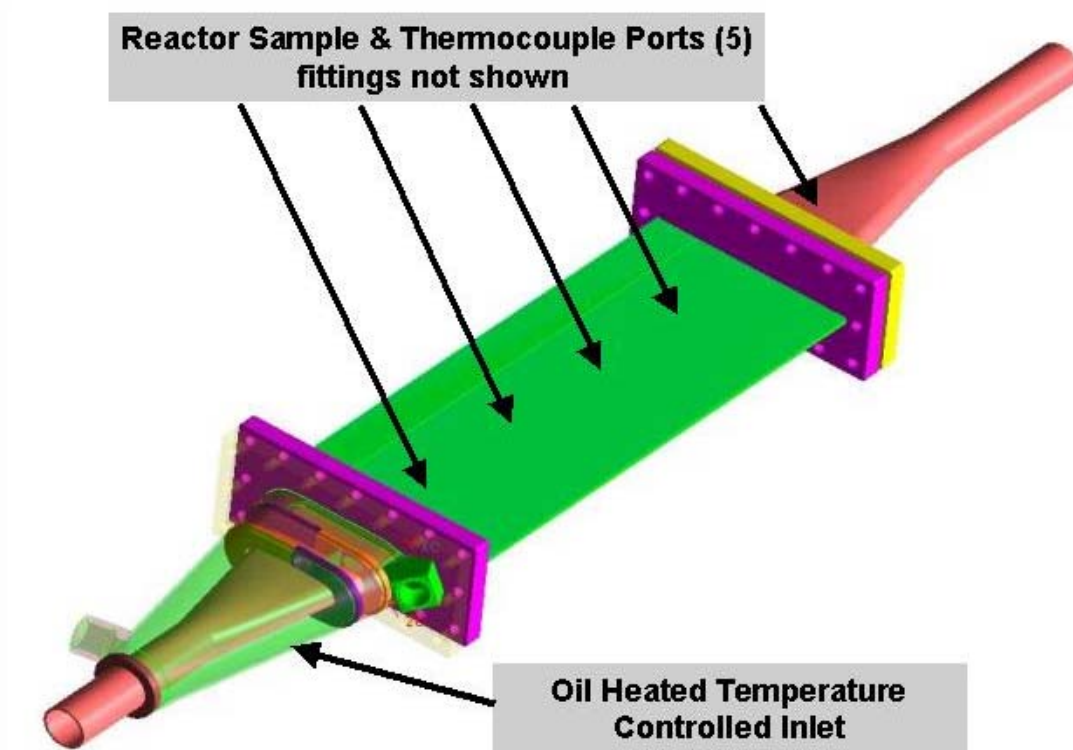
Figure 4.3.2.7.2-1: Single Planar Reactor

4.3.2.7.3   H1 Reactor – See Figure 4.3.2.7.3-1

At least 2 integrated reformers were fully concepted (i.e. 3D models completed). H1 was selected as the concept to further develop based on our familiarity and success with a similarly constructed Energy Recovery Unit, built and tested earlier in the program. In addition, the ability to integrate the various flow streams within a package that had a high degree of manufacturability was very desirable.
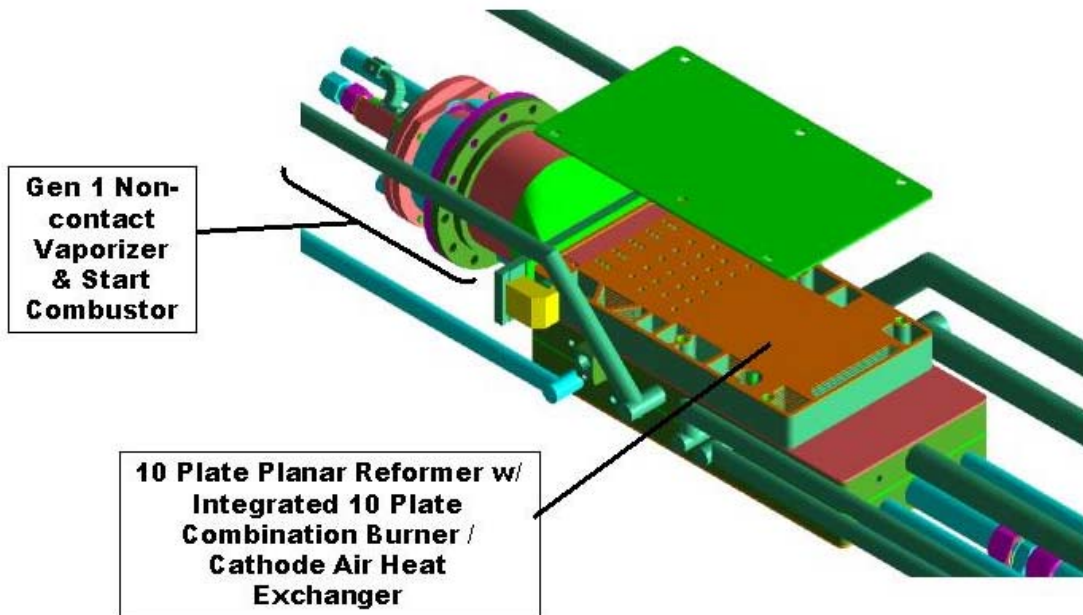
Figure 4.3.2.7.3-1: H1 10 Plate ReforWER

The basic functions of reforming, waste energy recovery, reformer air preheat, and cathode air heating are combined into a single multi-plate unit. Figures 4.3.2.7.3-2 and 4.3.2.7.3-3 describe the 2 sides of a "reformer plate". Initial construction involved double-sided etching and allowed unique flow path geometry on each face of the plate. Figure 4.3.2.7.3-2 shows the 3 flow streams involved on the reformer / air heating side of the plate. Air and fuel vapor enter from the left move over a catalytic surface and are reformed before exiting to common manifolds. Cold air enters from one side and exits on the other after heating up due to heat exchange from the combustor side (and to a lesser extent proximity to the reforming section).
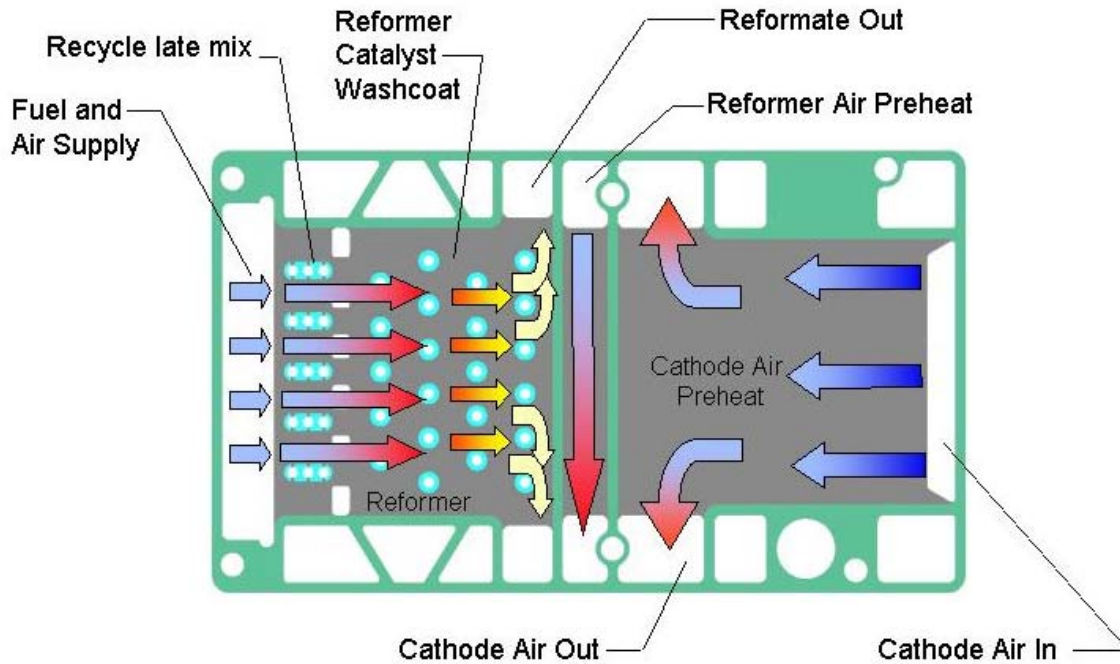
Figure 4.3.2.7.3-2 -- H1 Reformer/Air Heating Function
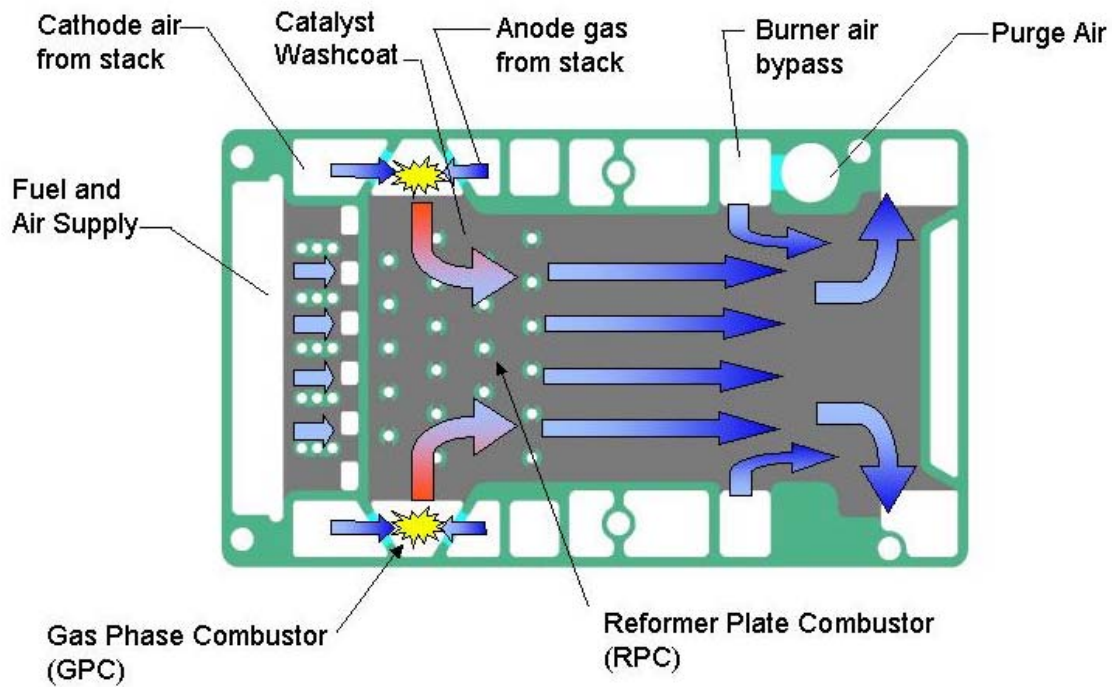
Figure 4.3.2.7.3-3: H1 Combustor Function

The H1 design saw considerable testing and as a result generated important information. Initial testing employed a lab heated mixing inlet (Figure 4.3.2.7.3-4), but later an actual product intent NCV was used.

Several questions were raised before and during testing and these became the focus of H1 testing.
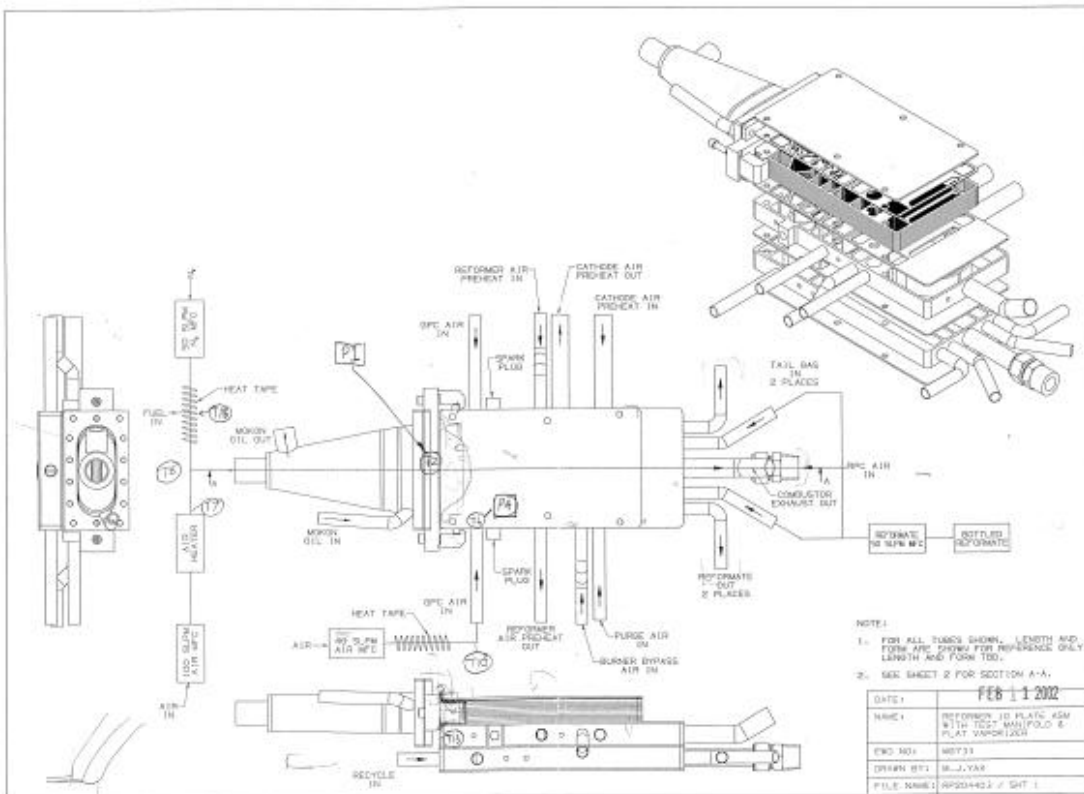
Figure 4.3.2.7.3-4 -- Lab A/F prep + H1 10 Plate + Fixture

4.3.2.7.4   Reformer Efficiency – See Figure 4.3.2.7.4-1

Combustor Ability to Control Reformer Plate Temperatures
The ability to control reformer plate temperatures through the use of the GPC process was an objective of initial H1 testing. Figure 4.3.2.7.4-1 shows a collection of various operating points plotted together showing the ability of the GPC to be run at an appropriate temperature to maintain reforming plate temperature at the desired range.
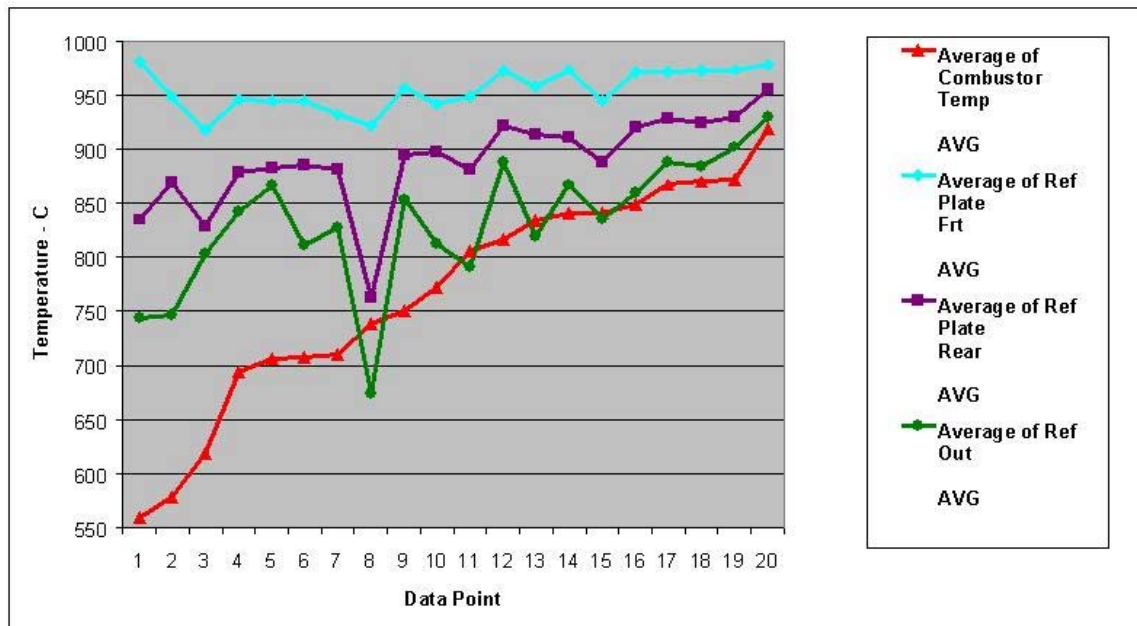
Figure 4.3.2.7.4-1: Combustor Control of Reformer Plate Temperature

Reactor Gas Hourly Space Velocity (GHSV) vs Conversion
Another area of investigation was the capacity of the reactor (i.e max GHSV for good conversion) to assure that overall size of the design was adequate. Figure 4.3.2.7.4-2 shows a "scale sweep" where fuel delivery increases along the X axis. The expected relationship is for conversion (i.e. reformer efficiency) to be constant at or below the maximum GHSV (plotted here as its inverse – residence time). Above the maximum GHSV, conversion would not be complete and would be seen in lower reforming efficiency.

While the data is not a modal as expected, the data points at 0.40 and 0.45 scale (0.25 and 0.28 grams per second, gps, fueling respectively) show this change in conversion. As this was for a 10 plate assembly and an actual APU Reformer would have ~30 plates, this indicates that the reformer will have sufficient initial capacity for 5 kW APU (which would require ~0.6 gps to be converted to reformate at ~75% reforming

efficiency). It does point out that there is little durability margin and will need to be addressed in future designs.
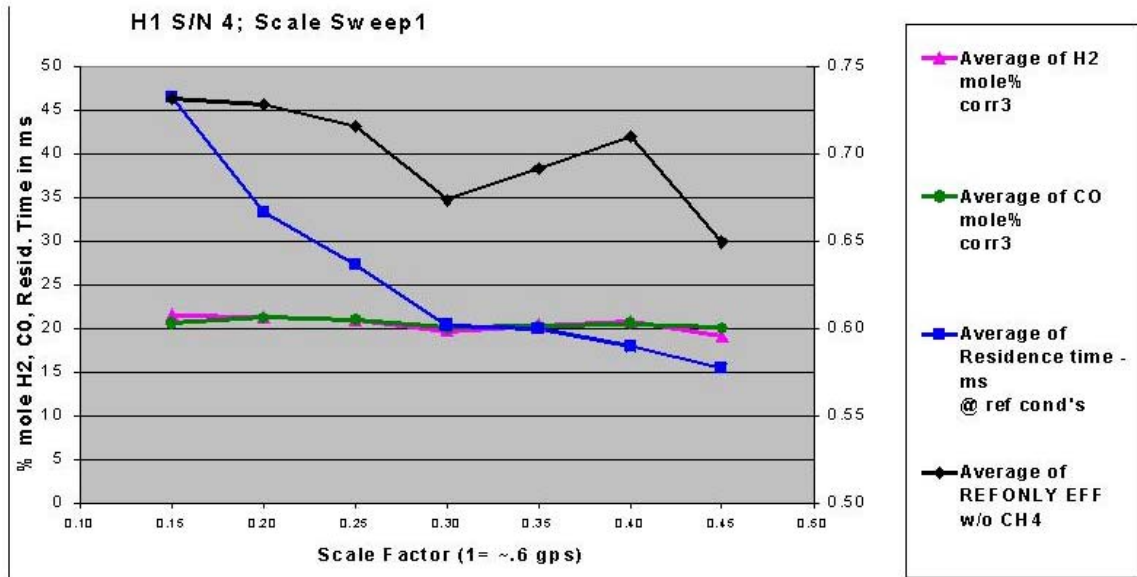
Figure 4.3.2.7.4-2: H1 Scale Sweep

Lead Edge Temperature Management
H1 testing also uncovered a thermal management problem at the lead edge of the reformer. We found that normal operating conditions resulted in temperatures in excess of 950 ºC at thermocouples located near the entrance to the reactor. In order to control these temperatures and not damage the wachcoat, it was necessary to dilute the inlet feedstream with N_2. This increases the heat capacity of the feedstream and potentially dilutes concentrations of reactants, thus delaying their exotherm until further into the reactor. Alternative designs for the lead edge are being evaluated

.
Combustor Emissions
Combustor capability was of interest in that ultimately the system will need to meet SULEV emissions levels without the assistance of an after treatment catalyst (ATC) downstream of the reformer (during run modes only). Initial testing of the H1 combustor performance can be found in Table 4.3.2.7.4-1. Several design weaknesses were found in the H1 design, including inadequate mixing and low/zero velocity areas in the combustor plate. Both of these issues will be addressed in the next generation design.

	time	Total HC ppm	Nox ppm	CO %	CO2 %	Source of Data
Ref Ramp up; combustor out	13:42	250	3	0.01	7.50	from Normal start w/ comb w/ emiss.xls (MG733C-15)
	13:44	2500	0	2.70	3.40	
	13:46	1000	0	0.18	6.93	
Steady State; combustor out	13:56	47	0	0.04	5.60	from Normal start w/ comb w/ emiss.xls (MG733C-15)
	13:57	226				

Table 4.3.2.7.4-1:   Combustor Emissions

4.3.2.7.5   H2 Reactor, See Figure 4.3.2.7.5-1 and 4.3.2.7.5-21

The intent of the H2 design was to remove the real and expected deficiencies in the H1 design. Coincident to its creation, revisions in the APU enclosure design and layout were also being considered. The primary thrust of the APU revision was to lower the surface area of the "hot zone" to reduce thermal losses. The H2 design allowed the revised APU hot zone enclosure to be "square" shaped as compared to the "tee" shaped hot zone required by the H1 design and thus allowed lower thermal losses to be realized. The key changes in H2 design as compared with H1 design are as follows:

1. Removal of Cathode Air Heat Exchange function (the "square" hot zone design would use 2 separate heat exchangers mounted to each side of the reformer – see Figure 4.1.2.1-A2, Appendix A in the system section of this report.
2. A single combustor, centrally located with the combustor flowstream in crossflow with the reformer flowstream. This greatly simplified manifolding with only the combustor outlet having a duplicated port.
3. Integration of the NCV2 vaporizer and start combustor.
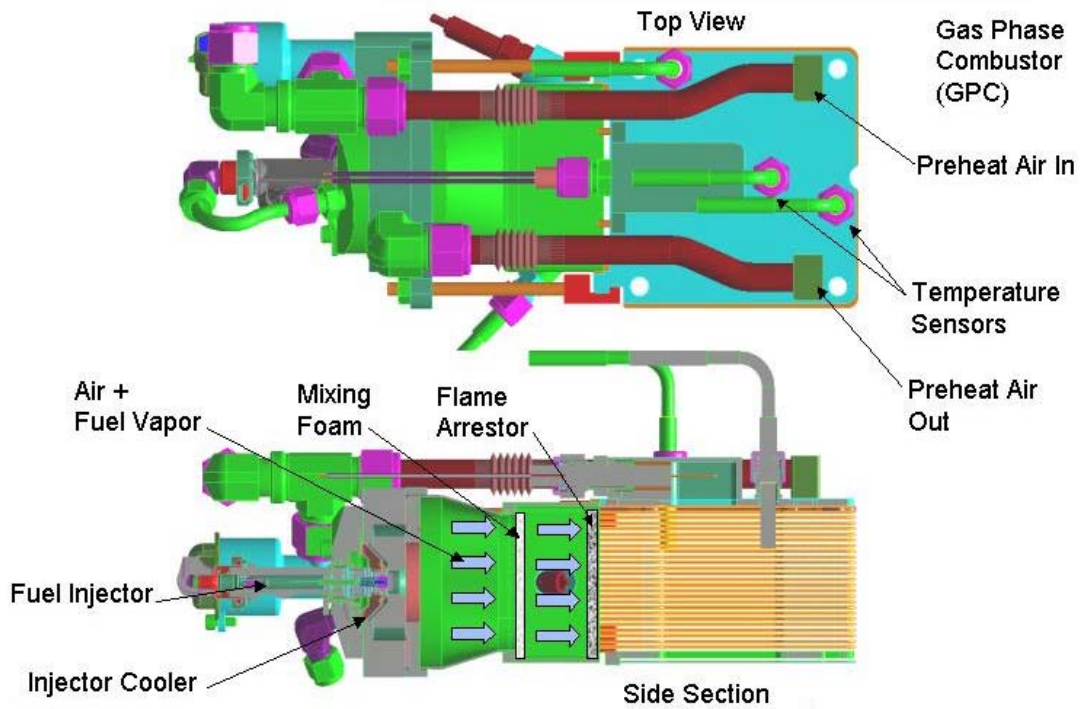
Figure 4.3.2.7.5-1:   H2 ReforWER
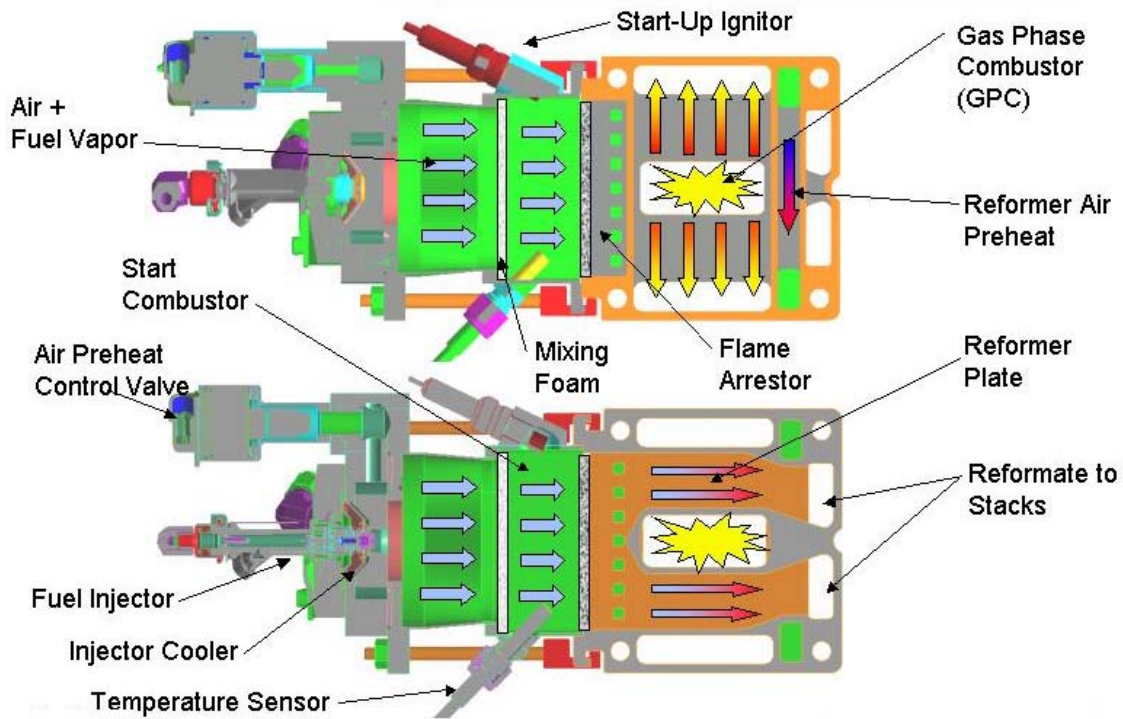
Figure 4.3.2.5.-2:   Top Section – H2 Reactor

Pressure / Flow Analysis

Several iterations of CFD modeling were conducted in order to achieve good distribution with the ~30 reforming and 30 combustion plates. Figure 4.3.2.7.5-3 and 4.3.2.7.5-4 show the distribution of the proposed H2 design which incorporated vertical manifolds at the lead edge to distribute recycle gas to each reformer layer (See Figure 4.3.2.7.5-5). Additionally, the design incorporated a feature that uses reforming areas on both plates (reforming and combustor) for the initial 20mm of the reactor. The reforming area on the combustor is referred to as the "slave" area as it feeds the master layers above or below it (see Figure 4.3.2.7.5-1).

While Figures 4.3.2.7.5-3 and 4.3.2.7.5-4 show relatively good massflow distribution on both the master and slave reforming areas, this unfortunately did not translate to good massflow distribution where the 2 streams join (the portion of the reforming plate downstream of the transfer ports – See Figure 4.3.2.7.5-4). The cause of this was considerable massflow up and down the recycle chimneys. This feature was eliminated subsequently (as was the use of recycle in the system). Figure 4.3.2.7.5-6 shows Total Assembly Pressure Drop plotted alongside Average Cell Pressure Drop.

The difference in these values for a given design represents the manifold or chimney losses, which were minimized as the design was modified. Similar analysis was conducted on the combustor.
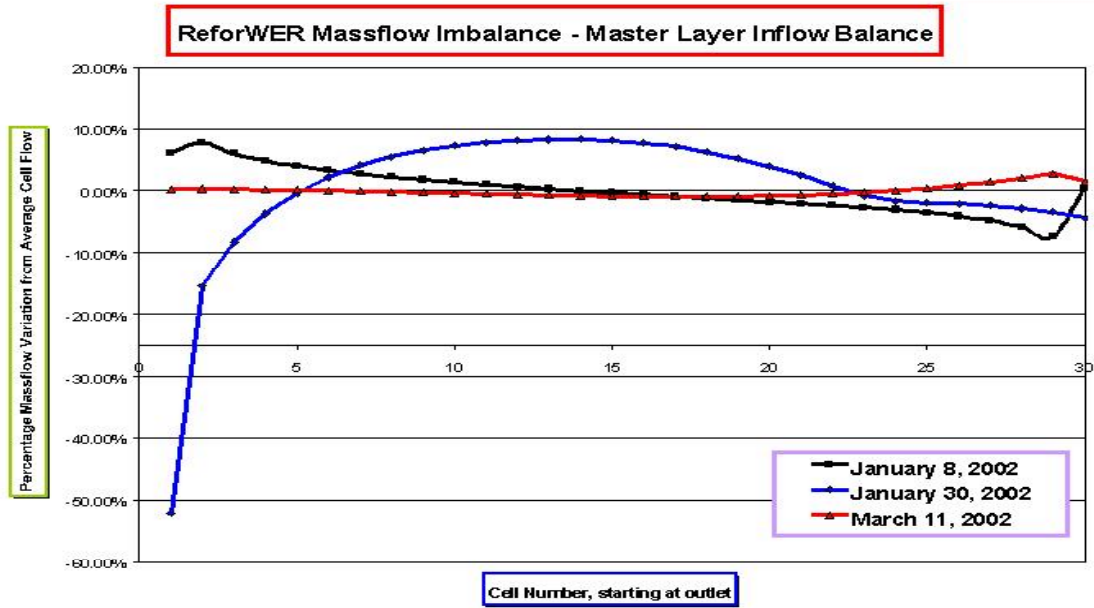
Figure 4.3.2.7.5-3: ReforWER Massflow Imbalance - Master
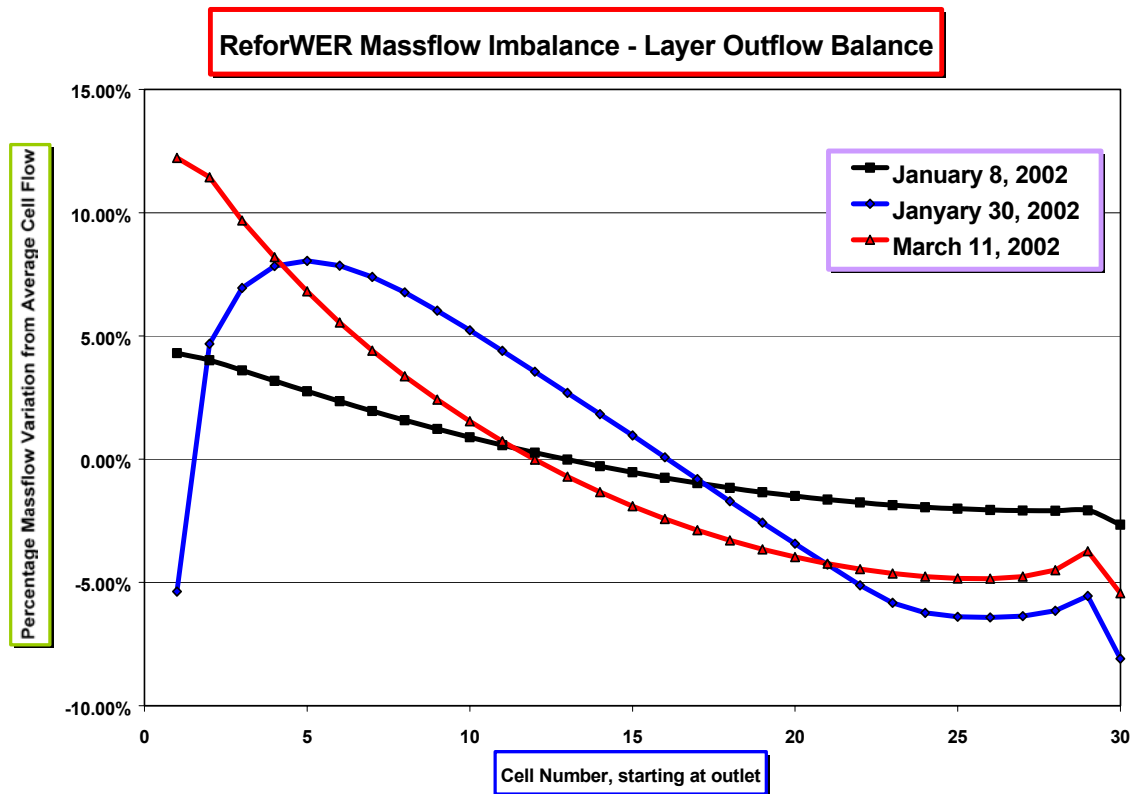
Figure 4.3.2.7.5-4: ReforWER Layer Outflow Balance
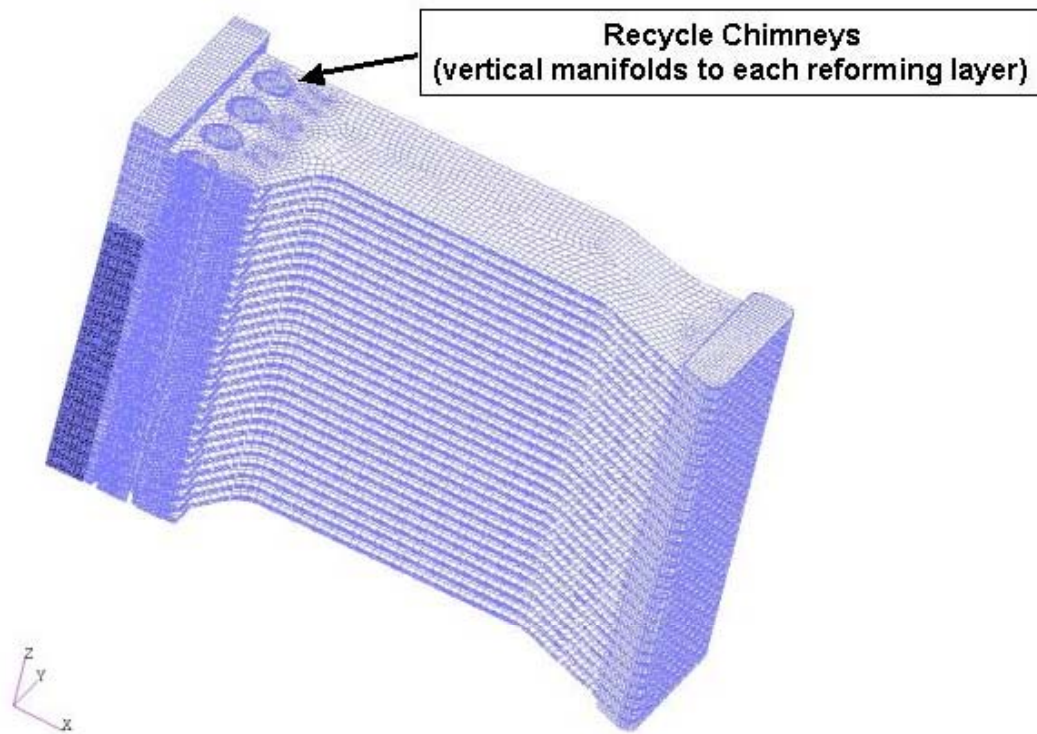
Figure 4.3.2.7-5: Recycle Chimney
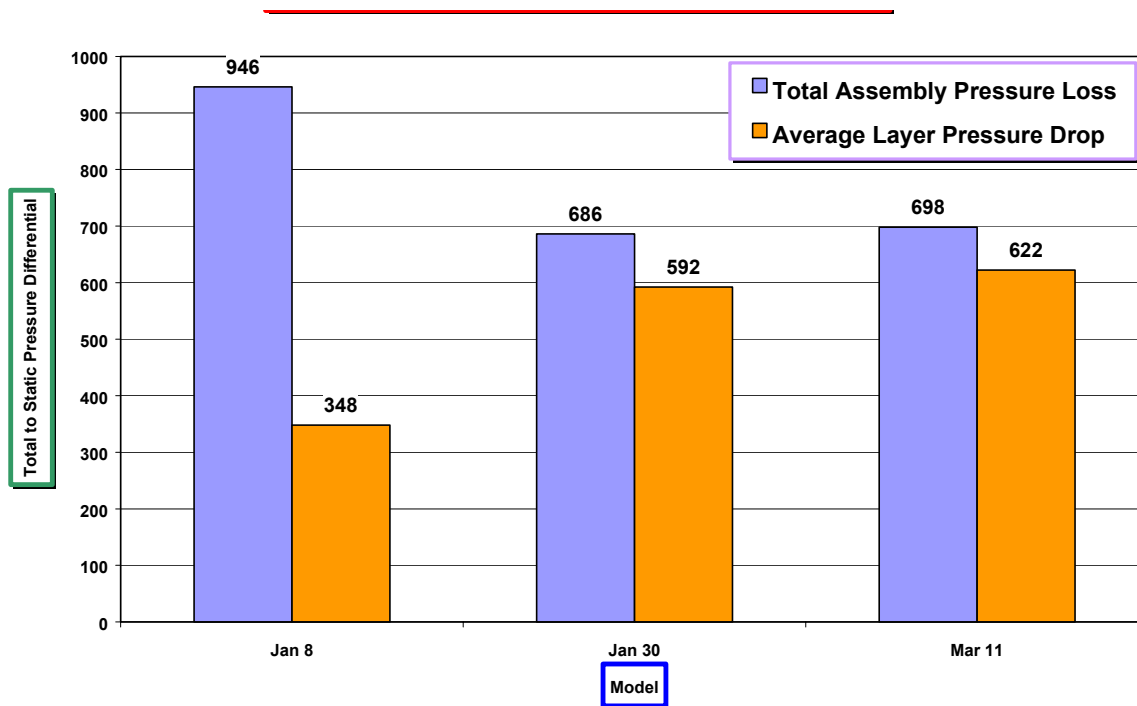
FIGURE 4.3.2.7.5-6 Assembly versus Layer Average Pressure Drop

4.3.3 Develop Catalysts

4.3.3.1 Catalyst Formulation and Characterization

Alumina-based Washcoats

Significant progress has been made in catalyst formulation. The catalyst is considered to consist of a shaped substrate carrying a washcoat containing active metals. Earlier testing has revealed that zirconia-toughened alumina to be amongst the best choice of substrates, and rhodium to be a good choice of active metal. While having good activity, the earliest generation of catalysts exhibited limited durability, thought to be due to instability of the washcoat. Exposed to high temperatures for long time intervals, the Al_2O_3 principal component of the washcoat is known to undergo phase transition, to the more stable α form, and also undergo sintering; both transformations contributing to encapsulation or loss of active metal, and loss in catalyst performance.

A series of different alumina oxides were obtained from suppliers, and tested in the as-received and thermally treated forms. Thermal treatment results in greater physical stability in that the alumina resists further sintering and loss of surface area. These aluminas were selected based on availability in commercial quantities and on properties thought to be important to reforming. A summary of the alumina-based compositions evaluated is given in Table 4.3.3.1-A1 in Appendix A. Testing is summarized in Figure 4.3.3.1-A1 and Figure 4.3.3.1-A2, in

Appendix A, conducted according to the 'rigorous' testing protocol. This set of alumina washcoat materials were characterized by basic physical methods, summarized in Table 4.3.3.1-A2 in Appendix A.

All of the catalysts exhibited good initial activity; however, only the most stable washcoat formulation, Al_2O_3-TG, had good durability over the duration of testing, having nearly the same activity after over 50 hours of testing as for the fresh catalyst. This can be attributed to the stability of α-Al_2O_3 and the reasonable stabilized surface area of the washcoat material, likely resulting in good Rh dispersion.

Several features of this data set should be noted. The behavior of product selectivity to CO and H_2 does not track in parallel, see Figures 4.3.3.1-A1 and 4.3.3.1-A2 in Appendix A. While the catalyst exhibited differing degrees of deactivation for H_2 production, nearly the same amount of CO was produced by all of the catalysts over most testing intervals. We have found that only when significant loss in H_2 production occurs, being less than 17% in the product gas, does diminishment of CO production occur, indicative of severe loss in catalyst performance. This decoupling of H_2 and CO selectivity's is an indication of differing reaction pathways for the formation of the two primary products. The sensitivity of H_2 selectivity to washcoat properties, and so presumably to Rh availability on the washcoat, can be an indication of the H_2 formation pathway involving surface-phase chemistry, while the CO formation pathway may have significant gas-phase contributions.

Another interesting feature of the data is the extremely low Rh dispersion, as measured by CO chemisorptions, Table 4.3.3.1-A2 in Appendix A. For example, Rh supported on the NC washcoat is almost completely lost, yet the tested catalyst still retains over 80% of the fresh H_2 production. Similar behavior is observed on the CNC washcoat material. This result implies that little Rh is required for the reaction to proceed, perhaps indicating that active surface sites have extremely high turn-over frequencies.

Future work will focus on understanding the relationship between H_2 and CO reaction pathways, selectivity's, Rh dispersion and microstructure and alumina stability, with the goal of producing well-characterized and understood highly stable washcoat and active metal compositions.

Zirconia-based Washcoats

A parallel development effort to test zirconium based washcoats was undertaken. Zirconium oxide was selected based on the material's well known stability at very high temperatures. Materials were obtained from MEI, Flemington, NJ, and washcoats were prepared, with the same active metal and substrate and testing procedure employed with the alumina-based washcoats.. Samples tested are listed in Table 4.3.3.1-A3 in Appenidix.

Results of testing are contained in Figures 4.3.3.1-A3 and 4.3.3.1-A4 in Appendix A, with comparison to the best alumina-based washcoat, Al_2O_3-TG. In general, the zirconium oxide based washcoat materials have equivalent CO production activity, and while having less H_2 production activity, exhibit the same stability over 50 hours of testing, as compared to alumina-TG. Characterization of the Zirconia-based washcoats was not completed due to the immediate focus on the better performing Alumina-based washcoats. Future Zirconia work, when resources become available, will focus on improving the activity of zirconium based catalysts while maintaining their stability.

4.3.3.2   Process Development

Thermodynamic Considerations

Of concern to reformer design is the amount of heat generated by the partial oxidation reaction, and how selectivity to the desired products, CO and H_2, and undesired products, such as carbon, change as a function of processing parameters, including O/C molar ratio and reaction temperature. To this end, a simple model was developed, using ASPEN process simulation software. Limitations of this tool include: use of Gibbs free-energy minimization model, which does not consider reaction chemistry, kinetics, or catalytic effects; assumption that reactants and products are at equilibrium; 'zero-dimensional' model which does not consider geometrical, spatial, or time-dependant inputs. Fuel feed, CARB Phase II gasoline, was modeled by a multi-component mixture, listed in Table 4.3.3.2-1 adjusted to give the same distribution of paraffins, iso-paraffines, cycloparaffins, and aromatics, as well as the same C:H:O ratio, as the representative fuel. Results of the modeling are presented in Figures 4.3.3.2-1 through 4.3.3.2-4.

The modeling indicates that situations of poor mixing can lead to either poor yields and excessive heat generation in cases of higher O/C, or carbon formation in cases of lowered O/C. Additionally, operating at 900 °C, provided sufficient residence time is provided to reach equilibrium, is sufficient to approach maximum H_2 and CO production, while minimizing hydrocarbon production. Operating at above 950 °C, while helpful in preventing carbon deposition when O/C is close to unity, provides no additional benefits, and in fact may be detrimental due to increased catalyst and material degradation.

Operating Regime Definition

Based on knowledge obtained from catalyst testing (see section 4.3.3, above) and the thermodynamic considerations discussed previously, some preliminary recommendations and constraints on reformer operations were proposed, listed in Table 4.3.3.1-A3. These results are based on cylindrical catalyst testing experience, using both flow-rate and temperature-based criteria, and the amounts of washcoats that can be added to planar substrates.

Some questions that future work will address include: 1) benefits of increasing washcoat loading per in² vs. increased risk of washcoat adhesion failure and increased pressure drop, 2) how to define a meaningful GHSV for planar configuration and 3) interactions between temperature, GHSV, and catalyst loading on conversion, selectivity, and deactivation.

Multi-component composition used for modeling CARB Phase II gasoline. Actual and modeled formula is $C_{7.07}H_{13.73}O_{0.13}$.

	mole fraction
n-hexane	0.1792
2,4 dimethyl hexane	0.2809
cyclohexane	0.0645
ethylbenzene	0.2836
n-heptane	0.0638
MTBE	0.1279

Table 4.3.3.2-1: Modeled Multi-Component Mixture Composition

Results of equilibrium modeling, predicted energy produced by the reaction as a function of O/C and product H_2 concentration, using multi-component gasoline composition simulation.

Figure 4.3.3.2-1: Equilibrium Modeling Results – Carbon Formation

Results of equilibrium modeling, predicted product compositions at O/C of 1.05, using multi-component gasoline composition simulation.
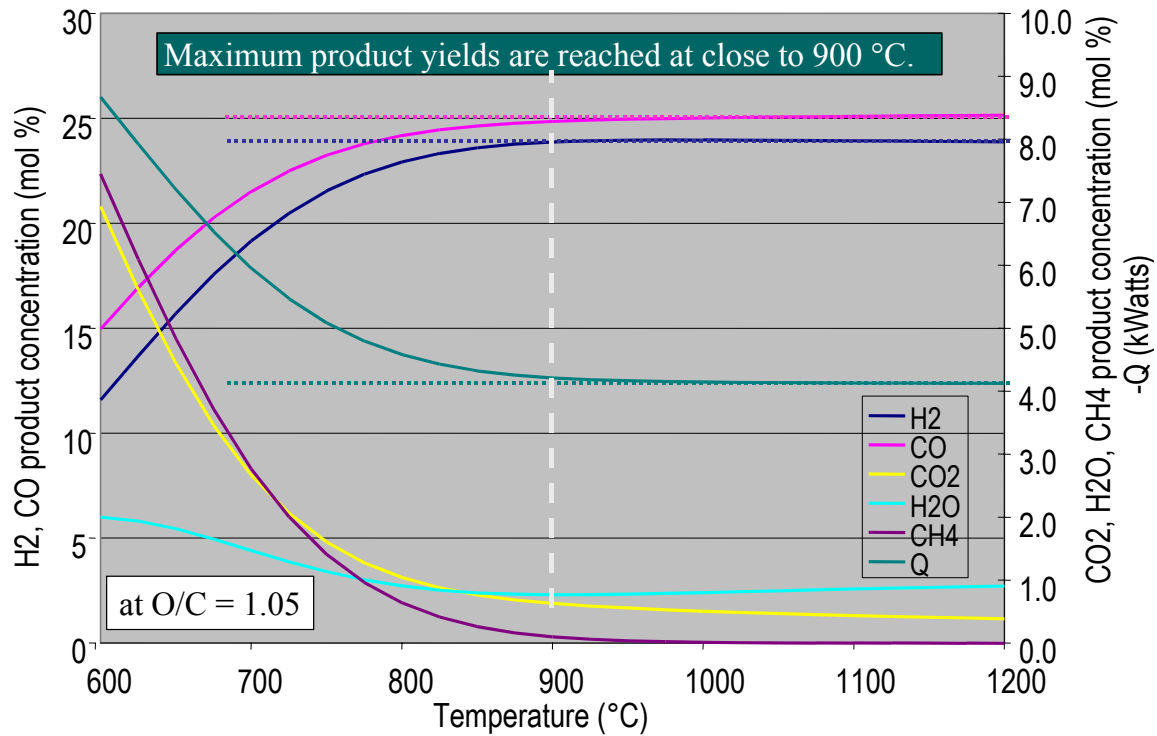
FIGURE 4.3.3.2.2-2: Equilibrium Modeling Results Product Compositions

Results of equilibrium modeling, predicted energy produced by the reaction as a function of O/C and product H_2 concentration, using multi-component gasoline composition simulation.
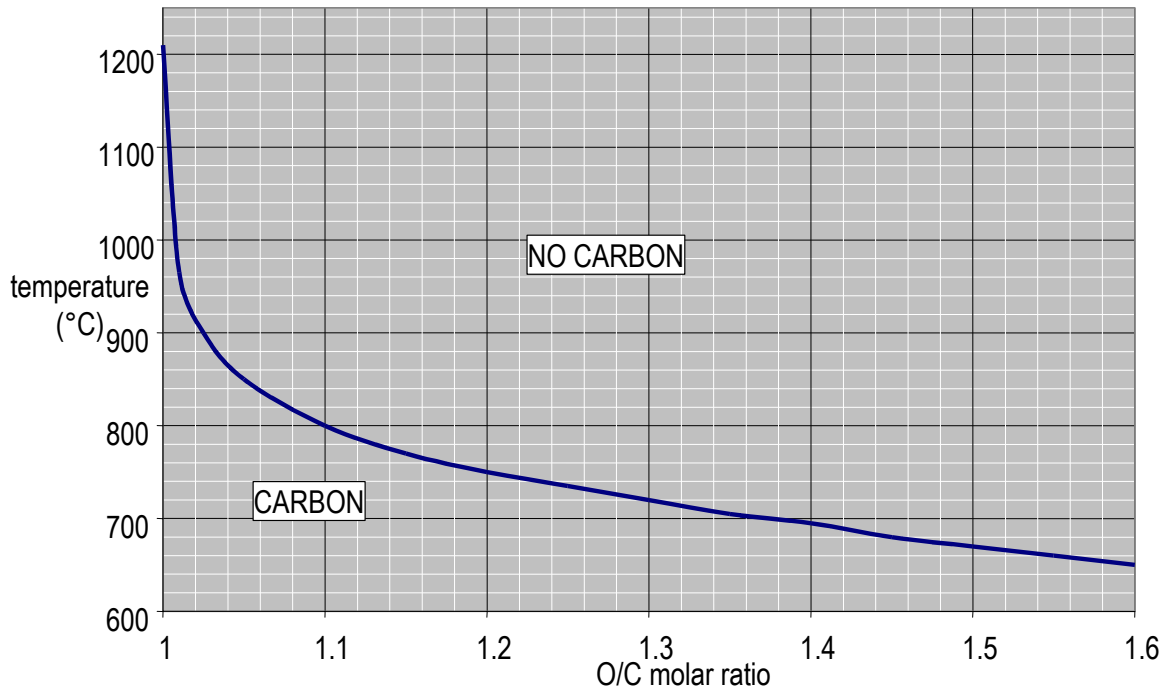
Results of equilibrium modeling, predicted H_2 product concentrations at various O/C, using multi-component gasoline composition simulation.
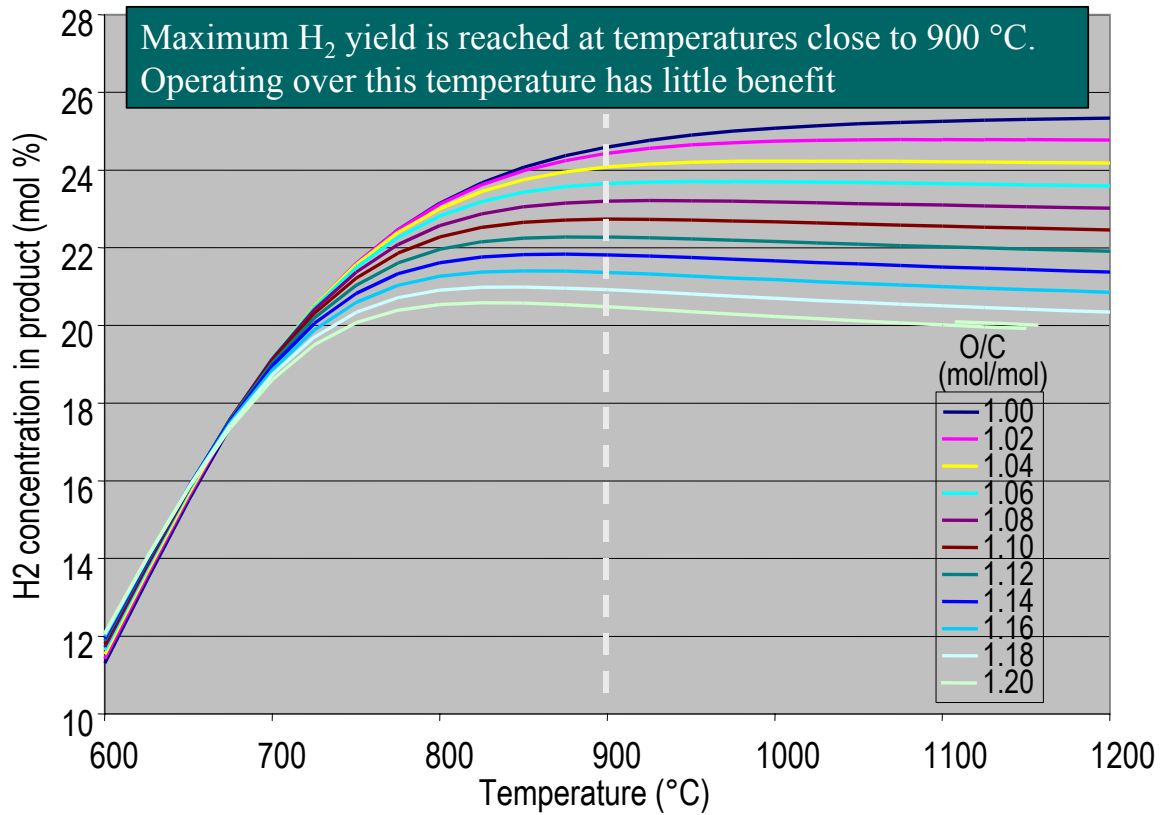
Figure 4.3.3.2-3: Equilibrium Modeling Results H_2 Product Concentrations
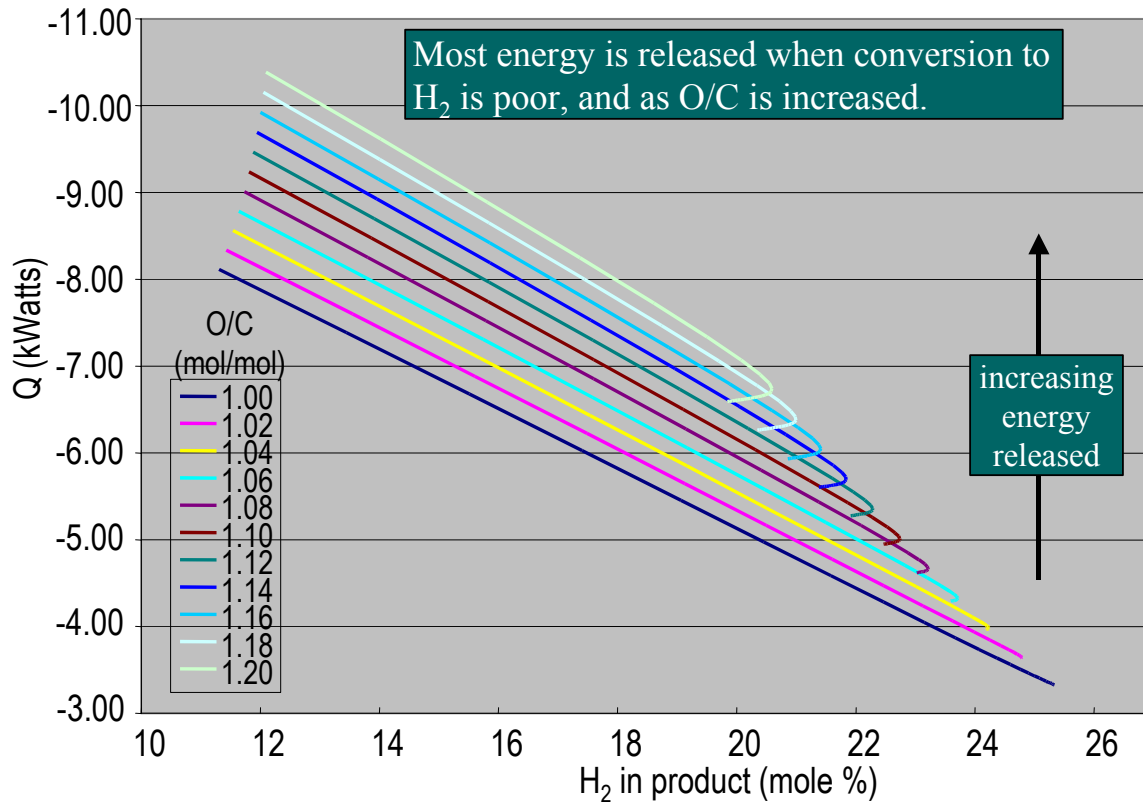
Figure 4.3.3.2-4 Equilibrium Modeling Results – Produced Energy

4.3.3.3   Testing Protocol Development

The ability to discriminate between catalyst formulations via testing is paramount to identifying the best formulation. Experience testing gasoline partial oxidation catalysts at the recommended temperatures of from 900 to 950 °C results in nearly identical levels of product H_2 and CO for all but the least appropriate compositions. Consequently, processing parameters and reactor wall temperatures are adjusted so that average catalyst center temperatures are about 1050-1100 °C. In this way, the catalysts are exposed to thermal stress and exhibit rapid aging, and so permitting elimination of all but the best catalyst formulations within a reasonably short period of time, usually after 20 to 50 hours of testing.

4.3.4 Develop a Desulfurization System

No work was completed under this subtask.

4.3.5 Develop Reformer and System—General

4.3.5.1   Lab Test System Development

Lab Test System Development discussion is covered in 4.3.1 through 4.3.3.

4.3.6 Investigate Integration of Reformer and ERU Functions

This subject covered under 4.3.2 Develop CPO Reformer above.

4.3.7 Fabricate Developmental Reformers

This subject covered under 4.3.2.

5.0   CONCLUSIONS

5.1   System Design and Integration

Working within the fixed package size has been an extremely challenging engineering task; however, one that has produced many innovations in both system mechanization and design concept.   The integration of the subsystems into the APU product was undertaken in an engineering evaluation mock-up. While executed mainly as a packaging verification exercise, many functional parts were used.   The subsystems, now in various stages of development, have been guided by the integrated product requirements. The emphasis on the end-product form factor has produced a workable concept with realizable performance in a much smaller size than would normally have been attempted.

5.2   SOFC Stack Development

The Delphi Battelle team has successfully developed the Generation 2 stack design. Modeling under steady state and transient conditions has provided us a good understanding of the performance characteristics of this design.   Parts have been fabricated and extensive testing has been carried out to evaluating sealing concepts and electrode contact concepts.   Progress has also been made on improving cathode to generate high power density.   Finally, short stacks with full sized cells have been fabricated and tested under different conditions to validate the design.

5.3   Reformer Developments

Catalyst and process conditions can be selected to give good performance, selectivity, and durability for gasoline partial oxidation. Additional work is required for optimization of catalyst compositions and the corresponding processes in which the catalysts are to be used.

6.0   Science & Technology Innovations and Transfers

1) The basic cell fabrication technique was developed on the CTP and transferred to the D-BP at its outset. The technique involves tape casting of the ceramic powders, tape lamination, and then cosintering of the bilayer. **– Jeff Stevenson**

2) The Lanthanum Strontium Ferrite (LSF) cathode and associated CeO2 barrier layer and associated processing were developed by the CTP and passed on to D-BP at the outset. These layers are screen printed onto the sintered bilayer and then fired. **– Jeff Stevenson**

3) Three modeling tools that are used extensively on the B-DP were first developed by the CTP. These are:
   a) Spreadsheet model of cell electrochemical performance. This is the algorithm that calculates cell voltage as a function of current, temperature, fuel composition and cell physical characteristics.
   b) Electrochemical modeling of stacks. This technique uses a computational fluid dynamics (CFD) code with the spreadsheet electrochemistry algorithm embedded to model the spatial distributions of electrochemical activity, temperature and fuel depletion for multi-cell stacks.
   c) Thermal cycle modeling. This technique uses CFD and finite element analysis (FEA) codes to model the heat transfer and resulting temperature and stress distributions in stacks during thermal cycles. These modeling tools were developed by the CTP over about a two year period starting in mid FY 2000. Transfer to and use by the D-BP started in mid FY 2001. Refinements continue on the models under the CTP. **– Moe Khaleel**

7.0 APPENDICES

Per Cooperative Agreement DE-FC26-02NT41246 Limited Rights Data considered restricted, proprietary, and confidential to Delphi are presented in Appendix A to this document per FAR 52.227-14, Rights in Data-General.

8.0 LIST OF ACRONYMS AND ABBREVIATIONS

A	
AC	Alternating Current
ADAM	Advanced Data Acquisition And Control Module
A/F	Air/Fuel Ratio
APU	Auxiliary Power Unit
AR&TD	Advanced Research And Technology Development
ASME	American Society Of Mechanical Engineers
ASR	Area Specific Resistance
ATC	After Treatment Catalyst
B	
BCI	Bulk Current Injection
BOP	Balance-Of-Plant
BTU	British Thermal Unit
C	
CAD	Computer-Aided Design
CARB	California Air Resources Board
CEO	Chief Executive Officer
CHEX	Cathode Air Preheat Heat Exchanger
CFD	Computational Fluid Dynamics
COR	Contracting Officer's Representative
CPO	Catalytic Partial Oxidation
CPU	Central Processing Unit
CRADA	Cooperative Research And Development Agreement
CTE	Coefficient Of Thermal Expansion
CTP	Core Technology Program
D	
DC	Direct Current
DI	Direct Injection
DIN	Deutsches Institut für Normung e.V. (Germany Industrial Standards)
DoD	Department Of Defense
DOE	Department Of Energy
E	
EHC	Electrically Heated Catalyst
EMC	Electro-Magnetic Compatibility
EMS	Engine Management System
EPRI	Electric Power Research Institute
ERU	Energy Recovery Unit
ESCO	Energy Service Companies
ESD	Electro-Static Discharge
F	
FEM	Finite Element Method
FMB	Fuel Meter Body
FMEA	Failure Modes And Effects Analysis

G	
GPC	Gas Phase Combuster
GSM	Global System Mobile Communication
GHSV	Gas Hourly Space Velocity
H	
HC	Hydrocarbons
HEX	Heat Exchanger
HVAC	Heating, Vacuum, And Air Conditioning
HZM	Hot Zone Module
I	
ICE	Internal Combustion Engine
ICM	Integrated Component Manifold
I/O	Input/Output
IRU	Interconnect Resistance Unit
ISM	Integrated Stack Module
L	
LHV	Lower Heating Value
LO	Light Off
LOT	Light Off Temperature
LSF	Lanthanum Strontium Ferrite
LZT	Lanthanum-Promoted Zinc Titanate
M	
MMC	Metal Matrix Composite
N	
NASA	National Aeronautics And Space Administration
NCV	Non-Contact Vaporizer
NETL	National Energy Technology Laboratory
NFPA	National Fire Protection Association
NPV	Net Present Value
NREL	National Renewable Energy Laboratory
O	
O:C	Oxygen:Carbon Ratio
OD	Outside Diameter
OTM	Oxygen Transport Membrane
P	
PDG	Product Development Group
PDP	Product Development Process
PEM	Polymer Electrolyte Membrane
PG&E	Pacific Gas & Electric Company
PLC	Programmable Logic Controller
PLIF	Planar Laser Induced Fluorescence
PLM	Plant Support Module
POC	Proof Of Concept
POX	Partial Oxidation
PSM	Plant-Support-Module
Pt	Platinum

PTC	Positive Temperature Coefficient
Q	
Q&R	Quality And Reliability
R	
ReforWER	Integrated Reformer And Waste Energy Recovery Unit
RFG	Reformulated Gasoline
S	
SAE	Society of Automotive Engineers
SECA	Solid State Energy Conversion Alliance
SEM	Scanning Electron Microscope
SOFC	Solid Oxide Fuel Cell
SOP	Start Of Production
SPC	Statistical Process Control
SS	Stainless Steel
SULEV	Super Ultra Low Emission Vehicle
SUV	Sport Utility Vehicle
T	
TDP	Technology Development Process
TEC	Thermal Expansion Coefficient
U	
ULEV	Ultra-Low Emission Vehicle
V	
V5	Version 5
W	
WBS	Work Breakdown Structure
WRU	Water Recovery Unit
Y	
YSZ	Yttria-Stabilized Zirconia